



UNIVERSITÀ DEGLI STUDI DI MILANO

FACOLTÀ DI SCIENZE E TECNOLOGIE

Corso di Laurea Magistrale in Fisica

Tesi di Laurea in Fisica

Threshold resummation in SCET vs. direct QCD: a systematic comparison

Relatore interno: Prof. S. Forte

Correlatore: Prof. G. Ridolfi

Luca Rottoli
matr. 808317

Anno Accademico 2012/2013

Contents

1	Strong interaction physics	1
1.1	Quantum Chromodynamics	1
1.2	The running coupling constant and the Landau pole	3
1.3	The parton model	4
1.4	Improved parton model	8
1.5	DGLAP equations	10
2	Resummation	15
2.1	Why resummation?	15
2.2	Soft-gluon effects in QCD cross-sections	16
2.3	Soft-gluon resummation and exponentiation in N -space	18
2.4	Soft gluon resummation and renormalization group approach	23
2.5	The Landau pole	29
2.6	Minimal prescription	31
2.7	Borel prescription	32
3	Phenomenology of threshold resummation in dQCD	35
3.1	Higgs production at the LHC	35
3.2	Higgs production in gluon-gluon fusion at fixed perturbative order	36
3.3	Higgs resummed results	40
4	Resummation in the SCET approach	43
4.1	Resummation in the Drell-Yan process	44
4.1.1	Fixed-order calculation of the Drell-Yan process	44
4.1.2	Factorization formula for the hard-scattering kernel	45
4.1.3	Resummation in momentum space	46
4.2	Resummation for the Higgs production process	48
4.2.1	Fixed-order expressions and factorization formula for Higgs production	48
4.2.2	Resummation in momentum space	49
4.3	The Becher-Neubert scale choice	51

4.4	Phenomenology	52
5	Resummation in SCET and in dQCD: an analytic comparison	55
5.1	Threshold resummation	55
5.2	Resummation of the Drell-Yan process in SCET and dQCD	56
5.2.1	Perturbative resummation in dQCD	56
5.2.2	Resummation in the SCET approach	57
5.3	Comparison at NNLL	58
5.3.1	Drell-Yan production	58
5.3.2	Higgs boson production	60
5.3.3	Master formula	62
5.4	Comparison in hadronic space	63
6	Resummation in SCET and in dQCD: a phenomenological comparison	67
6.1	Comparison of the resummed results	67
6.2	The resummation region for $gg \rightarrow H$ production mechanism	70
6.2.1	Saddle point argument	70
6.2.2	The saddle point in SCET	72
6.2.3	Results	73
6.2.4	Factorization violation in SCET	78
6.3	Higgs resummed results: N -space comparison	80
6.4	Detailed comparison	82
6.4.1	Connection with the analytical comparison	82
6.4.2	The Becher-Neubert scale choice	85
6.4.3	Summary and outlook	87
	Conclusions	89
A	Analytical expressions	91
A.1	Soft-gluon resummation formulae in dQCD	91
A.1.1	Drell-Yan process	92
A.1.2	Higgs production	94
A.1.3	Matching	95
A.2	Soft-gluon resummation formulae in SCET	96
A.2.1	Drell-Yan production	96
A.2.2	Higgs production	99
	References	101

Introduction

The discovery of a Higgs boson at the LHC brought enthusiasm to the high energy physics community and made physicists even more aware that accurate theoretical predictions are of the utmost importance in order to achieve a deeper understanding of the fundamental laws of nature. The next years will be dedicated to the study of the detailed properties of this new particle and to extend the energy frontier looking for physics beyond the Standard Model. For this reason, a detailed study of high-energy processes will be necessary in order to understand whether we are observing Standard Model physics or new physics when performing precision measurement in hadron colliders.

In order to obtain reliable predictions for the cross-sections it is necessary to compute all the relevant corrections. Higher order perturbative QCD calculations are necessary in order to obtain a detailed comprehension of hadronic final states properties. In some cases, enhanced logarithmically contributions appear at any order in perturbation theory. It is thus necessary to go beyond fixed-order perturbation theory and sum these contributions to all orders in the strong coupling constant α_s : hence resummation, which basically consists in a reorganization of the perturbative expansion by an all-order summation of classes of logs. This organization has been carried out in a variety of ways in a standard “direct” QCD (dQCD) approach.

In recent years an alternative approach to resummation, based on soft-collinear effective theory (SCET) has been proposed. In this latter approach the soft scale whose logarithms are resummed is a soft scale μ_s . Several choice for the soft scale μ_s are possible. In particular, one can choose the soft scale as a function of the dimensionless hadronic variable τ . This choice avoids problems related to the Landau pole in the strong coupling, which have to be faced in the traditional dQCD formalism.

An increasing interest in a deeper comprehension of the main similarities and differences between the two approaches has grown. In particular, the analytic equivalence of the dQCD and SCET approaches has been explored at various level. However, it would be interesting to investigate the phenomenological implications of this state of affairs.

In this Thesis we will perform a systematic comparison of soft-gluon resummation in SCET and in dQCD, both from an analytical and a phenomenological point of view. In particular, we will concentrate on Higgs boson production in gluon-gluon fusion in a hadron-hadron collider. It is indeed well known that the main contribution to Higgs production in the gluon-gluon channel

comes from the threshold region; for this reason, it is interesting to compare the predictions of the two approaches in order to obtain a deeper comprehension of possible differences in the resummation procedure. In particular, we will show how a systematic approach can be more easily performed by means of a saddle-point argument. We will present the results we have obtained with this strategy and we will discuss some open issues which would be interesting to further investigate.

The Thesis is organized as follows. In Chapter 1 we will present a very short review of QCD in order to introduce some notation which we will use in the following Chapters. In Chapter 2 we will summarize some general features of soft-gluon (or threshold) resummation for inclusive cross-sections. We will then apply soft-gluon resummation in the dQCD approach to a specific process, the Higgs production at LHC in gluon-gluon fusion, in Chapter 3. In the next Chapter, we will introduce the SCET approach to soft-gluon resummation, focusing on Drell-Yan process and Higgs production. In Chapter 5 we will then compare soft-gluon resummation in QCD as performed in the standard perturbative dQCD formalism, to resummation based on SCET in the Becher-Neubert approach. In the final Chapter we will perform a systematical comparison of soft-gluon resummation in SCET and in dQCD. In particular, we will present results for Higgs boson production in gluon-gluon fusion at the LHC.

Strong interaction physics

The following Chapter is dedicated to a brief overview of Quantum Chromodynamics (QCD), the modern theory of strong interactions. We intend this chapter as a very short review in order to introduce some notations that will be useful in the next Chapters. For a complete review, we refer the reader to [1].

1.1 Quantum Chromodynamics

Quantum Chromodynamics is a gauge theory based on the gauge group $SU(3)$, with Lagrangian

$$\mathcal{L}_{\text{QCD}} = \sum_f \bar{\psi}_i^{(f)} (i\bar{D}_{ij} - m_f \delta_{ij}) \psi_j^{(f)} - \frac{1}{4} F_a^{\mu\nu} F_{\mu\nu}^a, \quad (1.1)$$

where we have introduced the covariant derivative

$$D_{ij}^\mu \equiv \partial^\mu \delta_{ij} + ig_s t_{ij}^a A_a^\mu \quad (1.2)$$

and the field strength

$$F_{\mu\nu}^a = \partial_\mu A_\nu^a - \partial_\nu A_\mu^a - g_s f_{abc} A_\mu^b A_\nu^c. \quad (1.3)$$

By looking at Eq. (1.1) we notice that a single parameter, g_s , regulates the strength of the interaction. The fermionic fields, called quarks, have all the same coupling to the gauge fields, i.e. QCD is flavour blind. Eight self-interacting gauge fields, the gluons, have been introduced in order to preserve local gauge invariance.

As we have stated above, the gauge group of QCD is $SU(N)$, with $N = 3$. The indexes i, j in Eq. (1.1) run from 1 to N , whereas the group indexes a, b, c run from 1 to $N^2 - 1$, which is the dimension of the fundamental representation of $SU(N)$. The eight matrixes t_{ij}^a are usually normalized as

$$\text{Tr}(t_a t_b) = T_F \delta_{ab} \quad (1.4)$$

with $T_F = \frac{1}{2}$. They satisfy the Lie algebra

$$[t_a, t_b] = f_{ab}^c t_c, \quad (1.5)$$

flavour	d	u	s	c	b	t
name	down	up	strange	charm	bottom	top
mass	~ 2.5 MeV	~ 5 MeV	0.1 GeV	1.3 GeV	4.2 GeV	173 GeV
charge	$-1/3$	$2/3$	$-1/3$	$2/3$	$-1/3$	$2/3$

Table 1.1: Masses and charges of the quarks.

where f_{abc} are the real structure constants of the $SU(N)$ algebra, and are fully antisymmetric. The invariants C_F and C_A are defined by

$$\sum_a t_{ij}^a t_{kj}^a = C_F \delta_{ij} \quad (1.6)$$

$$\sum_{cd} f^{acd} f^{bdc} = C_A \delta^{ab}, \quad (1.7)$$

where

$$C_F = T_F \frac{N^2 - 1}{N} \quad (1.8)$$

$$C_A = N. \quad (1.9)$$

Thus for QCD we obtain

$$C_F = \frac{4}{3}, \quad C_A = 3. \quad (1.10)$$

In order to quantize the classical lagrangian Eq. (1.1) it is necessary to introduce gauge fixing and ghost terms. We refer the reader to any QFT textbook for details. The physical vertices in Eq. (1.1) include not only a gluon-quark-antiquark vertex, which is analogous to the electromagnetic vertex in QED, but also a 3-gluon and a 4-gluon vertex, which have no analogue in QED.

The theory has an additional exact $U(1)$ symmetry, which corresponds to the conservation of the baryon number. Furthermore, it is well known that the QCD spectrum presents an extra accidental symmetry, which corresponds to the conservation of the isospin number. The masses of the up quark and of the down quark are very small with respect to the lightest bound states:

$$m_u, m_d \ll m_\pi, m_N. \quad (1.11)$$

For all practical purposes, the two lightest quarks can be considered massless. The theory has therefore an additional approximate global $U(2)$ flavour symmetry, i.e. isospin. If we neglect the mass of the strange quark, the symmetry can be enlarged to an approximate $U(3)$ symmetry, which is at the basis of the Gell-Mann quark model.

Since the two chiral components of quark fields are independent in the massless limit, if the masses of the up and down quark are neglected the Lagrangian has the larger symmetry

$$SU_L(2) \times SU_R(2) \times U(1)_L \times U(1)_R, \quad (1.12)$$

or equivalently, considering vector and axial combinations,

$$SU_A(2) \times SU_V(2) \times U(1)_A \times U(1)_V. \quad (1.13)$$

$U(1)_V$ and $SU(2)_V$ are good symmetry in nature, which correspond respectively to the conservation of the baryon number and isospin number. The axial symmetry is spontaneously broken; in this case we expect to find the existence of four Goldstone bosons in the QCD spectrum. However, we observe only three Goldstone bosons, the pions. The absence of the fourth boson was known as the $U(1)_A$ problem: $U(1)_A$ is not realized neither à la Goldstone, neither à la Wigner-Weyl. The solution of the $U(1)_A$ problem was separately found by Jackiv and 't Hooft and relies on the highly non trivial topological vacuum structure of QCD.

1.2 The running coupling constant and the Landau pole

We define the QCD coupling constant as

$$\alpha_s = \frac{g_s^2}{4\pi}. \quad (1.14)$$

The renormalization group equation reads

$$\mu^2 \frac{d}{d\mu^2} \alpha_s(\mu^2) = \beta(\alpha_s(\mu^2)), \quad (1.15)$$

where the β -function starts at order α_s^2 and has the expansion

$$\beta(\alpha_s) = -\alpha_s^2(\beta_0 + \beta_1\alpha_s + \beta_2\alpha_s^2 + \dots). \quad (1.16)$$

One finds

$$\beta_0 = \frac{11C_A - 2n_f}{12\pi}, \quad (1.17)$$

which is positive provided $n_f \leq 16$. If the coupling constant is small it is possible to compute the β -function in perturbation theory. The sign in front of β_0 is crucial: it decides the slope of the coupling. Since in QCD β is negative at small α_s , the running coupling decreases as μ increases.

A theory like QCD, where the running coupling vanishes asymptotically at high energies is called (ultraviolet) *asymptotically free*. It has been proven that in 4 spacetime dimensions all and only non-abelian gauge theories are asymptotically free.

We can write the solution for α_s at one loop (leading log approximation):

$$\alpha_s(\mu^2) = \frac{\alpha(Q^2)}{1 + \beta_0 \alpha(Q^2) \log \frac{\mu^2}{Q^2}} \quad (1.18)$$

with the initial condition $\alpha_s(Q^2)$. Usually in QCD one defines

$$\frac{1}{\alpha(Q^2)} = \beta_0 \log \frac{Q^2}{\Lambda_{QCD}^2} \quad (1.19)$$

so that we can trade the parameter Q for the dimensional parameter Λ_{QCD} and we can write

$$\alpha(\mu^2) = \frac{1}{\beta_0 \log \frac{\mu^2}{\Lambda_{QCD}^2}}. \quad (1.20)$$

The scale Λ_{QCD} is of the order of a few hundred MeV. Eqs. (1.18)-(1.20) clarify what we intend for asymptotic freedom: the coupling constant decreases logarithmically with μ^2 . In the leading log approximation the coupling constant has been replaced in a way by the value of Λ_{QCD} . Λ_{QCD} depends on the particular definition of α_s , not only on the defining scale Q but also on the renormalization scheme (beyond leading order). Moreover, it also depends on the active number n_f of coupled flavours. In QED and QCD, the effects of heavy quarks are power suppressed and can be taken separately into account. This is very important, since all applications of perturbative QCD so far apply to energies below m_t . In conclusion, in QED and QCD, quarks with a mass higher than the scale μ do not contribute to n_f in the coefficients of the relevant β function.

One notes the presence of a singularity in Eqs. (1.19,1.20) called the Landau pole. The coupling constant α_s blows up at

$$\mu_L^2 = \Lambda_{QCD}^2 = Q^2 \exp \left(-\frac{1}{\beta_0 \alpha_s(\mu^2)} \right). \quad (1.21)$$

In this region, where $\mu \sim \Lambda_{QCD}$, QCD is non-perturbative. The scale Λ_{QCD} is typically of the order of some hundreds of MeV. The problem of the definition and the behaviour of the physical coupling in the region around the perturbative Landau pole is an issue that lies outside the domain of perturbative QCD.

Due to the failure of perturbation theory, we cannot predict the behavior of the coupling constant at low energy. We however observe that in this regime QCD is strongly coupled. Moreover, quarks can form bound states, which are the well-known hadrons. We have only a phenomenological knowledge of the nonperturbative QCD. When a bound $q\bar{q}$ pair is forced to separate, the potential between the quarks increases. At some separation length, it becomes convenient for the $q\bar{q}$ pair to split up in two $q\bar{q}$ pairs. The strong color attraction precludes the possibility of observing isolated quarks. This experimentally checked effect is known as *confinement* and it is observed whenever a high-energy collision takes place. The additional quarks or gluons produced in the collisions dress themselves into hadrons and form jets of particle which are seen in the detectors.

The most important non-perturbative method at present is the technique of lattice simulations which has produced very valuable results on confinement, phase transitions, bound states, and so on, and it is by now an established basic tool. Nevertheless, a full non-perturbative explanation of confinement has not been achieved yet.

1.3 The parton model

Scattering experiments have been the main source of information on hadronic structure in the second half of the twentieth century. In a typical scattering experiment a beam of high-energy leptons (usually electrons) is made to collide with hadrons. When the momentum transfer of the

virtual photon which mediates the collision is sufficiently large, a system with a large number of hadrons is produced:

$$e^-(k) + N(p) \rightarrow e^-(k') + X. \quad (1.22)$$

This process is called deep inelastic scattering (DIS).

The differential cross-section for electron-nucleon scattering can be parametrized by structure functions $F_i(x_{Bj}, Q^2)$, which are determined by experiment, where

$$Q^2 = -(k - k')^2 = -q^2, \quad x_{Bj} \equiv \frac{Q^2}{2p \cdot q}. \quad (1.23)$$

The experimental data show that in the limit $Q^2 \rightarrow \infty$, but for finite value of x_{Bj} the structure functions obey approximate Bjorken scaling (which in reality is broken by logarithmic corrections that can be computed in QCD, as we will see):

$$F_i(Q^2, x_{Bj}) \xrightarrow{Q^2 \rightarrow \infty} F_i(x_{Bj}). \quad (1.24)$$

Bjorken and Feynman proposed a simple model, the so-called *parton model*, in order to explain this phenomenon. The basic assumption of this model is that the proton is made up of a smaller point-like, non interacting constituents, called partons. Among these constituents one can find the fermions which carry electric charge, namely the quarks (and antiquarks), and possibly other neutral constituents. In the parton model, each parton is characterized by the fraction x of the hadron's total momentum that it carries. Consequently, for each species i of parton, there is a function $f_i(x)$ which express the probability that a parton i carries a fraction x of the total momentum of the nucleon. The functions $f_i(x)$ are called *parton distribution functions* (PDF) and must be experimentally determined.

We naively expect the validity of the momentum sum rule, which expresses the conservation of incoming total momentum:

$$\int_0^1 dx \sum_i x f_i^{(p)}(x) = 1. \quad (1.25)$$

We also expect the proton flavour to be conserved. For example,

$$\int_0^1 dx \left(f_u^{(p)}(x) - f_{\bar{u}}^{(p)}(x) \right) = 2 \quad \int_0^1 dx \left(f_d^{(p)}(x) - f_{\bar{d}}^{(p)}(x) \right) = 1. \quad (1.26)$$

Measurements confirm these naive expectations. One discovers however that the fraction of total momentum carried by valence and sea quarks is about one-half; the remaining half is in fact carried by the neutral gluons, the quanta of the strong nuclear force.

In conclusion, the parton model enables the computation of several high energy processes with hadrons in the initial state using only a simple set of assumptions: the hadrons are made of partons, whose momenta are distributed according to PDFs. Finally, transverse momenta and masses of the partons must be neglected.

We can now apply the parton model to inclusive DIS and verify that, despite its simplicity, it imposes strong constraints on the cross-section. The kinematics variables of the process are shown in Fig. 1.1. We defined the additional variables

$$s = (k + p)^2, \quad y = \frac{p \cdot q}{k \cdot p}. \quad (1.27)$$

The observation of the outgoing electrons enables a determination of s , x_{Bj} and y , which is the electron fractional energy loss in the laboratory frame of a fixed target experiment¹.

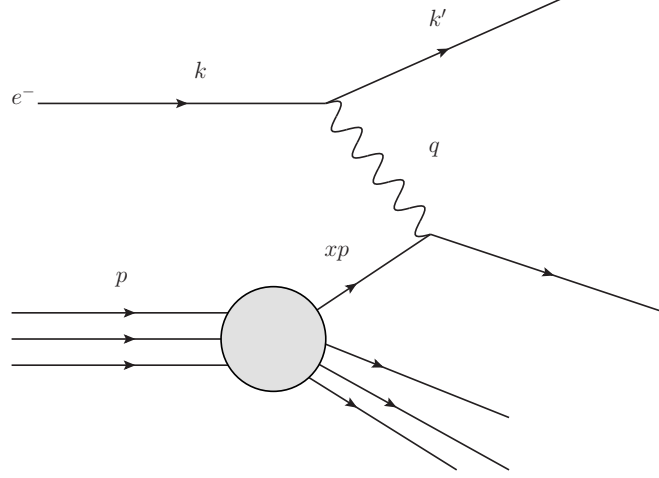


Figure 1.1: Kinematics for the DIS process in the parton model framework.

The Feynman rules of QED allow for a computation the partonic cross-section

$$\frac{d\hat{\sigma}}{d\hat{y}} = q_l^2 \frac{\hat{s}}{Q^4} 2\pi\alpha^2 (1 + (1 - \hat{y})^2) \quad (1.28)$$

where q_l is the electric charge of the (anti)quark l and

$$\begin{aligned} \hat{p} &= xp, & \hat{s} &= (k + \hat{p})^2 = 2k \cdot p, & (\hat{p} + q)^2 &= 2\hat{p} \cdot q - Q^2 = 0, \\ \hat{y} &= \frac{\hat{p} \cdot q}{k \cdot \hat{p}} = y, & x_{Bj} &= \frac{Q^2}{2p \cdot q} = x \frac{Q^2}{2\hat{p} \cdot q} = x. \end{aligned} \quad (1.29)$$

According to the parton model, the hadronic cross-section can be computed as

$$\frac{d\sigma}{dy} = \int dx \sum_l f_l(x) \frac{d\hat{\sigma}_l}{dy}. \quad (1.30)$$

We thus have

$$\begin{aligned} \frac{d\sigma}{dy dx_{Bj}} &= \sum_l f_l(x) \frac{d\hat{\sigma}}{dy} \\ &= \frac{2\pi\alpha^2 s x_{Bj}}{Q^4} (1 + (1 - y)^2) \sum_l q_l^2 f_l(x_{Bj}). \end{aligned} \quad (1.31)$$

Looking at Eq. (1.31) we learn that the parton model, in its simplicity, makes remarkable predictions. It shows that at fixed x_{Bj} and y the cross-section scales with the energy s . Moreover,

¹In the centre-of-mass of the electron-quark system, $y = \frac{1 - \cos \theta_{el}}{2}$ where θ_{el} is the electron scattering angle.

it fully predicts the y -dependence of the cross-section, which is typical of vector interaction with fermions (Callan-Gross relation). It is customary to write the cross-section Eq. (1.31) introducing the structure function $F_2(x)$, which obeys Bjorken scaling:

$$\frac{d\sigma}{dydx} = \frac{2\pi\alpha^2 s}{Q^4} (1 + (1-y)^2) F_2(x) \quad F_2(x) = \sum_l x q_l^2 f_l(x). \quad (1.32)$$

In particular, for electron scattering on proton,

$$F_2(x) = x \left(\frac{4}{9} u_p(x) + \frac{1}{9} d_p(x) \right), \quad (1.33)$$

whereas for electron scattering on a neutron

$$F_2^n(x) = x \left(\frac{1}{9} d_n(x) + \frac{4}{9} u_n(x) \right) = x \left(\frac{4}{9} d_p(x) + \frac{1}{9} u_p(x) \right) \quad (1.34)$$

and therefore knowledge of F_2^n and F_2^p allows a determination of u_p and d_p separately.

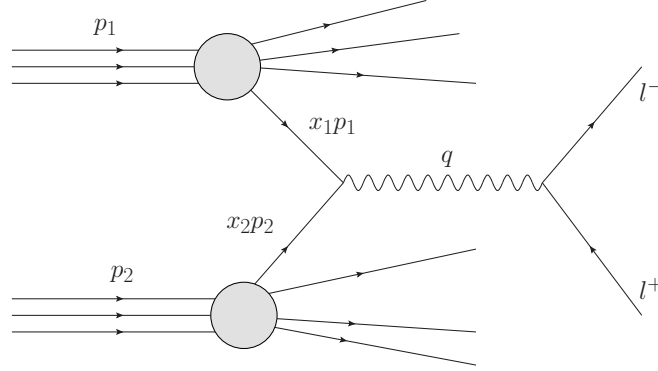


Figure 1.2: Kinematics for the DY process in the parton model framework.

The parton model can be used also for other processes. In the so-called Drell-Yan process, a massive lepton pair emerges from a $q\bar{q}$ annihilation in a hadron-hadron collision. The Drell-Yan process is depicted in Fig. 1.2 in the parton model interpretation. In this case, the partonic kinematic variables are

$$\hat{p}_i = x_i p_i, \quad i = 1, 2, \quad s = (p_1 + p_2)^2 = 2p_1 \cdot p_2, \quad Q^2 = q^2. \quad (1.35)$$

The partonic cross-section is

$$\frac{d\hat{\sigma}^{DY}}{dQ^2} = q_l^2 \frac{4\pi\alpha}{9Q^2} \delta(\hat{s} - Q^2). \quad (1.36)$$

where $\hat{s} = x_1 x_2 s$. The hadronic cross-section in the parton model interpretation, where Q^2 is large, is then

$$\frac{d\sigma^{DY}}{dQ^2} = \sum_l \int dx_1 dx_2 \left(f_l^{(H_1)}(x_1) f_{\bar{l}}^{(H_2)}(x_2) + (l \leftrightarrow \bar{l}) \right) \delta(x_1 x_2 s - Q^2) \sum_l q_l^2 \frac{4\pi\alpha}{9Q^2}. \quad (1.37)$$

In the parton model interpretation we can compute the cross-section for several scattering processes, in which also gluons could enter in the initial state. However not all hadronic processes can be computed in this way. There is a rule of thumb which enables one to decide whether the process is a hard process or not, in the parton model context. If the process is insensitive to the initial transverse momentum of the partons, which is of the order of typical hadronic scales, we can obtain cross-sections in the parton model safely. The parton densities, in fact, do not carry any information about the initial transverse momentum of the partons.

The parton model works well at the first order, but it is completely useless at the next order correction, because of the appearance of collinear singularities. For simplicity, let us consider again DIS. To first order in the coupling it is necessary to consider the emission of one real gluon and a virtual one (see Fig. 1.3). If one adds real and virtual contributions, the partonic cross-section reads

$$\sigma^{(1)} = \frac{C_F \alpha_s}{2\pi} \int dz \frac{dk_{\perp}^2}{k_{\perp}^2} \frac{1+z^2}{1-z} \left(\sigma^{(0)}(z\hat{p}) - \sigma^{(0)}(\hat{p}) \right). \quad (1.38)$$

We see that there is a singularity at $z = 1$ which cancels between real and virtual corrections. This region corresponds to the soft limit. The cross-section Eq. (1.38) thus does not have soft singularities. However, there is also a collinear singularity in the limit $k_{\perp} \rightarrow 0$ for finite z . This singularity does not cancel.

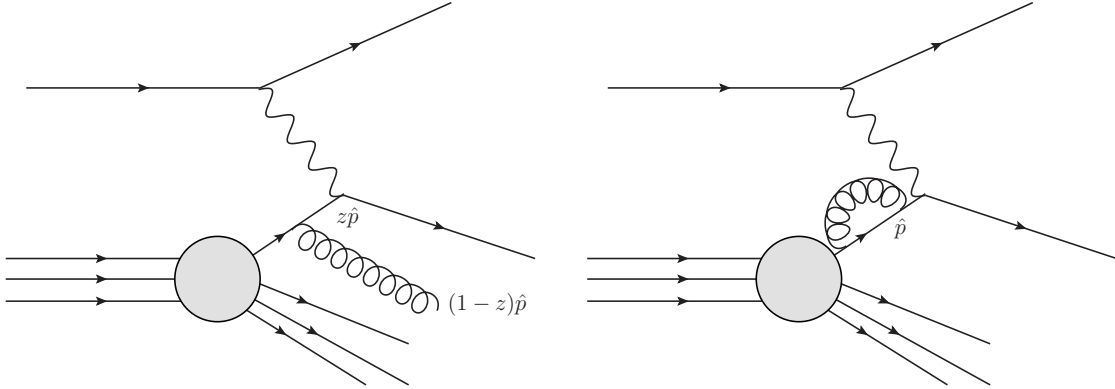


Figure 1.3: Virtual and real radiative contribution to DIS.

The naive parton model therefore does not survive radiative corrections. As we will see in the next Section, collinear divergences from initial state emissions are absorbed into parton distribution functions, similarly to what happens when UV divergences are renormalized.

1.4 Improved parton model

The presence of collinear divergences makes clear that the parton model is, if not totally wrong, rather incomplete. The parton model today is viewed as an approximate consequence of the leading order perturbative treatment of QCD, the modern theory of strong interactions.

In the real world, divergences do not exist. There are several remedies we could take in order to make the divergences go away, for example by introducing the quark masses, or put

a lower cutoff λ in the transverse momentum integral. If we do so, however, the cross-section would acquire a strong dependence upon low energy details, such as quark masses or confinement effects. These dependences would in the end spoil the parton model, since by assumptions these details should not count.

It is possible however to rescue the parton model if we make some improvements. We now fix some notation which will be useful in the following Chapters. We define the Altarelli-Parisi splitting function

$$P_{qq}^{(0)}(z) = C_F \left(\frac{1+z^2}{1-z} \right)_+, \quad (1.39)$$

where we have introduced the *plus prescription*. The plus distribution naturally arises from the cancellation of soft divergences; it is defined as

$$\int_0^1 dz [f(z)]_+ g(z) = \int_0^1 dz f(z) [g(z) - g(1)]. \quad (1.40)$$

We introduce a cutoff λ and we rewrite Eq. (1.38) as

$$\sigma^{(1)} = \frac{\alpha_s}{2\pi} \log \frac{Q^2}{\lambda^2} \int dz P_{qq}^{(0)}(z) \sigma^{(0)}(z\hat{p}). \quad (1.41)$$

The partonic cross-section is found to be

$$\sigma(\hat{p}) = \sigma^{(0)}(\hat{p}) + \sigma^{(1)}(\hat{p}) = \int dz \left(\delta(1-z) + \frac{\alpha_s}{2\pi} \log \frac{Q^2}{\lambda^2} P_{qq}^{(0)}(z) \right) \sigma^{(0)}(z\hat{p}). \quad (1.42)$$

If we insert this formula in the parton model formula for the hadronic cross-section we obtain

$$\sigma(p) = \int dy dz f_q(y) \Gamma_{qq}(z, Q^2) \sigma^{(0)}(zyp) \quad (1.43)$$

where we have defined

$$\Gamma_{qq}(z, Q^2) = \delta(1-z) + \frac{\alpha_s}{2\pi} \log \frac{Q^2}{\lambda^2} P_{qq}^{(0)}(z). \quad (1.44)$$

We then introduce an intermediate scale μ_F and we recombine the logarithms using

$$\log \frac{Q^2}{\lambda^2} = \log \frac{Q^2}{\mu_F^2} + \log \frac{\mu_F^2}{\lambda^2} \quad (1.45)$$

and we rewrite the hadronic cross-section (up to $\mathcal{O}(\alpha_s^2)$ corrections) as

$$\sigma(p) = \int dx f_q(x, \mu_F^2) \hat{\sigma}(xp, \mu^2) \quad (1.46)$$

where

$$f_q(x, \mu_F^2) = \int dy dz f_q(y) \Gamma_{qq}(z, Q^2) \delta(x - zy). \quad (1.47)$$

This means that the radiative corrections to the parton process can be absorbed redefining the parton densities, which acquire a scale dependence. This redefinition is universal and does not depend upon the hard process we are considering. In the improved parton model the physical cross section can be defined in terms of the new scale-dependent PDFs. We can write (we omit the sum over flavours)

$$\sigma = \int dx_1 dx_2 f_1^{(P_1)}(x_1, \mu^2) f_2^{(P_2)}(x_2, \mu_F^2) \hat{\sigma}(x_1 x_2 s, \mu_F^2). \quad (1.48)$$

In the QCD-improved parton model a short distance cross-section $\hat{\sigma}$ appears, which is obtained by subtracting the long distance part from the partonic cross-section. In this way it is possible to rely on perturbation theory. The introduction of the factorization scale allows to shift the divergent contribution into non-perturbative PDF. A choice of the factorization scale μ_F similar to Q avoids large logarithms in the short distance cross-section.

The argument we have presented was carried out only at leading order in perturbation theory. However, there are several arguments which show that Eq. (1.48) holds to all orders in perturbation theory. This result is known as factorization theorem. In case of DIS, a solid proof of the theorem, which relies on a clever analytic continuation property of the DIS cross-section, exists. For production processes in hadronic collisions the situation is more difficult. All-order arguments for factorization have been given in Ref. [4]. Today the factorization theorem is widely accepted.

One can improve the accuracy of the hadronic cross-section by extracting from experiment PDFs at higher order and computing the short distance cross-section at the desired level of accuracy:

$$\hat{\sigma} = [\hat{\sigma}_0 + a\hat{\sigma}_1 + a^2\sigma_2^2 + \dots] \quad (1.49)$$

with² $a = \alpha_s(\mu_R)/(2\pi)$.

1.5 DGLAP equations

We have seen how collinear singularities due to an initial state parton do not cancel. Fortunately, it is possible to include into the PDFs initial state emission with k_\perp below a given scale. The price to pay is the introduction of a factorization scale μ , which separates the non-perturbative, low energy dynamics from the perturbative hard cross section. As for the renormalization scale, the dependence of cross-section on μ is due to the fact that the perturbative expansion has been truncated. The μ -dependence becomes milder when including higher orders.

The new scale-dependent PDFs contains uncalculable long distance effects. These effects can be measured by using Eq. (1.48) with some reference hard process. In this way it is possible to obtain the PDF at a given scale μ . It is however possible to obtain the μ dependence of PDFs by deriving Eq. (1.47). By doing so, the master equation of QCD, the Altarelli-Parisi (AP) equation (or Dokshitzer-Gribov-Lipatov-Altarelli-Parisi equation) is obtained:

$$\mu^2 \frac{\partial f_q(x, \mu^2)}{\partial \mu^2} = \int_x^1 \frac{dy}{y} f_q(y, \mu^2) P_{qq}^{(0)}\left(\frac{x}{y}\right). \quad (1.50)$$

²The coupling constant α_s is evaluated at the renormalization scale μ_R , which is in principle different from the factorization scale μ_F . For simplicity, from now on we will consider only one scale $\mu = \mu_F = \mu_R$.

Therefore, even if we cannot compute PDFs, we can predict how they evolve from one scale to another. Since the splitting functions are universal, it is possible to measure PDFs in one process and use them as inputs for another one.

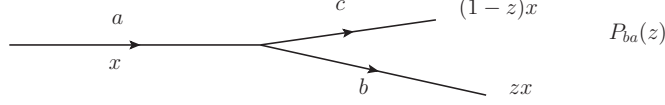


Figure 1.4: Standard conventions for splitting functions.

It is necessary to take account of the different species of partons. The standard notation for the splitting functions is shown in Fig. 1.4. The DGLAP equations are a system of coupled integro/differential equations which are usually written in compact notation as³

$$\mu^2 \frac{\partial f_i(x, \mu^2)}{\partial \mu^2} = \sum_j P_{ij} \otimes f_j(\mu^2). \quad (1.51)$$

with

$$P_{ij}(x) = \frac{\alpha_s}{2\pi} P_{ij}^{(0)} + \left(\frac{\alpha_s}{2\pi}\right)^2 P_{ij}^{(1)} + \dots \quad (1.52)$$

The splitting functions are now known up to $P_{ij}^{(2)}$. The determination of $P_{ij}^{(2)}$ is an essential input in order to determinate NNLO PDFs. In the following, we limit our discussions to $P_{ij}^{(0)}$. At leading order the splitting functions are

$$P_{qq}^{(0)}(z) = P_{\bar{q}\bar{q}}^{(0)}(z) = C_F \left(\frac{1+z^2}{1-z} \right)_+, \quad (1.53)$$

$$P_{qg}^{(0)}(z) = P_{\bar{q}g}^{(0)}(z) = T_F(z^2 + (1-z)^2), \quad (1.54)$$

$$P_{gq}^{(0)}(z) = P_{g\bar{q}}^{(0)}(z) = C_F \frac{1+(1-z)^2}{z}, \quad (1.55)$$

$$P_{gg}^{(0)}(z) = 2C_A \left[z \left(\frac{1}{1-z} \right)_+ + \frac{1-z}{z} + z(1-z) + \left(\frac{11}{12} - \frac{n_f}{6C_A} \right) \delta(1-z) \right]. \quad (1.56)$$

At higher orders components $P_{q_i q_j}$ with $i \neq j$, $P_{q_i \bar{q}_j}$ for any i, j arise.

We can take the difference of Eq. (1.51) for a quark (antiquark) flavour i with itself for a quark (antiquark) flavour j :

$$\mu^2 \frac{\partial}{\partial \mu^2} (f_i(\mu) - f_j(\mu)) = \sum_k (P_{ik} \otimes f_k(\mu) - P_{jk} \otimes f_k(\mu)). \quad (1.57)$$

Since the gluon contributions cancels out, we get

$$\mu^2 \frac{\partial}{\partial \mu^2} (f_i(\mu) - f_j(\mu)) = P_{qq} \otimes (f_i(\mu) - f_j(\mu)). \quad (1.58)$$

³The \otimes product is defined as $f_1 \otimes f_2 \otimes \dots \otimes f_n(x) = \int_0^1 dx_1 dx_2 \dots dx_n f_1(x_1) f_2(x_2) \dots f_n(x_n) \delta(x - x_1 x_2 \dots x_n)$.

With n_f flavours there are therefore $2n_f - 1$ independent combination of PDFs which evolve independently, called non-singlet components. On the other hand, we can take the sum of the DGLAP equations for all quark and antiquark flavours. In this way we get

$$\sum_{i \neq g} \frac{\partial}{\partial \mu^2} f_i(\mu) = P_{qq} \otimes \sum_{i \neq g} f_i(\mu) + 2n_f P_{ig} \otimes f_g(\mu). \quad (1.59)$$

We can finally consider Eq. (1.51) for the gluon:

$$\frac{\partial}{\partial \mu^2} f_g(\mu) = \sum_{i \neq g} P_{gi} \otimes f_i(\mu) + P_{gg} \otimes f_g(\mu). \quad (1.60)$$

If we define

$$S(\mu) = \sum_{i \neq g} f_i(\mu) \quad (1.61)$$

we have the following system of equations for the singlet component S and the gluon:

$$\mu^2 \frac{\partial}{\partial \mu^2} f_g(\mu) = P_{gq} \otimes S(\mu) + P_{gg} \otimes f_g(\mu) \quad (1.62)$$

$$\mu^2 \frac{\partial}{\partial \mu^2} S(\mu) = P_{qq} \otimes S(\mu) + 2n_f P_{ig} \otimes f_g(\mu). \quad (1.63)$$

We then learn that the singlet component mixes with the gluon density in its evolution, contrary to the non-singlet components, which evolve independently.

In Fig. 1.5 it is possible to observe some typical features of parton distribution functions. In particular, the gluon distribution is very large and dominates at small x . The sea distributions grow at small x , too. The valence distributions present a peak around $x = 0.1 - 0.2$. Finally, the largest uncertainties are at very small, or very large x .

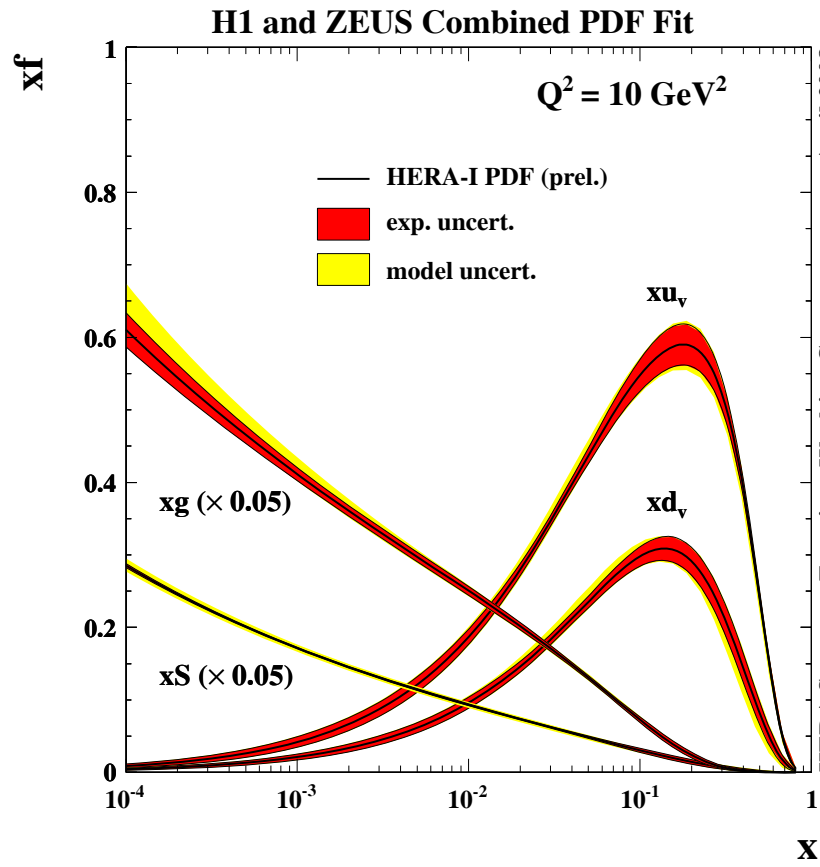


Figure 1.5: Typical features of PDFs.

Higher order perturbative QCD calculations are necessary in order to obtain a detailed understanding of hadronic final states properties. In some cases, logarithmically enhanced contributions appear at all order in perturbation theory. It is thus necessary to go beyond fixed-order perturbation theory and sum these contributions to all orders in α_s . The LHC provides very precise measurements of many processes, such as Drell-Yan, Higgs or top production. Accurate theoretical predictions are necessary in order to understand whether we are observing Standard Model physics or new physics signals. There is therefore great interest in assessing the impact of threshold resummation in order to obtain accurate phenomenological predictions.

In this Chapter we summarize some general features of soft-gluon (or threshold) resummation for inclusive cross-sections. In Sect. 2.1 we introduce the idea of resummation classifying the enhanced contributions which appear when physical observable are calculated. In Sects. 2.2 and 2.3 we present a simplified argument which sheds light on the main features of soft resummation – factorization and exponentiation. In Sect. 2.4 we present a proof of all-order resummation which follows a renormalization group argument. Finally, in Sect. 2.5 we introduce the reader to the well known problem of the Landau pole which appears in the resummed expressions and in Sect. 2.6 and 2.7 we present two different solutions which remove it.

2.1 Why resummation?

When we compute a cross-section in dQCD we may run into several (logarithmically) enhanced contributions, which we can classify into three main categories:

- logarithms of ultra-violet (UV) origin;
- logarithms of collinear origin;
- logarithms of soft origin.

We have seen how logarithms of collinear origin can be absorbed into scale-dependent PDFs thanks to DGLAP equations; in the same way UV logarithms are absorbed into the running coupling constant α_s . How can we deal with the last kind of logarithms?

Since any particle detector has a finite energy resolution, a generic physical cross-section is always inclusive over arbitrary soft particles which are produced in the final state. Thanks to

this inclusiveness, the radiation of undetected real gluons cancels exactly the divergences which appear when calculating perturbative contributions due to virtual gluons. However, despite the cancellation theorems of soft-gluon singularities, soft-gluon effects can still be large in kinematic configurations where high unbalance between real and virtual contributions persists. In this case, the convergence of fixed-order expansion is spoiled, and calculations to all orders of perturbation theory are necessary in order to achieve reliable predictions. An all-order exact treatment is hopeless, and an improved perturbative expansion must be found: hence resummation, which basically consists of a reorganization of the perturbative expansion by an all-order summation of classes of logs.

The idea of resummation should not sound completely new; in fact we have encountered another example of resummation when we have considered the solution of the renormalization group equation for the running coupling constant α_s Eq. (1.20). In the case of UV resummation we have to deal with single logs. In the case of soft-gluon resummation we have to deal with double logs, which originate because soft logs are usually accompanied by collinear logs. Complications arise because of the non-abelian nature of QCD; gluons carry colour charge and multiple gluon emission is affected by dynamical correlations.

2.2 Soft-gluon effects in QCD cross-sections

In this Section and in the next Section, we will introduce soft-gluon resummation by following a simplified approach [15, 16] which nevertheless emphasizes the key ideas which enable a determination of resummed expression. We consider a generic process where a system of invariant mass M is produced in a collision with centre of mass energy s . At the first order in α_s , the cross-section is affected by emission of virtual and real gluons, with emission probabilities given by

$$\frac{d\omega_{1,v}(z)}{dz} = -4A_1\alpha_s\delta(1-z)\int_0^{1-\xi} dz' \frac{\log(1-z')}{1-z'} \quad (2.1)$$

$$\frac{d\omega_{1,r}(z)}{dz} = 4A_1\alpha_s \frac{\log(1-z)}{1-z} \Theta(1-z-\xi), \quad (2.2)$$

where $1-z$ is the energy fraction carried by unobserved final state particles, where $z = M^2/\hat{s}$, and A_1 is process-dependent ($A_1 = C_F/\pi$ for the DY case and $A_1 = C_A/\pi$ for the Higgs case). As we have previously said, the combination of the bremsstrahlung spectrum and of the collinear spectrum leads to double-logs. The virtual term has the same kinematics of the LO cross-section, and thus contributes only on threshold, whereas the real contribution, which is singular as well in $z = 1$, is spread out in the whole interval $[\tau, 1]$ where τ is the energy fraction of the tagged final state, $\tau = M^2/s$.

In order to regularize the infrared divergences, we have introduced an unphysical cut-off ξ . Once the two contributions have been added, we can safely perform the physical limit $\xi \rightarrow 0$ and we thus obtain a finite emission probability:

$$\frac{d\omega_1(z)}{dz} = 4A_1\alpha_s \left(\frac{\log(1-z)}{1-z} \right)_+ . \quad (2.3)$$

If we integrate over z we finally obtain that the final leftover of infrared cancellation is therefore a double-logarithmic factor:

$$\int_{\tau}^1 dz \frac{d\omega_1(z)}{dz} = 2A_1\alpha_s \log^2(1-\tau). \quad (2.4)$$

In the elastic limit $\tau \rightarrow 1$, when the final state carries a large fraction of the total energy, a perturbative expansion become meaningless because when $\alpha_s \log^2(1-\tau) \sim 1$ all the terms in the perturbative series are of the same order, even if the coupling constant is small.

We can generalize our argument and convince ourselves that a generic partonic coefficient function $C(z, \alpha_s)$ is enhanced in the elastic limit $z \rightarrow 1$. To this purpose, we consider a quark parton line which emits n gluons. For each emission, the energy decreases by a factor $z = z_1 z_2 \dots z_n$ where $1 - z_i$ is the energy fraction carried by the i -th gluon. In the elastic limit, each gluon emission leads to an enhanced term in the partonic coefficient. In the end, we end up with a tower of terms which have the following form:

$$\alpha_s^n \left(\frac{\log^k(1-z)}{1-z} \right)_+, \quad 0 \leq k \leq an - 1, \quad (2.5)$$

where in general a is process-dependent. In particular, $a = 1$ for DIS and $a = 2$ for Drell-Yan and Higgs boson production. From now on, we will consider the latter case, and thus $a = 2$. The higher-order soft contributions of Eq. (2.5) produced by multiple soft radiation have to be resummed in order to achieve a reliable theoretical prediction.

One could ask when soft-gluon resummation is relevant for phenomenology. As we have seen, the inclusive cross-section (differential only in M) for the production of a system of a large mass M can be written in factorized form as

$$\begin{aligned} \frac{d\sigma}{dM^2} &= \sum_{ij} \int dx_i dx_j f_i^{(1)}(x_i, \mu) f_j^{(2)}(x_j, \mu) \times \hat{\sigma}_{ij}(M^2, \hat{s}, \mu, \alpha_s(\mu)) \\ &= \tau \sigma_0 \sum_{ij} \int \frac{dx_i}{x_i} \frac{dx_j}{x_j} f_i^{(1)}(x_i, \mu) f_j^{(2)}(x_j, \mu) \times C_{ij}(z, \mu, M^2, \alpha_s(\mu)) \\ &= \tau \sigma_0 \sum_{ij} \int_{\tau}^1 \frac{dz}{z} \mathcal{L}_{ij}\left(\frac{\tau}{z}\right) C_{ij}(z, \mu, M^2, \alpha_s(\mu)) \end{aligned} \quad (2.6)$$

where we have defined the *parton luminosity*

$$\mathcal{L}_{ij}(x) = \int_x^1 \frac{dy}{y} f_i^{(1)}\left(\frac{x}{y}, \mu\right) f_j^{(2)}(y, \mu) \quad (2.7)$$

and the sum runs over the flavour indexes i, j . We have introduced some conventional notation that we will use in the next Chapters:

$$\tau \equiv \frac{M^2}{s}, \quad z \equiv \frac{\tau}{x_i x_j} = \frac{M^2}{\hat{s}} \quad (2.8)$$

where $\hat{s} = x_i x_j s$; \sqrt{s} is the hadronic center-of-mass energy whereas $\sqrt{\hat{s}}$ is the partonic center-of-mass energy. We can then identify true threshold, $s \rightarrow M^2$, and partonic threshold, $x_i x_j s \rightarrow M^2$,

in the limits $\tau \rightarrow 1$ and $z \rightarrow 1$. We have understood how the partonic coefficient functions are enhanced when z get close to 1; this means that soft-gluon resummation becomes relevant when the partonic process is close to threshold. Hence soft-gluon resummation is also called threshold resummation.

When a system of high mass M^2 is produced, and thus τ tends to 1, the contribution to the cross-section Eq. (2.6) comes entirely from the threshold region. In this case, soft resummation is obviously necessary. Among the systems where we encounter such a behavior there are DIS, Drell-Yan processes where a very massive lepton pair of invariant mass M^2 is produced, production of heavy $q\bar{q}$ pairs and pairs of jets with large transverse momentum.

However, the relevance of resummation is determined by partonic kinematics, which can be quite different from hadronic kinematics. Therefore the effect of soft-gluon resummation can be relevant even relatively far from the hadronic threshold, since the hadronic cross-sections are found by convoluting a partonic cross-section with a parton luminosity. In particular, the effect of soft-gluon resummation is found to be not negligible for Drell-Yan production at hadron colliders.

Furthermore, it has to be noticed that the effect of soft resummation could be significant even when τ is small and the process is very far from threshold, as for example Higgs boson production at the LHC. This region is clearly perturbative; however, the size of the soft corrections depends in a non-trivial way on the shape of the parton distribution functions. For this reason, threshold resummation is expected to be relevant if the PDFs are peaked at small x . In this case it turns out that, partly because of the partonic kinematics, partly because of the cross-section shape, most of the cross-section is governed by the logarithmically enhanced terms.

2.3 Soft-gluon resummation and exponentiation in N -space

For the sake of simplicity, we omit the sum over parton subprocesses and we write perturbative QCD factorization as

$$\sigma(\tau, M^2) = \int_{\tau}^1 \frac{dz}{z} \mathcal{L}\left(\frac{\tau}{z}\right) C(z, M^2), \quad (2.9)$$

where we have defined a dimensionless cross-section as

$$\sigma(\tau, M^2) = \frac{1}{\tau \sigma_0} \frac{d\sigma}{dM^2} \quad (2.10)$$

by imposing that at the Born level the coefficient function at LO is simply $C(z, M^2) = \delta(1 - z)$. Without loss of generality, we choose $\mu_F^2 = \mu_R^2 = M^2$.

The physical basis for soft-gluon resummation relies on factorization. In particular, it is possible to prove that in the soft limit the n -gluon probability can be written in a factorized form:

$$\frac{d\omega_n(z_1, \dots, z_n)}{dz_1 \dots dz_n} \simeq \frac{1}{n!} \prod_{i=1}^n \frac{d\omega_1(z_i)}{dz_i}. \quad (2.11)$$

The proof, which is based on the *eikonal approximation*, is rather easy in QED, but is more cumbersome in a non-abelian theory like QCD, where the gluons are not neutral but carry color

charge instead. The coefficient function can be written as

$$C(z, M^2) = \delta(1 - z) + \sum_{n=1}^{\infty} \int_0^1 dz_1 \dots dz_n \frac{d\omega_n(z_1, \dots, z_n)}{dz_1 \dots dz_n} \delta(z - z_1 \dots z_n). \quad (2.12)$$

The presence of $\delta(z - z_1 \dots z_n)$ due to the longitudinal-momentum conservation spoils the factorization in Eq. (2.12). However, we can obtain a fully factorizable expression performing a *Mellin transform* and moving to N -space. We define the Mellin transform of a function $f(x)$ defined in the range $(0, 1)$ as

$$f(N) \equiv \mathcal{M}[f](N) \equiv \int_0^1 dx x^{N-1} f(x). \quad (2.13)$$

The Mellin transform is a Laplace transform where a change of variables have been performed. If $x = e^{-\xi}$,

$$\int_0^1 dx x^{N-1} f(x) = \int_0^{\infty} d\xi e^{-\xi N} f(x(\xi)). \quad (2.14)$$

The inverse Mellin transform is then

$$f(x) = \frac{1}{2\pi i} \int_{c-i\infty}^{c+i\infty} dN x^{-N} g(N), \quad (2.15)$$

where c is greater than the real part of the rightmost singularity. Under Mellin transform, the convolution product diagonalizes:

$$\begin{aligned} (f \otimes g)(N) &= \int_0^1 dx x^{N-1} \int_x^1 \frac{dy}{y} f(y) g\left(\frac{x}{y}\right) = \int_0^1 dx x^{N-1} \int_0^1 dy \int_0^1 dz f(y) g(z) \delta(x - yz) \\ &= \int_0^1 dy y^{N-1} f(y) \int_0^1 dz z^{N-1} g(z) = f(N) g(N). \end{aligned} \quad (2.16)$$

The cross-section Eq. (2.9) can consequently be written in N -space as

$$\sigma(N, M^2) = \int_0^1 d\tau \tau^{N-1} \sigma(\tau, M^2) = C(N, M^2) \mathcal{L}(N). \quad (2.17)$$

Upon Mellin transform, the n -particle longitudinal phase space factorizes:

$$\int_0^1 dz z^{N-1} \delta(z - z_1 \dots z_n) = z_1^{N-1} \dots z_n^{N-1}. \quad (2.18)$$

This means that in N -space the coefficient function is fully factorized and can be recast in exponential form:

$$\begin{aligned} C(N, M^2) &= 1 + \sum_{n=1}^{\infty} \int_0^1 dz_1 \dots dz_n \frac{d\omega_n(z_1, \dots, z_n)}{dz_1 \dots dz_n} z_1^{N-1} \dots z_n^{N-1} \\ &= 1 + \sum_{n=1}^{\infty} \frac{1}{n!} \int_0^1 dz_1 \frac{d\omega_1(z_1)}{dz_1} z_1^{N-1} \dots \int_0^1 dz_n \frac{d\omega_1(z_n)}{dz_n} z_n^{N-1} \end{aligned}$$

$$= \exp \left[\int_0^1 dz \, z^{N-1} \frac{d\omega_1(z)}{dz} \right] \quad (2.19)$$

In the large N limit, one can show that by inserting Eq. (2.3) in Eq. (2.19) the exponential reduces to the exponential of a double-log:

$$C(N, M^2) = \exp \left[4A_1 \alpha_s \int_0^1 dz \, z^{N-1} \frac{z^{N-1} - 1}{1 - z} \right] = \exp \left[2A_1 \alpha_s (\log^2 N + \mathcal{O}(N)) \right]. \quad (2.20)$$

In N -space the threshold region $z \sim 1$ corresponds to the large N region, and the tower of logs Eq. (2.5) converts into

$$\alpha_s^n \log^k \frac{1}{N}, \quad 0 \leq k \leq 2n. \quad (2.21)$$

However, in Eq. (2.20), only the highest power $k = 2n$ is resummed. The result we have obtained is said to hold at leading-logarithmic (LL) accuracy.

In this simplified presentation we have not taken into account running coupling effects. The argument in this form would be complete in QED, where it is called *Sudakov* resummation. Nevertheless, it shows that the physical basis for soft resummation are the factorization of the multi-gluon amplitudes, which follows from QCD dynamics, and the factorization of the phase space, which can take place only by working in N -space.

In order to correctly take into account the running of α_s , one must consider the longitudinal momenta of the gluons, which fix the energy scale of gluon emission. Taking into account the running coupling effects, the exponential Eq. (2.19) becomes

$$C(N, M^2) = \exp \left[\int_0^1 dz \, z^{N-1} 2A_1 \left(\frac{1}{1-z} \int_{M^2}^{(1-z)^2 M^2} \frac{d\mu^2}{\mu^2} \alpha_s(\mu^2) \right) \right]_+ \quad (2.22)$$

which reduces to the previous result when α_s is constant. The expression, however, is ill-defined; by integrating in z up to $z = 1$ at some point the coupling constant has to be evaluated in the non-perturbative region and hits the Landau pole. This singularity has thus to be properly regularized. The problem can be circumvented by expanding the integrand in powers of α_s , computing the Mellin transform of each term in the large- N limit and finally resumming the series, obtaining a finite result. However, we will see that the Landau pole problem will make a reappearance again.

Even if Eq. (2.22) includes the proper running coupling effects, it still holds only at LL accuracy. One can prove that the most general expression for the N -space resummed coefficient function is

$$C^{\text{res}}(N, M^2) = \bar{g}_0(\alpha_s) \exp \bar{\mathcal{S}} \left(M^2, \frac{M^2}{N^2} \right), \quad (2.23)$$

where the *Sudakov form factor* is

$$\bar{\mathcal{S}} \left(M^2, \frac{M^2}{N^2} \right) = \int_0^1 dz \, z^{N-1} \left[\frac{1}{1-z} \int_{M^2}^{M^2(1-z)^2} \frac{d\mu^2}{\mu^2} 2A(\alpha_s(\mu^2)) + D(\alpha_s([1-z]^2 M^2)) \right]_+, \quad (2.24)$$

log approx.	g_i up to	g_0 up to order	accuracy: $\alpha_s^n \log^k \frac{1}{N}$
LL	$i = 1$	$(\alpha_s)^0$	$k = 2n$
NLL	$i = 2$	$(\alpha_s)^1$	$2n - 2 \leq k = 2n$
NNLL	$i = 3$	$(\alpha_s)^2$	$2n - 4 \leq k = 2n$

Table 2.1: Orders of logarithmic approximations and accuracy of the predicted logarithms.

which reduces to Eq. (2.22) at LL accuracy. The functions $\bar{g}_0(\alpha_s)$, $A(\alpha_s)$ and $D(\alpha_s)$ are power series in α_s , with $\bar{g}_0(\alpha_s) = 1 + \mathcal{O}(\alpha_s)$. The functions $D(\alpha_s)$ and $\bar{g}_0(\alpha_s)$ are process-dependent, whereas $A(\alpha_s)$ is order by order the coefficient of the soft singularities in the Altarelli-Parisi splitting function for the relevant partonic process.

Using the notation of Ref. [9], the resummed coefficient function can be written in the form

$$C^{\text{res}}(N, M^2) = g_0(\alpha_s) \exp \mathcal{S}(\bar{\alpha}L, \bar{\alpha}) \quad (2.25)$$

$$\bar{\alpha} \equiv 2\beta_0\alpha, \quad L \equiv \log \frac{1}{N}, \quad (2.26)$$

where g_0 collects all the constant terms and can be written as

$$g_0(\alpha_s) = 1 + \sum_{j=1}^{\infty} g_{0j} \alpha_s^j, \quad (2.27)$$

and \mathcal{S} has a logarithmic expansion

$$\mathcal{S}(\bar{\alpha}L, \bar{\alpha}) = \frac{1}{\bar{\alpha}} g_1(\bar{\alpha}L) + g_2(\bar{\alpha}L) + \bar{\alpha} g_3(\bar{\alpha}L) + \bar{\alpha}^2 g_4(\bar{\alpha}L) + \dots \quad (2.28)$$

The functions g_i can be obtained performing the integrals Eq. (2.25), and they are determined by a small number of coefficients of the expansion of the functions A and D , and are of order $g_1(\bar{\alpha}L) = \mathcal{O}(\alpha_s^2)$, $g_i(\bar{\alpha}L) = \mathcal{O}(\alpha_s)$ for $i > 1$. We note that the functions g_0 and \mathcal{S} do not coincide with the functions \bar{g}_0 and $\bar{\mathcal{S}}$ since by definition \mathcal{S} does not contain not logarithmically enhanced terms and g_0 includes non-logarithmic contribution both from \bar{g}_0 and from $\bar{\mathcal{S}}$.

If contributions up to g_n are included in \mathcal{S} , $\log C^{\text{res}}(N, M^2)$ is determined up to $\mathcal{O}(\alpha_s^{k+(n-1)} L^k)$ subleading corrections. In order to achieve the exact predictions of all the coefficients of the logarithms it is mandatory to include up to the relevant order the function g_0 , because of its interference with the logarithmically enhanced contributions. In particular, at the next^k-to-leading logarithmic (N^kLL) accuracy it is necessary to include functions up to g_{k+1} and compute g_0 up to order α_s^k . At LL accuracy only the largest power of $\log \frac{1}{N}$ are correctly predicted; by adding one order in each of the functions g_i , g_0 the NLL accuracy, which predicts two powers more, is achieved, and so on. We show in Tab. 2.1 the order up to which the expansion of g_0 and g_i should be included in order to get a given logarithmic accuracy and the terms which are correctly predicted. Consider for example the result at NLL accuracy. We can write

$$g_k(\lambda) = (2\beta_0)^{2-k} \sum_{j=1}^{\infty} g_{kj} \left(\frac{\lambda}{2\beta_0} \right)^j, \quad g_{11} = 0. \quad (2.29)$$

log approx.	$A(\alpha_s)$	$D(\alpha_s)$	$\bar{g}_0(\alpha_s)$	accuracy: $\alpha_s^n \log^k \frac{1}{N}$
LL	1-loop	—	tree-level	$k = 2n$
NLL*	2-loop	1-loop	tree-level	$2n - 1 \leq k \leq 2n$
NLL	2-loop	1-loop	1-loop	$2n - 2 \leq k \leq 2n$
NNLL*	3-loop	2-loop	1-loop	$2n - 3 \leq k \leq 2n$
NNLL	3-loop	2-loop	2-loop	$2n - 4 \leq k \leq 2n$

Table 2.2: Orders of logarithmic approximations and accuracy of the predicted logarithms for the $N^k\text{LL}$ and the $N^k\text{LL}^*$ counting. The last columns refers to the coefficient function.

If we expand C^{res} in powers of α_s , we obtain

$$\begin{aligned}
C^{\text{res}}(N, \alpha_s) = & 1 + \alpha_s [g_{12}L^2 + g_{21}L + g_{01}] \\
& + \alpha_s^2 \left[\frac{g_{12}^2}{2}L^4 + (g_{12}g_{21} + g_{13})L^3 + \left(\frac{g_{21}^2}{2} + g_{22} + g_{12}g_{01} \right) L^2 + \mathcal{O}(L) \right] \\
& + \mathcal{O}(\alpha_s^3).
\end{aligned} \tag{2.30}$$

As expected, the order α_s and the coefficients of the powers $k = 4, 3, 2$ of L at order α_s^2 depend only on the NLL contributions g_1 , g_2 and g_{01} .

We emphasize that the functions g_i depend on a few coefficients of the expansion of the functions A and D ; g_1 depends on the coefficient A_1 previously introduced, and g_2 on a couple of other coefficients. In particular, the function A is fully determined by the Altarelli-Parisi anomalous dimension. It is therefore necessary to compute the $N^p\text{LO}$ anomalous dimension in order to compute g_{p+1} , which is necessary for the result with $N^p\text{LL}$ accuracy. On the other hand, the process-dependent functions can be fixed by matching the expansion of the resummed coefficient function in α_s with a fixed order computation. In conclusion, in order to obtain LL, NLL, NNLL accuracy it is necessary to know the GLAP anomalous dimension respectively at 1, 2, 3 loop, whereas the fixed order expressions at NLO and NNLO are needed for NLL and NNLL accuracy.

It has been pointed out that if one exponentiates g_0 (or equivalently \bar{g}_0) and then performs the power counting at the level of exponent it may be more natural to include one order less in g_0 . However, this decreases the logarithmic accuracy of the coefficient function by half of a logarithmic order; for example, the coefficient of L^2 at order α_s^2 in Eq. (2.30) is not correctly predicted without g_{01} . This is sometimes called $N^k\text{LL}^*$ accuracy. For phenomenology it is often more convenient to examine the accuracy of the predicted logarithms by considering the functions $A(\alpha_s)$, $D(\alpha_s)$ and $\bar{g}_0(\alpha_s)$ in Eq. (2.24). A summary for the first orders both for the $N^k\text{LL}$ and the $N^k\text{LL}^*$ counting is given in Tab. 2.2.

Correct predictions for phenomenology with $N^p\text{LO}+N^k\text{LL}$ accuracy are obtained by combining the resummed coefficient function expanded in powers of α_s with the fixed-order coefficient function and then subtracting the double-counting terms:

$$C_{N^k\text{LL}}^{N^p\text{LO}}(N, \alpha_s) = \sum_{j=0}^p \alpha_s^j C^{(j)}(N) + C_{N^k\text{LL}}^{\text{res}}(N, \alpha_s) - \sum_{j=0}^p \frac{\alpha_s^j}{j!} \left[\frac{d^j C_{N^k\text{LL}}^{\text{res}}(N, \alpha_s)}{d\alpha_s^j} \right]_{\alpha_s=0}. \tag{2.31}$$

2.4 Soft gluon resummation and renormalization group approach

In the previous Sections we have present a simplified discussion of the resummation mechanism, which however has shed light on the fundamental ideas which allow for a determination of resummed expressions for physical observables.

Exponentiation formulae have been obtained first at LO and subsequently extended at NLO by recurring to eikonal [9] or factorization [8] techniques. The exponentiation of soft logs related to gluon emission has been then proved at all orders in [10, 11]. In all these approaches soft-gluon resummation is performed in N -space, after the Mellin transformation of the cross-section which factorizes into the product of a partonic cross-section and a parton luminosity Eq. (2.17). More recently threshold resummation was based on direct diagrammatic analysis in Refs. [17, 18]. In the latter approach factorization and resummation are performed without the need of a Mellin transform by recurring to path-integral methods.

A complete review of these proofs is beyond the scope of this Thesis. In this Section we present a simple proof of all-order soft-logarithms exponentiation in QCD by following the argument presented in [11]. The result is essentially based on kinematics arguments and renormalization-group techniques.

For the sake of simplicity, we will consider a DIS-like process. We consider the total cross-section $\sigma(x, Q^2)$ in the vicinity of the kinematic boundary $x = 1$. Let $\sigma(N, Q^2)$ be its Mellin transform which can be written in factorized form as

$$\sigma(N, Q^2) = C \left(N, \frac{Q^2}{\mu^2}, \alpha_s(\mu^2) \right) F(N, \mu^2) \quad (2.32)$$

where $F(N, \mu^2)$ are Mellin moments of parton densities $F(x, \mu^2)$. In the case of Drell-Yan process or Higgs production Eq. (2.32) should be appropriately modified in order to take into account that there are two partons in the initial state. Since resummation takes the form of an exponentiation, it is convenient to introduce the physical anomalous dimension, which is defined as the log-derivative of the cross-section

$$Q^2 \frac{\partial \sigma(N, Q^2)}{\partial Q^2} = \gamma(N, \alpha_s(Q^2),) \sigma(N, Q^2). \quad (2.33)$$

We can thus write the cross-section as

$$\sigma(N, Q^2) = \exp[E(N, Q_0^2, Q^2)] \sigma(N, Q_0^2) \quad (2.34)$$

with

$$E(N, Q_0^2, Q^2) = \int_{Q_0^2}^{Q^2} \frac{dk^2}{k^2} \gamma(N, \alpha_s(k^2)). \quad (2.35)$$

We observe that by comparison of Eq. (2.33) and Eq. (2.32)

$$\gamma(N, \alpha_s(Q^2)) = \frac{\partial}{\partial \log Q^2} \log C \left(N, \frac{Q^2}{\mu^2}, \alpha_s(\mu^2) \right). \quad (2.36)$$

The only assumption we make is the validity of the standard factorization Eq. (2.32). This means that the coefficient function can be multiplicatively renormalized. We can therefore

remove all the divergences from the so-called bare coefficient function $C^{(0)}(N, Q^2, \alpha_0, \epsilon)$ by introducing a process-independent factor Z_C

$$C\left(N, \frac{Q^2}{\mu^2}, \alpha_s(\mu^2), \epsilon\right) = Z_C(N, \alpha_s(\mu^2), \epsilon) C^{(0)}(N, Q^2, \alpha_0, \epsilon) \quad (2.37)$$

such that the renormalized coefficient function is finite at $\epsilon = 0$ since the multiple poles in Z_C cancel out the infinities of the bare coefficient function. We have introduced a renormalized coupling constant $\alpha_s(\mu^2)$ which is related to the bare coupling constant α_0 by the implicit equation

$$\alpha_0(\mu^2, \alpha_s(\mu^2), \epsilon) = \mu^{2\epsilon} \alpha_s(\mu^2) Z_\alpha(\alpha_s(\mu^2), \epsilon). \quad (2.38)$$

Both Z_α and Z_C are computable in perturbation theory and are Q^2 -independent with a convenient choice of the factorization scheme (such as the $\overline{\text{MS}}$ scheme). Therefore the physical anomalous dimension is, according to Eq. (2.33)

$$\begin{aligned} \gamma &= \frac{\partial}{\partial \log Q^2} \log C^{(0)}(N, Q^2, \alpha_0, \epsilon) \\ &= -\epsilon \alpha_0 \frac{\partial}{\partial \alpha_0} \log C^{(0)}(N, Q^2, \alpha_0, \epsilon). \end{aligned} \quad (2.39)$$

When we have derived Eq. (2.39) we have taken into account the fact that for dimensional reason the dependence on Q^2 of the bare coefficient function is through the combination $\alpha_0 Q^{-2\epsilon}$.

In order to obtain a resummed expression for the physical anomalous dimension it is necessary to understand the structure of the bare coefficient function in N -space. The bare coefficient function and its Mellin transform can be expanded in powers of the bare coupling constant α_0 :

$$C^{(0)}(x, Q^2, \alpha_0, \epsilon) = \sum_{n=0}^{\infty} \alpha_0^n C_n^{(0)}(x, Q^2, \epsilon) \quad (2.40)$$

$$C^{(0)}(N, Q^2, \alpha_0, \epsilon) = \sum_{n=0}^{\infty} \alpha_0^n C_n^{(0)}(N, Q^2, \epsilon). \quad (2.41)$$

The main result of [11], which we will not prove here, consists in showing first that the N -dependence of the bare coefficient function is determined by the kinematic structure of the k -particle phase space at tree-level, and secondly that loop integrations do not affect this result. One first proves that

$$C_n^{(0)}(x, Q^2, \epsilon) = (Q^2)^{-n\epsilon} \left[C_{n0}^{(0)}(\epsilon) \delta(1-x) + \sum_{k=1}^n \frac{C_{nk}^{(0)}(\epsilon)}{\Gamma(-ak\epsilon)} (1-x)^{-1-ak\epsilon} \right] + \mathcal{O}[(1-x)^0] \quad (2.42)$$

where we have denoted by $\mathcal{O}[(1-x)^0]$ terms which are not divergent as $x \rightarrow 1$ when ϵ tends to 0, and $a = 1$ for DIS, where Q^2 is the virtuality of the exchanged boson, and $a = 2$ for DY or Higgs boson production processes, where the hard scale Q is the invariant mass of the final state. Since

$$\int_0^1 dx x^{N-1} (1-x)^{-1-ak\epsilon} = \frac{\Gamma(N) \Gamma(-ak\epsilon)}{\Gamma(N-ak\epsilon)} = \Gamma(-ak\epsilon) N^{ak\epsilon} + \mathcal{O}(1/N), \quad (2.43)$$

whereas the Mellin transform of any function of x which is not divergent as $x \rightarrow 1$ vanishes in the large N limit, one has

$$C_n^{(0)}(N, Q^2, \epsilon) = \sum_{k=0}^n C_{nk}^{(0)}(\epsilon) (Q^2)^{-(n-k)\epsilon} \left(\frac{Q^2}{N^a} \right)^{-k\epsilon} + \mathcal{O}(1/N). \quad (2.44)$$

Furthermore, one can see that the coefficients $C_{nk}^{(0)}$ have a pole of order $2n$ in ϵ . These poles are related to infrared singularities, and despite the fact that they cancel in the coefficient function, their interference with the powers of ϵ in the series expansion of $N^{-\epsilon}$ leads to powers of $\log N$ in $\sigma(N, Q^2)$ (which are related to powers of $\log(1-x)$ under Mellin transform). The presence of soft logs is therefore a consequence of an incomplete cancellation of real and virtual contributions to $C_n^{(0)}$ in the soft limit.

We can conclude that when $N \rightarrow \infty$, the regularized cross-section depends on N only through integer powers of a dimensionful variable $(Q/N^a)^{-\epsilon}$. The fact that the coupling constant in d dimension has the dimensions of $Q^{2\epsilon}$ relates the dependence of $(Q/N^a)^{-\epsilon}$ to the running of the coupling through the renormalization group. We will see how this fact is sufficient in order to prove all-order resummation.

From Eq. (2.44) and Eq. (2.39) we get

$$\begin{aligned} \gamma(N, Q^2, \alpha_0, \epsilon) &= \sum_{i=1}^{\infty} \alpha_0^i \sum_{j=0}^i \gamma_{ij}(\epsilon) (Q^2)^{-(i-j)\epsilon} \left(\frac{Q^2}{N^a} \right)^{-j\epsilon} + \mathcal{O}(1/N) \\ &= \sum_{i=1}^{\infty} \sum_{j=0}^i \gamma_{ij}(\epsilon) [(Q^2)^{-\epsilon} \alpha_0]^{i-j} \left[\left(\frac{Q^2}{N^a} \right)^{-\epsilon} \alpha_0 \right]^j + \mathcal{O}(1/N), \end{aligned} \quad (2.45)$$

which is a power series with N -independent coefficients. It is possible to obtain a renormalized expression of the physical anomalous dimension by expressing the bare coupling in terms of the renormalized bare coupling. It is convenient to introduce the function

$$\begin{aligned} \bar{\alpha}_0 \left(\frac{Q^2}{\mu^2}, \alpha_s(\mu^2), \epsilon \right) &= Q^{-2\epsilon} \alpha_0(\mu^2, \alpha_s(\mu^2), \epsilon) \\ &= \left(\frac{Q^2}{\mu^2} \right)^{-\epsilon} \alpha_s(\mu^2) Z_{\alpha_s}(\alpha_s(\mu^2), \epsilon). \end{aligned} \quad (2.46)$$

which is invariant under renormalization group transform:

$$\frac{d\bar{\alpha}_0}{d \log \mu^2} = 0. \quad (2.47)$$

In particular, when $\mu = Q$,

$$\bar{\alpha}_0 \left(\frac{Q^2}{\mu^2}, \alpha_s(\mu^2), \epsilon \right) = \bar{\alpha}_0(1, \alpha_s(Q^2), \epsilon) = \alpha_s(Q^2) Z_{\alpha_s}(\alpha_s(Q^2), \epsilon). \quad (2.48)$$

We can therefore write the renormalized anomalous dimension as

$$\gamma \left(N, \frac{Q^2}{\mu^2}, \alpha_s(\mu^2), \epsilon \right) = \sum_{i=1}^{\infty} \sum_{j=0}^i \gamma_{ij}(\epsilon) [\bar{\alpha}_0(1, \alpha_s(Q^2), \epsilon)]^{i-j} \left[\bar{\alpha}_0 \left(1, \alpha_s \left(\frac{Q^2}{N^a} \right), \epsilon \right) \right]^j + \mathcal{O}(1/N)$$

$$= \sum_{m=1}^{\infty} \sum_{n=0}^m \gamma_{mn}^R(\epsilon) \alpha_s^{m-n}(Q^2) \alpha_s^n \left(\frac{Q^2}{N^a} \right) + \mathcal{O}(1/N) \quad (2.49)$$

where the coefficients γ_{mn}^R depends on $\gamma_{ij}(\epsilon)$ and Z_{α_s} . The fact that the physical anomalous dimension is finite as $\epsilon \rightarrow 0$ however does not imply that it admits an expansion of the same form of Eq. (2.49) since the coefficients $\gamma_{mn}^R(\epsilon)$ might not be finite in the $\epsilon \rightarrow 0$ limit. In order to obtain an expression for the four-dimensional physical anomalous dimensions in terms of finite quantities it is convenient to separate the N -independents terms in Eq. (2.49) ($n = 0$) from the N -dependent terms ($n > 0$) by defining

$$\begin{aligned} \hat{\gamma}^{(l)} \left(\alpha_s(Q^2), \alpha_s \left(\frac{Q^2}{N^a} \right), \epsilon \right) &\equiv \sum_{i=1}^{\infty} \sum_{j=1}^i \gamma_{ij}(\epsilon) [\bar{\alpha}_0(1, \alpha_s(Q^2), \epsilon)]^{i-j} \left[\bar{\alpha}_0 \left(1, \alpha_s \left(\frac{Q^2}{N^a} \right), \epsilon \right) \right]^j \\ &= \sum_{m=0}^{\infty} \sum_{n=1}^{\infty} \gamma_{m+n,n}^R(\epsilon) \alpha_s^m(Q^2) \alpha_s^n \left(\frac{Q^2}{N^a} \right) \end{aligned} \quad (2.50)$$

and

$$\begin{aligned} \hat{\gamma}^{(c)}(\alpha_s(Q^2), \epsilon) &\equiv \sum_{i=1}^{\infty} \gamma_{i0}(\epsilon) [\bar{\alpha}_0(1, \alpha_s(Q^2), \epsilon)]^i \\ &= \sum_{m=1}^{\infty} \gamma_{m0}^R(\epsilon) \alpha_s^m(Q^2) \end{aligned} \quad (2.51)$$

such that

$$\gamma \left(N, \frac{Q^2}{\mu^2}, \alpha_s(\mu^2), \epsilon \right) = \hat{\gamma}^{(l)} \left(\alpha_s(Q^2), \alpha_s \left(\frac{Q^2}{N^a} \right), \epsilon \right) + \hat{\gamma}^{(c)}(\alpha_s(Q^2), \epsilon) + \mathcal{O}(1/N). \quad (2.52)$$

Eq. (2.52) implies that, though $\hat{\gamma}^{(l)}$ and $\hat{\gamma}^{(c)}$ might not separately be finite in the $\epsilon \rightarrow 0$, they can be made finite by adding an appropriate counterterm Z_{γ} :

$$\gamma^{(l)} \left(\alpha_s(Q^2), \alpha_s \left(\frac{Q^2}{N^a} \right), \epsilon \right) = \hat{\gamma}^{(l)} \left(\alpha_s(Q^2), \alpha_s \left(\frac{Q^2}{N^a} \right), \epsilon \right) - Z_{\gamma}(\alpha_s(Q^2), \epsilon), \quad (2.53)$$

$$\gamma^{(c)}(\alpha_s(Q^2), \epsilon) = \hat{\gamma}^{(c)}(\alpha_s(Q^2), \epsilon) + Z_{\gamma}(\alpha_s(Q^2), \epsilon) \quad (2.54)$$

where now $\gamma^{(l)}$ and $\gamma^{(c)}$ have a finite $\epsilon \rightarrow 0$ limit. The counterterm has to be N -independent since $\hat{\gamma}^{(c)}$ is N -independent. A particularly convenient choice is

$$Z_{\gamma}(\alpha_s(Q^2), \epsilon) = \hat{\gamma}^{(l)}(\alpha_s(Q^2), \alpha_s(Q^2), \epsilon). \quad (2.55)$$

With this choice $\gamma^{(l)}$ vanishes for $N = 1$ (and therefore is finite), but thanks to the N -independence of the counterterm this holds for any N . This means that a different choice of the counterterm consists in a redefinition of the finite part, which is therefore a mere reshuffle of the finite N -independent term in $\gamma^{(l)}$ and $\gamma^{(c)}$. With the peculiar choice Eq. (2.55) $\gamma^{(l)}$ is purely logarithmic; in fact it vanishes at $N = 1$, where $\log N = 0$. With this choice

$$\gamma^{(l)} \left(\alpha_s(Q^2), \alpha_s \left(\frac{Q^2}{N^a} \right), \epsilon \right) = \hat{\gamma}^{(l)} \left(\alpha_s(Q^2), \alpha_s \left(\frac{Q^2}{N^a} \right), \epsilon \right) - \hat{\gamma}^{(l)}(\alpha_s(Q^2), \alpha_s(Q^2), \epsilon), \quad (2.56)$$

$$\gamma^{(c)}(\alpha_s(Q^2), \epsilon) = \hat{\gamma}^{(c)}(\alpha_s(Q^2), \epsilon) + \hat{\gamma}^{(l)}(\alpha_s(Q^2), \alpha_s(Q^2), \epsilon), \quad (2.57)$$

and the physical anomalous dimension is thus

$$\begin{aligned} \gamma\left(N, \frac{Q^2}{\mu^2}, \alpha_s(\mu^2), \epsilon\right) &= \gamma^{(l)}\left(\alpha_s(Q^2), \alpha_s\left(\frac{Q^2}{N^a}\right), \epsilon\right) + \gamma^{(c)}(\alpha_s(Q^2), \epsilon) + \mathcal{O}(1/N) \\ &= \gamma^{(l)}\left(\alpha_s(Q^2), \alpha_s\left(\frac{Q^2}{N^a}\right), \epsilon\right) + \mathcal{O}(N^0). \end{aligned} \quad (2.58)$$

Now both $\gamma^{(l)}$ and $\gamma^{(c)}$ are finite in the $\epsilon \rightarrow 0$ limit. The function $\gamma^{(l)}$ provides an expression of the resummed physical anomalous dimension up to non-logarithmic in the large N limit. The choice Eq. (2.55) let us notice that

$$\gamma^{(l)}\left(\alpha_s(Q^2), \alpha_s\left(\frac{Q^2}{N^a}\right), \epsilon\right) = \int_1^{N^a} \frac{dn}{n} g\left(\alpha_s(Q^2), \alpha_s\left(\frac{Q^2}{n}\right), \epsilon\right) \quad (2.59)$$

where we have defined

$$\begin{aligned} g(\alpha_s(Q^2), \alpha_s(\mu^2), \epsilon) &\equiv -\frac{\partial}{\partial \log \mu^2} \hat{\gamma}^{(l)}(\alpha_s(Q^2), \alpha_s(\mu^2), \epsilon) \\ &= -\beta^{(d)}(\alpha_s(\mu^2), \epsilon) \frac{\partial}{\partial \alpha_s(\mu^2)} \hat{\gamma}^{(l)}(\alpha_s(Q^2), \alpha_s(\mu^2), \epsilon), \end{aligned} \quad (2.60)$$

where $\beta^{(d)}$ is the d -dimensional beta function, defined as

$$\begin{aligned} \frac{\partial}{\partial \log \mu^2} \alpha_s(\mu^2) &\equiv \beta^{(d)}(\alpha_s(\mu^2), \epsilon) \\ &= -\epsilon \alpha_s(\mu^2) + \beta(\alpha_s(\mu^2)). \end{aligned} \quad (2.61)$$

It follows that

$$g(\alpha_s(Q^2), \alpha_s(\mu^2), \epsilon) = \sum_{m=0}^{\infty} \sum_{n=1}^{\infty} g_{mn}(\epsilon) \alpha_s^m(Q^2) \alpha_s^n(\mu^2). \quad (2.62)$$

We have therefore obtained that the resummed physical anomalous dimension is

$$\gamma^{\text{res}}(N, \alpha_s(k^2)) = \int_1^{N^a} \frac{dn}{n} g\left(\alpha_s(k^2), \alpha_s\left(\frac{k^2}{n}\right)\right) + \mathcal{O}(N^0) \quad (2.63)$$

$$g\left(\alpha_s(k^2), \alpha_s\left(\frac{k^2}{n}\right)\right) = \sum_{m=0}^{\infty} \sum_{n=1}^{\infty} g_{mn} \alpha_s^m(k^2) \alpha_s^n\left(\frac{k^2}{n}\right); \quad g_{11} = 0. \quad (2.64)$$

The coefficients g_{mn} can be obtained by comparing the resummed result with the fixed-order expressions. In the $N^{k-1}\text{LL}$ approximation it is necessary to know all the $\frac{k(k+1)}{2}$ coefficients g_{mn} with $n+m \leq k$, and thus [12] a full $N^{2k-1}\text{LO}$ fixed-order calculation is needed.

The result obtained coincides with the all-order resummation obtained in [10] but it is less predictive, since in [10] one assumes the validity of a factorization formula more restrictive than

Eq. (2.32). In the latter approach in fact the coefficient function is written in the large N limit as

$$C\left(N, \frac{Q^2}{\mu^2}, \alpha_s(\mu^2)\right) = C^{(l)}\left(\frac{Q^2}{\mu^2 N^a}, \alpha_s(\mu^2)\right) C^{(c)}\left(\frac{Q^2}{\mu^2}, \alpha_s(\mu^2)\right), \quad (2.65)$$

which implies that the bare coefficient function is therefore

$$C^{(0)}(N, Q^2, \alpha_0, \epsilon) = C^{(0,l)}\left(\frac{Q^2}{N^a}, \alpha_0, \epsilon\right) C^{(0,c)}(Q^2, \alpha_0, \epsilon). \quad (2.66)$$

It follows that the the physical anomalous dimension has the form

$$\gamma\left(N, \frac{Q^2}{\mu^2}, \alpha_s(\mu^2), \epsilon\right) = \gamma^{(l)}\left(\frac{Q^2}{\mu^2 N^a}, \alpha_s(\mu^2), \epsilon\right) + \gamma^{(c)}\left(\frac{Q^2}{\mu^2}, \alpha_s(\mu^2), \epsilon\right), \quad (2.67)$$

where $\gamma^{(l)}$ depends on $\alpha_s\left(\frac{Q^2}{N^a}\right)$ only. If one follows the lines of the proof above, one obtains that $g = g(\alpha_s(\mu^2), \epsilon)$, i.e. only the terms with $m = 0$ in Eq. (2.64) are left. Therefore the knowledge of the first k coefficients (which corresponds to a N^k LO calculation) is sufficient in order to obtain the N^{k-1} LL approximation. Eq. (2.66) is satisfied if and only if the coefficients $C_n^{(0)}(\epsilon)$ have the following structure in the large N limit:

$$C_n^{(0)}(\epsilon) = \sum_{k=0}^n F_k(\epsilon) G_{n-k}(\epsilon) (Q^2)^{-(n-k)\epsilon} \left(\frac{Q^2}{N^a}\right)^{-k\epsilon}. \quad (2.68)$$

It was shown in [13] that the validity of the factorization Eq. (2.66) holds for different process at various perturbative orders. However, an all-order proof of the validity of Eq. (2.68) is not yet available.

We can finally cast the results Eq. (2.63,2.64) in x -space, thanks to the relation between leading $\log \frac{1}{N}$ and leading $\log(1-x)$ resummation:

$$\gamma^{\text{res}}(N, \alpha_s(k^2)) = \int_0^1 dx x^{N-1} P^{\text{res}}(x, \alpha_s(k^2)) + \mathcal{O}(N^0) \quad (2.69)$$

$$P^{\text{res}}(x, \alpha_s(k^2)) \equiv \left[\frac{\hat{g}(\alpha_s(k^2), \alpha_s(k^2(1-x)^a))}{1-x} \right]_+ \quad (2.70)$$

$$\hat{g}(\alpha_s(k^2), \alpha_s(\mu^2)) = - \sum_{p=0}^{\infty} \frac{\Delta^{(p)}(1) a^p}{p!} \frac{d^p}{d \log^p \mu^2} g(\alpha_s(k^2), \alpha_s(\mu^2)), \quad (2.71)$$

where we have defined

$$\Delta(p) \equiv \frac{1}{\Gamma(p)}. \quad (2.72)$$

It is therefore possible to compute the resummed evolution factor $K^{\text{res}}(N; Q_0^2, Q^2)$ defined by

$$\begin{aligned} K^{\text{res}}(N; Q_0^2, Q^2) &= \exp[E^{\text{res}}(N, Q_0^2, Q^2)] \\ &= \exp \int_{Q_0^2}^{Q^2} \frac{dk^2}{k^2} \gamma^{\text{res}}(N, \alpha_s(k^2)). \end{aligned} \quad (2.73)$$

It is possible to obtain resummed expression for the coefficient function and anomalous dimension in any factorization scheme from Eq. (2.73). In particular, it is shown in Ref. [11] that the resummed coefficient function can be brought in the form of Eq. (2.25).

2.5 The Landau pole

We can rewrite [19] the resummed expression of the physical anomalous dimension Eq. (2.63) as

$$\gamma^{\text{res}}(N, \alpha_s(Q^2)) = \int_1^N \frac{dn}{n} \sum_{k=1}^{\infty} g_k \alpha_s^k \left(\frac{Q^2}{n} \right) + \mathcal{O}(N^0) \quad (2.74)$$

where the constants g_k can be determined by matching with fixed-order expression and we have neglected N -independent or power-suppressed terms. Without loss of generality, we have taken $a = 1$. The resummed expression of the physical anomalous dimension is necessary in order to obtain the resummed Mellin transform of the cross section $\sigma(N, Q^2)$. The physical cross section $\sigma(x, Q^2)$ can finally be calculated by inverting the Mellin transform. The resummed result Eq. (2.63) depends on N through the rescaled coupling $\alpha_s \left(\frac{Q^2}{N} \right)$. This means that $\gamma^{\text{res}}(N, \alpha_s(Q^2))$ and equivalently $\sigma(N, Q^2)$ have a branch cut along the real positive axis for $N > N_L$, where N_L is the location of the Landau pole in N -space:

$$N_L = \frac{Q^2}{\Lambda^2}. \quad (2.75)$$

As a consequence, $\sigma(N, Q^2)$ is not the Mellin transform of $\sigma(x, Q^2)$; in fact a Mellin transform always has a convergence abscissa, i.e. it is an analytic function in the half-plane $\Re(N) > c$, where c is a real constant.

For the sake of simplicity, let us consider the resummed physical anomalous dimension at LL accuracy:

$$\begin{aligned} \gamma_{LL}(N, \alpha_s(Q^2)) &= g_1 \int_1^N \frac{dn}{n} \alpha_s \left(\frac{Q^2}{n} \right) \\ &= -\frac{g_1}{\beta_0} \log \left(1 + \beta_0 \alpha_s(Q^2) \log \frac{1}{N} \right) \end{aligned} \quad (2.76)$$

where we have used the LL expression of α_s Eq. (1.18). We notice that the the LL expression of $\gamma(N, \alpha_s(Q^2))$ has a branch cut for $N \geq N_L$, which

$$N_L \equiv \exp \left(\frac{1}{\beta_0 \alpha_s(Q^2)} \right). \quad (2.77)$$

On the other hand, one can consider any finite truncation of the series expansion

$$\gamma_{LL}(N, \alpha_s(Q^2)) = \sum_{k=0}^{\infty} \alpha_s^k(Q^2) \gamma_k(N), \quad (2.78)$$

which is free of singularities for N large enough. The resummed expression in x space can be constructed as

$$P_{LL}(x, \alpha_s(Q^2)) = \sum_{k=0}^{\infty} \alpha_s^k P_k(x), \quad (2.79)$$

where the coefficients are computed as the inverse Mellin transform of the series expansion in N space:

$$P_k(x) = \mathcal{M}^{-1}[\gamma_k(N)](x). \quad (2.80)$$

In particular, one obtains

$$P_{LL}(x, \alpha_s(Q^2)) = - \lim_{k \rightarrow \infty} \frac{g_1}{\beta_0} \sum_{k=1}^K \frac{(-1)^{k+1}}{k} \beta_0^k \alpha_s^k(Q^2) \times \frac{1}{2\pi i} \int_{\bar{N}-i\infty}^{\bar{N}+i\infty} dN x^{-N} \log^k \frac{1}{N}, \quad \bar{N} > 0. \quad (2.81)$$

The series Eq. (2.81), however, does not converge. If it did converge, it would be possible to interchange the sum and the integral, but the sum

$$\frac{(-1)^{k+1}}{k} \beta_0^k \alpha_s^k(Q^2) \log \frac{1}{N} \quad (2.82)$$

is convergent for

$$\left| \beta_0 \alpha_s(Q^2) \log \frac{1}{N} \right| < 1, \quad (2.83)$$

whereas the integral involves values of N which are not in this range. However, if the inverse Mellin transform is taken at finite logarithmic accuracy, the perturbative series converges. In the LL case,

$$\frac{1}{2\pi i} \int_{\bar{N}-i\infty}^{\bar{N}+i\infty} dN x^{-N} \log^k \frac{1}{N} = k \left[\frac{\log^{k-1}(1-x)}{1-x} \right]_+ + \text{NLL}, \quad (2.84)$$

and therefore

$$\begin{aligned} P_{LLx}(x, \alpha_s(Q^2)) &= -g_1 \left[\frac{1}{1-x} \frac{\alpha_s(Q^2)}{1 + \beta_0 \alpha_s(Q^2) \log(1-x)} \right]_+ \\ &= -g_1 \left[\frac{\alpha_s(Q^2(1-x))}{1-x} \right]_+, \end{aligned} \quad (2.85)$$

where the scale Q^2 is replaced by $Q^2(1-x)$. Eq. (2.85) is convergent for

$$x < x_L \equiv 1 - \frac{\Lambda^2}{Q^2}. \quad (2.86)$$

Similar arguments apply to the expression of the resummed coefficient function Eq. (2.23); in particular, the series

$$C^{\text{res}}(z, \alpha_s) = \sum_{k=0} \alpha_s^k C_k^{\text{res}}(z) \quad (2.87)$$

acquires a nonzero convergence radius if the term-by-term inverse Mellin transform of

$$C^{\text{res}}(N, \alpha_s) = \sum_{k=0} \alpha_s^k C_k^{\text{res}}(N) \quad (2.88)$$

is performed at the relevant logarithmic level. Nevertheless, the convolution integral Eq. (2.9) extends to the region above the Landau pole where the series diverges. It is therefore necessary a definition of what these divergent series mean. We now introduce two prescriptions which provide resummed expressions to which the divergent series is asymptotic.

2.6 Minimal prescription

A simple solution in order to handle the Landau pole problem was first presented in Ref. [20]. The resummed hadronic cross-section could formally be written as a power expansion

$$\frac{1}{\tau\sigma_0} \frac{d\sigma}{dM^2} = \frac{1}{2\pi i} \sum_{k=0}^{\infty} \alpha_s^k \int_{c-i\infty}^{c+i\infty} dN \tau^{-N} \mathcal{L}(N) C_k^{\text{res}}(N) \quad (2.89)$$

with well-defined coefficients computed as the exact Mellin transform of the coefficients of the series in z space Eq. (2.87). However, as we have seen, the series Eq. (2.89) is not convergent because of the presence of the Landau pole. Equivalently, it is not possible to construct the hadronic cross-section as the inverse Mellin transform of the product of the N -space parton luminosity and coefficient function since in the integral

$$\frac{1}{\tau\sigma_0} \frac{d\sigma}{dM^2} = \frac{1}{2\pi i} \int_{c-i\infty}^{c+i\infty} dN \tau^{-N} \mathcal{L}(N) C(N, \alpha_s) \quad (2.90)$$

c does not exist because of the branch cut in the N -space. The minimal prescription (MP) consists of defining the resummed hadronic cross-section as

$$\frac{1}{\tau\sigma_0} \frac{d\sigma^{\text{MP}}}{dM^2} = \frac{1}{2\pi i} \int_{\text{MP}} dN \tau^{-N} \mathcal{L}(N) C^{\text{res}}(N, \alpha_s) \quad (2.91)$$

where the integration path is chosen in such a way that all the singularities, with the exception of the branch cut, are to the left of the integration contour. The numerical convergence of the integral is guaranteed by modifying the slope of the path as shown in Fig. 2.1. The MP is well defined for all τ and is exact for invertible functions. In Ref. [20] it was shown that the expansion Eq. (2.89) converges asymptotically to the MP formula Eq. (2.91) and that if one truncates the series expansion Eq. (2.89) at the order at which its terms are at a minimum, the difference between the truncated expansion and the full MP formula is suppressed by a more than power suppression factor

$$e^{-\frac{HQ(1-\tau)}{\Lambda}} \quad (2.92)$$

where H is a slowly varying positive function.

The MP, however, is not a convolution. In fact, if one defines the MP resummed coefficient function as

$$C^{\text{MP}}(z, \alpha_s) = \frac{1}{2\pi i} \int_{\text{MP}} dN z^{-N} C^{\text{res}}(N, \alpha_s) \quad (2.93)$$

and write $\mathcal{L}(N)$ as the Mellin transform of $\mathcal{L}(z)$, the resummed hadronic cross-section results in

$$\frac{1}{\tau\sigma_0} \frac{d\sigma^{\text{MP}}}{dM^2} = \int_{\tau}^{\infty} \frac{dz}{z} \mathcal{L}\left(\frac{\tau}{z}\right) C^{\text{MP}}(z, \alpha_s). \quad (2.94)$$

Because of the branch cut, in fact, $C^{\text{MP}}(z, \alpha_s)$ does not vanish when $z > 1$ and therefore the integral extends to ∞ . However, the contribution from the region $z > 1$ is exponentially

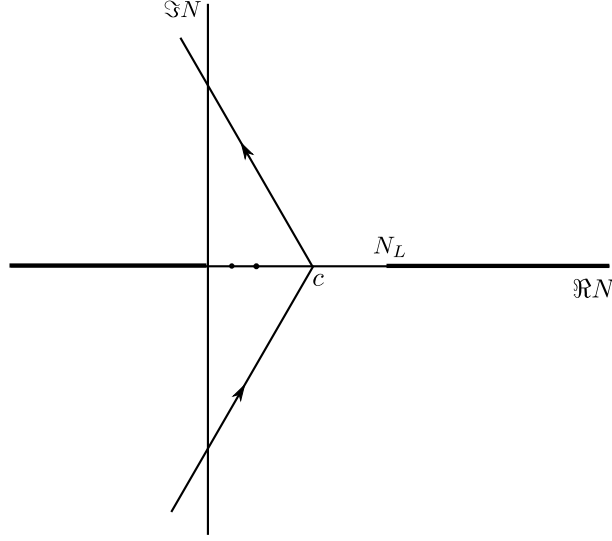


Figure 2.1: Minimal prescription path.

suppressed in $\frac{\Lambda}{M}$, see Eq. (2.92). In conclusion, the MP has good properties but presents some problems. Firstly, the hadronic cross-section receives contributions from an unphysical region; secondly, it was found in Ref. [23] that MP partonic cross-section strongly oscillates in the proximity of $z = 1$ and therefore problems in the numerical implementation arise. In order to solve this last problem different solutions have been suggested. In Ref. [20] the problem is handled by adding and subtracting the results of the minimal prescription evaluated with a toy luminosity. In Ref. [21] the use of parton distributions whose Mellin transform can be computed exactly at the initial scale has been proposed. This solution however restricts the choice of PDFs and therefore is not a suitable solution for precision phenomenology. In Ref. [23] the parton luminosities are expanded on a basis of Chebyshev polynomials, whose Mellin transform can be computed analytically.

2.7 Borel prescription

In Refs. [19, 22] an alternative prescription, based on Borel summation of divergent series, was developed. In this Section we will follow the simpler presentation given in Refs. [5, 23]. We consider the resummed coefficient function Eq. (2.25) which we write as

$$C^{\text{res}}(N, \alpha_s) = h_0(\alpha_s) + \tilde{\Sigma}(\bar{\alpha}L, \alpha_s) \quad (2.95)$$

where $h_0(\alpha_s)$ contains only terms constant in N and Σ , which includes only logarithmically enhanced contributions, can be expanded in series as

$$\tilde{\Sigma}(\bar{\alpha}L, \alpha_s) = \sum_{k=1}^{\infty} h_l(\alpha_s) (\bar{\alpha}L)^k. \quad (2.96)$$

The coefficient function in z space can be written as the series

$$C^{\text{res}}(z, \alpha_s) = \sum_{k=0}^{\infty} h_k(\alpha_s) \bar{\alpha}^k c_k(z), \quad (2.97)$$

where we have included the constant term in the sum and $c_k(z)$ are the inverse Mellin transform of $\log^k \frac{1}{N}$, which can be written in one of the following alternative forms:

$$\mathcal{M} \left[\log^k \frac{1}{N} \right] = \delta_{k0} \delta(1-z) + \left(\frac{d^k}{d\xi^k} \log^{\xi-1} \frac{1}{z} \Big|_{\xi=0} \right)_+ \quad (2.98)$$

$$= \delta_{k0} \delta(1-z) + \frac{k!}{2\pi i} \left(\oint \frac{d\xi}{\xi^{k+1}} \log^{\xi-1} \frac{1}{z} \right)_+ \Gamma(\xi). \quad (2.99)$$

In the last form the path of integration must inclose $\xi = 0$. Therefore by interchanging the sum and the integral the resummed coefficient function in z space becomes

$$C^{\text{res}}(z, \alpha_s) = \frac{1}{2\pi i} \oint \frac{d\xi}{\xi} \left(\frac{[\log^{\xi-1} \frac{1}{z}]_+}{\Gamma(\xi)} + \delta(1-z) \right) \sum_{k=0}^{\infty} h_k(\alpha_s) \left(\frac{\bar{\alpha}}{\xi} \right)^k k!. \quad (2.100)$$

The series in Eq. (2.100) is factorially divergent. However, we can sum the series using the Borel method:

$$\begin{aligned} C^{\text{res}} &= \frac{1}{2\pi i} \oint \frac{d\xi}{\xi} \left(\frac{[\log^{\xi-1} \frac{1}{z}]_+}{\Gamma(\xi)} + \delta(1-z) \right) \int_0^{\infty} d\omega e^{-\omega} \sum_{k=0}^{\infty} h_k(\alpha_s) \left(\frac{\bar{\alpha}\omega}{\xi} \right)^k \\ &= \frac{1}{2\pi i} \oint \frac{d\xi}{\xi} \left(\frac{[\log^{\xi-1} \frac{1}{z}]_+}{\Gamma(\xi)} + \delta(1-z) \right) \int_0^{\infty} d\omega e^{-\omega} \sum_{k=0}^{\infty} h_0 + \tilde{\Sigma} \left(\frac{\bar{\alpha}\omega}{\xi}, \alpha_s \right) \\ &= \frac{1}{2\pi i} \oint \frac{d\xi}{\xi} \left(\frac{[\log^{\xi-1} \frac{1}{z}]_+}{\Gamma(\xi)} + \delta(1-z) \right) \int_0^{\infty} d\omega e^{-\omega} \sum_{k=0}^{\infty} \Sigma \left(\frac{\bar{\alpha}\omega}{\xi}, \alpha_s \right) \end{aligned} \quad (2.101)$$

where we have used the definition Eq. (2.96) and we have defined the function $\Sigma(b, \alpha_s) = h_0(\alpha_s) + \tilde{\Sigma}(b, \alpha_s)$. We observe that the branch cut $-\infty < \bar{\alpha}L \leq -1$ of the function Σ has been mapped in terms of the new variable ξ onto the range $-\bar{\alpha}\omega \leq \bar{\alpha}\xi \leq 0$ in the complex ξ plane. Therefore the ξ integration path, which has to encircle the ξ pole order by order, is any closed curve encircling the cut. We further observe that the ω integral move the lower branch point to $-\infty$. This means that the inverse Borel of Eq. (2.101) does not exists because of the factorial growth of the function $1/\Gamma(\xi)$ as $\xi \rightarrow \infty$.

We now formulate the Borel prescription. It is convenient to recast the integral Eq. (2.101) into a different form by changing variable in the ω integral defining $\omega' = \bar{\alpha}\omega$:

$$C^{\text{res}} = \frac{1}{2\pi i} \oint \frac{d\xi}{\xi} \left(\frac{[\log^{\xi-1} \frac{1}{z}]_+}{\Gamma(\xi)} + \delta(1-z) \right) \int_0^{\infty} \frac{d\omega}{\bar{\alpha}} e^{-\frac{\omega}{\bar{\alpha}}} \sum_{k=0}^{\infty} \Sigma \left(\frac{\omega}{\xi}, \alpha_s \right). \quad (2.102)$$

This integral is divergent; to make it convergent, we put a upper cutoff at some finite value W of the Borel variable ω :

$$C^{\text{BP}}(z, \alpha_s, W) = \frac{1}{2\pi i} \oint \frac{d\xi}{\xi} \left(\frac{[\log^{\xi-1} \frac{1}{z}]_+}{\Gamma(\xi)} + \delta(1-z) \right) \int_0^W \frac{d\omega}{\bar{\alpha}} e^{-\frac{\omega}{\bar{\alpha}}} \sum_{k=0}^{\infty} \Sigma \left(\frac{\omega}{\xi}, \alpha_s \right). \quad (2.103)$$

In Refs. [19, 22] it is proved that the divergent series Eq. (2.103) is asymptotic to the original divergent series Eq. (2.97) and that the neglected terms due to the cutoff are higher twist:

$$\exp \frac{W}{\bar{\alpha}} = \left(\frac{\Lambda^2}{M^2} \right)^{W/2} \quad (2.104)$$

where Λ is the Landau pole scale. This means that the full and cutoff results differ for any truncation by a twist $2 + W$ (for Drell-Yan or Higgs production). Since the first subleading twist is twist 4, the parameter W can be chosen freely in the range $W \geq 2$. Different choices of the parameter W correspond to equivalent results which differ by power suppressed terms. It is therefore possible to use W as a parameter to estimate ambiguities in the resummation procedure. In Ref. [23] the “minimal” choice $W = 2$ was used. Finally, it is important to stress the fact that the resummed expression is at parton level and therefore does not spoil the convolution structure as the MP does.

Phenomenology of threshold resummation in dQCD

In this Chapter we will apply soft-gluon resummation in the dQCD approach to a specific process, Higgs production at LHC. In particular, we will concentrate on the $gg \rightarrow H$ production mechanism, which is the dominant mechanism for SM Higgs boson production at LHC. It is well known [24] that the main contribution to Higgs production in the gluon-gluon channel comes from the threshold region; for this reason, resummation arguments can be used in order to estimate higher order approximations of the cross-section [25]. In Sect. 3.1 we will briefly describe the main production modes of a SM Higgs boson at the LHC. We will discuss in more detail Higgs production in gluon-gluon fusion at fixed perturbative order in Sect. 3.2. We will finally see the effects of soft-gluon resummation on this process in Sect. 3.3.

3.1 Higgs production at the LHC

In this section we briefly describe the main Higgs production mechanisms at a high energy collider, such the LHC proton-proton collider. There are only a few production mechanisms which are relevant for the production of a Higgs boson with $m_H \sim 125$ GeV at the LHC. The cross-sections for such processes are represented in Fig. 3.1. In order of decreasing importance the measurable production modes are:

- (a) gluon-gluon fusion: $gg \rightarrow H$,
- (b) vector boson fusion (VBF): $qq \rightarrow qqH$, via W^+W^- , $ZZ \rightarrow H$,
- (c) associated production with vector bosons: $q\bar{q} \rightarrow WH$, ZH ,
- (d) associated production with top quarks: $gg, q\bar{q} \rightarrow Ht\bar{t}$.

The leading order Feynman diagrams for these mechanisms are shown in Fig. 3.2. The main contribution is the gluon-gluon fusion process, via a loop of heavy quarks (we recall that Yukawa Higgs couplings are proportional to masses). We will describe Higgs production in this channel more accurately in the next Section.

The next contribution, vector-boson fusion, has been calculated at NNLO QCD with the inclusion of NLO EW corrections and it presents a well-converging perturbative expansion. The third largest cross-section, the associated production with a massive vector boson, has been

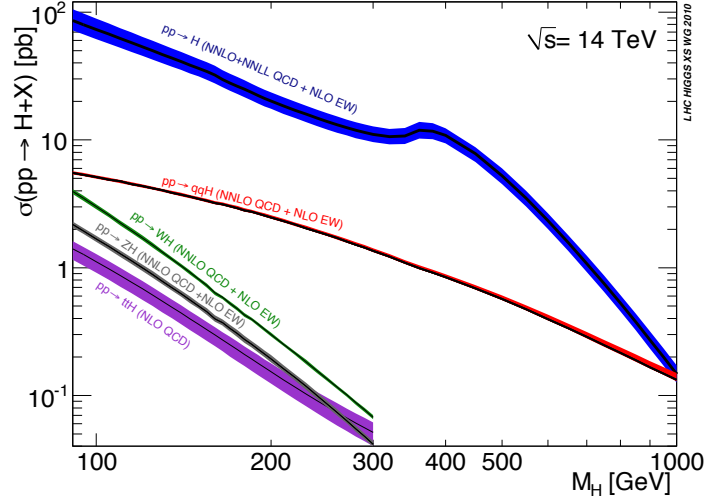


Figure 3.1: Higgs production cross-sections in the Standard Model, including parametric and systematic theoretical errors, for the LHC at c.m. energy 14 TeV.

calculated at NNLO QCD + NLO EW. The perturbative expansion has also in this case good properties of convergence. The fourth and less frequent production mechanism is the associated production with a couple of top quarks. At the moment this process is known less accurately. It has been calculated at NLO QCD and has therefore larger uncertainties. However, since the cross-section for this specific process increases rapidly with energy, there is an increasing interest in this latter process in prospect of the LHC upgrade at 14 TeV.

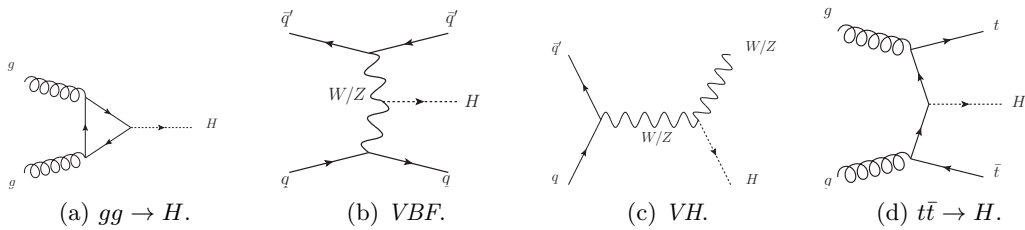
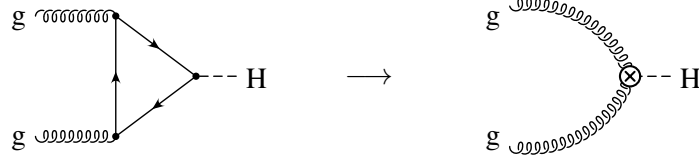


Figure 3.2: Higgs production mechanisms at the LHC.

3.2 Higgs production in gluon-gluon fusion at fixed perturbative order

The Higgs production in gluon-gluon fusion is the dominant Higgs production mechanism in the SM. The perturbative expansion of the cross-section is slowly convergent; it has been calculated

Figure 3.3: Effective vertex in the $m_t \rightarrow \infty$ limit.

with full-dependence on the top and bottom quarks at NLO and at NNLO in the heavy-top limit. In Refs. [27, 28] a computation of the cross-section with finite m_t mass in the limit of high partonic c.m.s. energy was presented. A recent approximate determination of the N³LO was presented in Ref. [25]. The cross-section for the threshold production of the Higgs boson at hadron-colliders at N³LO has been recently performed in Ref. [26]. A complete N³LO in the heavy-top limit is on the way. Mixed QCD+EW corrections have been calculated in Ref. [29].

The NLO corrections to this process, which arises mainly from the radiation of soft and collinear gluons, are very large. Gluon radiation gives the dominant contribution in the soft limit, where $\hat{s} \sim m_H^2$. This leading contribution, however, does not resolve the top quark loop in the large m_t limit, i.e. when $m_H \ll 2m_t$. Therefore, it is possible to calculate the NLO corrections with a good level of accuracy in the limit $m_t \rightarrow \infty$, which greatly reduces the complexity of the calculation since it is reduced by one order of loops. In the infinite top-quark mass limit the one loop ggH vertex is reduced to a tree level effective vertex (see Fig. 3.3) which can be derived by the effective lagrangian

$$\mathcal{L} = -\frac{1}{4v} W G_{\mu\nu}^a G^{a,\mu\nu} H, \quad v = \frac{1}{(2G_F^2)^{1/4}}. \quad (3.1)$$

The Wilson coefficient W in the $\overline{\text{MS}}$ scheme is given by [30, 31]

$$W = -\frac{\alpha_s}{3\pi} \left[1 + \frac{11}{4} \frac{\alpha_s}{\pi} + \left[\frac{2777}{288} + \frac{19}{16} \log \frac{\mu^2}{m_t^2} + n_f \left(-\frac{67}{96} + \frac{1}{3} \log \frac{\mu^2}{m_t^2} \right) \right] \left(\frac{\alpha_s}{\pi} \right)^2 + \mathcal{O}(\alpha_s^3) \right]. \quad (3.2)$$

In the infinite m_t limit it is possible to calculate the NLO and NNLO QCD corrections as corrections to the effective vertex. Since the NLO correction has been calculated with full m_t dependence, it has been possible to test how accurate is the infinite m_t approximation at NLO. The approximate and the exact results shows a remarkable agreement at the level of the total cross-section as one can see in Fig. 3.4 even for a heavy Higgs.

At NNLO the total cross-section requires the calculation of two-loop diagrams instead of the original three-loop diagrams. The cross-section has been calculated in the soft limit in Ref. [31]. The partonic cross-section $\hat{\sigma}_{ij}$ has the perturbative expansion

$$\hat{\sigma}_{ij}^{(n)} = \sum_{n=0}^{\infty} \left(\frac{\alpha_s}{\pi} \right)^n \hat{\sigma}_{ij}^{(n)}. \quad (3.3)$$

In the soft limit ($z \rightarrow 1$) it is possible to write the n -th term of the expansion by expanding

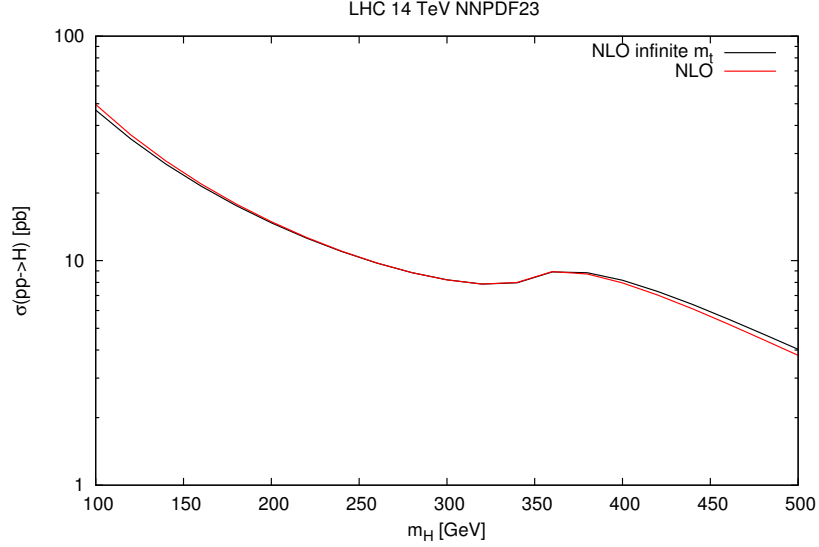


Figure 3.4: Comparison between the NLO exact cross-section and the cross-section calculated in the infinite m_t limit. The curves have been obtained with `ggHiggs` and using NNPDF23 NNLO PDF set.

about $z = 1$ and after separating off distributions from regular terms as

$$\hat{\sigma}_{ij}^{(n)} = \overbrace{a^{(n)}\delta(1-z) + \sum_{k=0}^{2n-1} b_k^{(n)} \left[\frac{\log^k(1-z)}{1-z} \right]_+}^{\text{purely soft terms}} + \overbrace{\sum_{l=0}^{\infty} \sum_{k=0}^{2n-1} c_{lk}^{(n)} (1-z)^l \log^k(1-z)}^{\text{collinear + hard terms}}. \quad (3.4)$$

The NNLO cross-section is obtained by calculating the perturbative coefficient $a^{(2)}$, $b^{(2)}$, $c_{lk}^{(2)}$ for $l \geq 0$ and $k = 0, \dots, 3$. The result obtained in this limit has been confirmed by the full calculation of Ref. [32].

The total cross section for the production of a Higgs boson in hadronic collisions at center-of-mass energy \sqrt{s} can be written as

$$\sigma(\tau, M^2) = \sum_{ij} \int_0^1 dx_1 \int_0^1 dx_2 \int_0^1 dz f_i(x_1) f_j(x_2) \hat{\sigma}_{ij}(z) \delta\left(z - \frac{\tau}{x_1 x_2}\right) \quad (3.5)$$

$$= \tau \sigma_0 \alpha_s^2 \sum_{ij} \int_{\tau}^1 \frac{dz}{z} \mathcal{L}_{ij}\left(\frac{\tau}{z}\right) C_{ij}(z) \quad (3.6)$$

where

$$\tau = \frac{M^2}{s}, \quad (3.7)$$

$$\sigma_0 = \frac{G_F}{288\pi\sqrt{2}} \left| \sum_q A(x_q) \right|^2, \quad x_q = \frac{4m_q^2}{m_H^2}, \quad (3.8)$$

$$A(x) = \frac{3}{2}x[1 + (1-x)f(x)], \quad f(x) = \begin{cases} \arcsin^2 \frac{1}{\sqrt{x}} & x \geq 1 \\ -\frac{1}{4} \left[\log \frac{1+\sqrt{1-x}}{1-\sqrt{1-x}} - i\pi \right]^2 & x < 1 \end{cases}, \quad (3.9)$$

\mathcal{L}_{ij} is the parton luminosity Eq. (2.7) and the coefficient functions C_{ij} are related to the partonic cross-section as

$$\hat{\sigma}_{ij}(z) = \sigma_0 z \alpha_s^2 C_{ij}(z, \alpha_s) \quad (3.10)$$

and have a perturbative expansion in α_s :

$$C_{ij} = C_{ij}^{(0)} + \alpha_s C_{ij}^{(1)} + \alpha_s^2 C_{ij}^{(2)} + \dots \quad (3.11)$$

At LO only C_{gg} contributes; the coefficient functions at NLO in the large- m_t limit can be found in Refs. [33, 34], whereas the full NNLO correction can be found in Ref. [32].

We show in Fig. 3.5 the cross-section for the Higgs production in gluon-gluon fusion calculated at LO, NLO and NNLO with **ggHiggs** [37] in the large- m_t limit. All the curves have been obtained using the NNPDF2.3 NNLO PDF set and $\alpha_s(m_Z) = 0.0117$ in order to show the perturbative behavior of the hard partonic cross-section. We observe that the cross-section has a slowly convergent expansion.

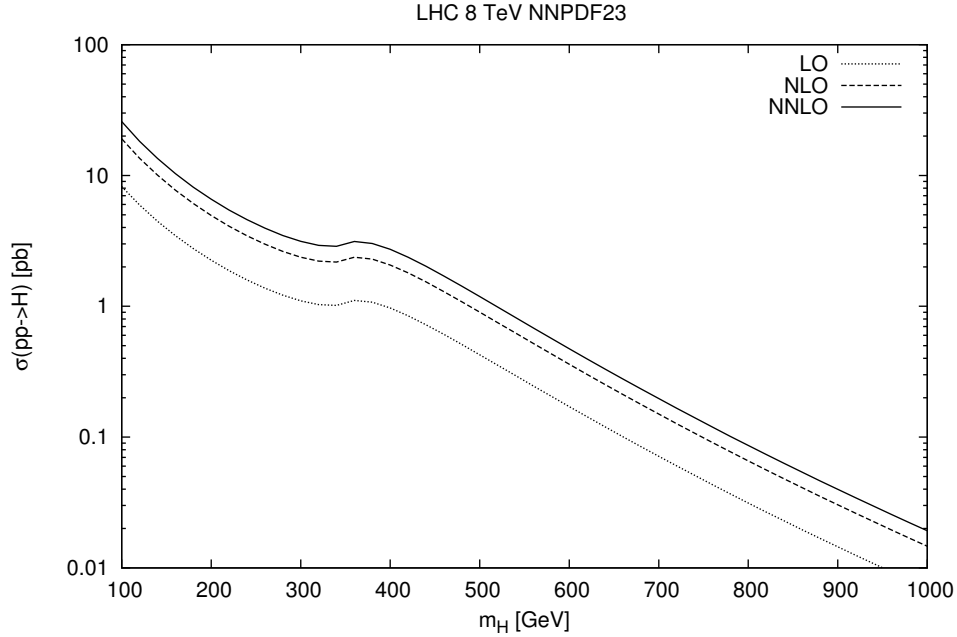


Figure 3.5: Total cross-section for $gg \rightarrow H$ as a function of the Higgs mass m_H at LO, NLO and NNLO at the LHC, setting $\mu_F = \mu_R = m_H$, computed with **ggHiggs** in the large- m_t approximation in the LHC 8 TeV kinematics.

3.3 Higgs resummed results

The NNLO cross section has been further improved in Ref. [35] by resumming up to NNLL accuracy. In this Section we present a phenomenological study of the impact of threshold resummation on the inclusive cross-section for the Higgs boson production process. Once the resummed coefficient functions have been computed, their convolution with PDFs provide us (after matching consistently with fixed-order results) with the resummed hadronic observables.

As we have seen in the previous Chapters, in dQCD resummation is performed in N space to finite logarithmic accuracy. After performing the Mellin inversion with one of the aforementioned prescriptions, retaining terms to all log orders in $1 - z$ the physical hadronic cross-section can be finally obtained. The most general expression for the resummed coefficient in the N space is, as we have seen,

$$C^{\text{res}}(N, \alpha_s) = g_0(\alpha_s) \exp \left[\frac{1}{\bar{\alpha}} g_1(\bar{\alpha}L) + g_2(\bar{\alpha}L) + \bar{\alpha} g_3(\bar{\alpha}L) + \dots \right]. \quad (3.12)$$

where $L = \log \frac{1}{N}$. The explicit expressions of the coefficients g_i can be found in Appendix A. The double-counting terms which have to be subtracted when matching with the fixed-order result can be found as the Taylor expansion in powers of α_s of $g_0(\alpha_s) \exp \mathcal{S}(\lambda, \bar{\alpha})$:

$$\begin{aligned} g_0(\alpha_s) \exp \mathcal{S}(\lambda, \bar{\alpha}) &= (1 + \alpha_s g_{01} + \alpha_s^2 g_{02}^2 + \dots) e^{\alpha_s \mathcal{S}_1 + \alpha_s^2 \mathcal{S}_2 + \dots} \\ &= 1 + (\mathcal{S}_1 + g_{01}) \alpha_s + \left(\frac{\mathcal{S}_1^2}{2} + \mathcal{S}_2 + \mathcal{S}_1 g_{01} + g_{02} \right) \alpha_s^2 + \mathcal{O}(\alpha_s^3). \end{aligned} \quad (3.13)$$

In Fig. 3.6 we show the results for the inclusive invariant mass distribution for Higgs boson production. The resummed result have been obtained with the minimal prescription described in Sect. 2.6 and then matched with the fixed-order results obtained with **ggHiggs**. Also in this case we have used the NNPDF2.3 NNLO PDF set. We have used a code by M. Bonvini which resums up to NNLL accuracy and is consistently matched with fixed-order corrections up to NNLO.

In order to obtain a better assesment of the effect of threshold resummation it is useful to introduce the K -factor defined as

$$K(\tau, M^2) = \frac{\sigma(\tau, M^2)}{\sigma^{\text{LO}}(\tau, M^2)}. \quad (3.14)$$

We show in Fig. 3.7 the K -factor for the fixed-order and the resummed cross-section as a function of the Higgs mass. We note once again that the NLO correction to the total cross-section is very large and it amounts to a correction by 100% of the LO cross-section, and that only at NNLO the perturbative series starts to show a better behaviour. We observe that the effects of soft-gluon resummation are small at LL. We have checked that this fact is due to subleading terms, which are known to be relevant in Higgs boson production since the process is far from threshold. On the other hand, the difference between NNLL and NNLO is about one half of the difference between NNLO and NLO. We observe that NLL correction is not very distant from the NNLO curve, and it gets closer as the Higgs mass grows.

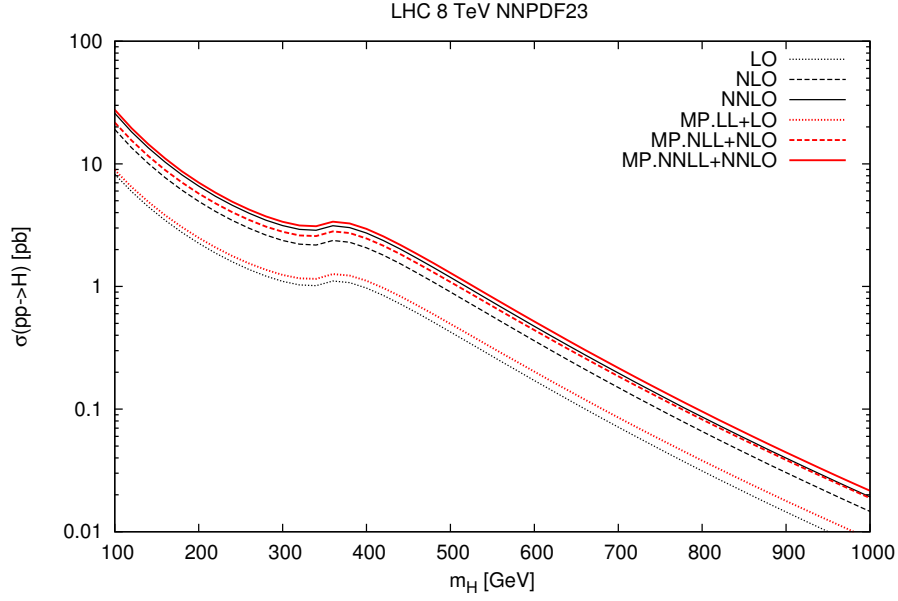


Figure 3.6: Resummed cross-section as a function of the Higgs mass m_H at LL, NLL and NNLL at the LHC. The curves have been calculated with NNPDF2.3 NNLO PDF set, with $\mu_F = \mu_R = m_H$.

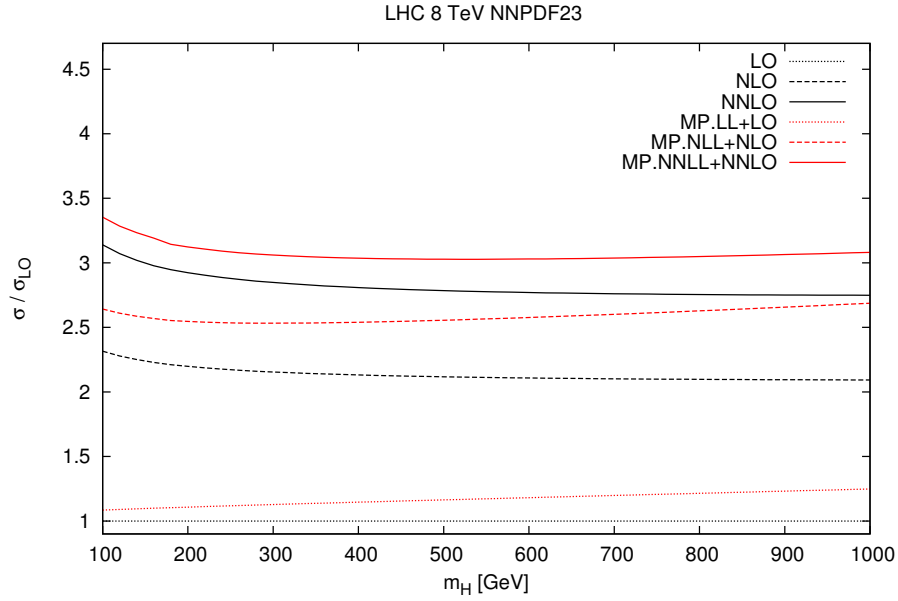


Figure 3.7: K -factor for the resummed cross-section as a function of the Higgs mass m_H at LL, NLL and NNLL at the LHC. The curves have been calculated with NNPDF2.3 NNLO PDF set, with $\mu_F = \mu_R = m_H$.

Resummation in the SCET approach

In recent years an alternative approach to resummation, based on soft-collinear effective theory¹ (SCET) has been proposed. Soft-collinear effective theory techniques provide a powerful way of performing resummation in the standard Mellin space [38]. However, since effective theory deals with hadronic degrees of freedom, resummed expressions can be derived in a SCET approach in terms of hadronic-related quantities, as it was pointed out in Ref. [39]. In this latter approach the scale whose logarithms are resummed is a soft scale μ_s fixed in terms of the hadronic momentum scale $M(1 - \tau)$. The Becher-Neubert (BN) choice of scale avoids the Landau pole problem, since the divergences related to the need to integrate over the parton kinematics disappear. The approach of Ref. [39] (that we will refer to as the SCET approach) has been subsequently extended to various physical processes, such as deep inelastic scattering [40], Drell-Yan [41], and Higgs production [42].

However, the hadronic scale choice leads to puzzling consequences, since the partonic coefficient function depends on hadron-level physics, a statement which is unclear in the standard dQCD approach. As a consequence of the BN scale choice the partonic coefficient function depends on τ through the convolution variable *and* through the soft scale μ_s . Hence the resummed result does not factorize under Mellin transform into the product of the coefficient function and a parton luminosity as in Eq. (2.17). For this reason, as we will see in the next Chapter, it is not possible to compare directly the SCET approach to the standard dQCD approach at the parton level.

In this Chapter we study the emergence of an effective physical scale that characterizes the soft emission using the approach to threshold resummation based on effective field theory. We follow the argument of Ref. [41], which considers as an example Drell-Yan production. We will then see [42] how it is possible to apply the same argument to Higgs-boson production at hadron colliders in Sect. 4.2. In Sect. 4.3 we will discuss in more detail the BN scale choice and its consequences. Finally, we will present predictions for the total resummed cross-section in case of Higgs boson production in gluon-gluon fusion in hadron collider in Sect. 4.4.

¹In this Thesis we are not interested in a discussion of soft-collinear effective theory and we will limit our discussion to its implications on phenomenology. An introduction to SCET is available online at http://physicslearning.colorado.edu/tasi/tasi_2013/notes/june13/Bauer1.pdf.

4.1 Resummation in the Drell-Yan process

4.1.1 Fixed-order calculation of the Drell-Yan process

We consider the production of a lepton pair of invariant mass M at a hadron collider with centre-of-mass energy \sqrt{s} . In particular, we limit our discussion for simplicity to the process

$$N_1 + N_2 \rightarrow \gamma^* + X \rightarrow l^- + l^+ + X. \quad (4.1)$$

We consider the cross-section

$$\frac{d^2\sigma}{dM^2 dY} = \frac{4\pi\alpha^2}{3N_c M^2 s} \sum_{ij} \int dx_1 dx_2 C_{ij}(x_1, x_2, s, M, \mu_f) f_{i/N_1}(x_1, \mu_f) f_{j/N_2}(x_2, \mu_f) \quad (4.2)$$

differential on $M^2 = q^2$ and $Y = \frac{1}{2} \log \frac{1^0 + q^3}{q^0 - q^3}$, where q is the virtuality of the photon and Y is the rapidity of the lepton pair in the centre-of-mass frame. The hard-scattering kernels C_{ij} have a power expansion in α_s . At LO only the $q\bar{q}$, $\bar{q}q$ channels contribute, while at NLO also the qg , gq , $\bar{q}g$, $g\bar{q}$ channels contribute.

It is useful to define new kernels C_{ij} in terms of the variable z Eq. (2.8) and the quantity

$$y = \frac{\frac{x_1}{x_2} e^{-2Y} - z}{(1-z)\left(1 + \frac{x_1}{x_2} e^{-2Y}\right)} \quad (4.3)$$

with $0 \leq y \leq 1$, $\tau \leq z \leq 1$. In particular,

$$\tilde{C}_{ij}(x_1, x_2, s, M, \mu_f) = \left| \frac{dz dy}{dx_1 dx_2} \right| \frac{C_{ij}(z, y, s, M, \mu_f)}{[[1 - y(1 - z)][1 - (1 - y)(1 - z)]]}. \quad (4.4)$$

The hard-scattering kernels at NLO can be found in Ref. [44] and at NNLO in Refs. [44, 45]. The coefficient functions C_{ij} contains terms which are singular at the partonic threshold $z = 1$. In particular, C_{ij} contains logarithms of the form

$$\log \frac{M^2(1-z)^2}{z^2 \mu_f^2} \quad (4.5)$$

which suggests that two mass scales are relevant in the DY process: a hard scale $\mu_h \sim M$ and a soft scale $\mu_s \sim M(1-z)/\sqrt{z}$, which characterize respectively the invariant mass of the lepton pair and the energy of the remnant X which is produced in the collision. As we have seen in Chapter 2, the goal of resummation is to resum these logarithms, which become large when a large separation between the hard and the soft scale exists (i.e. when $z \rightarrow 1$), to all order in perturbation theory.

The leading singular terms in the partonic threshold in the hard scattering kernels are contained in $C_{q\bar{q}}$. In the $z \rightarrow 1$ limit it is possible to rearrange the expression such that the singular terms are always accompanied by δ -distributions in the variable y :

$$C_{q\bar{q}} = \frac{\delta(y) + \delta(1-y)}{2} e_q^2 C(z, M, \mu_f) + C_{q\bar{q}}^{\text{subl}}. \quad (4.6)$$

The complete expression of the leading singular terms can be found in Appendix of Ref. [41] and it can be derived from the hard scattering kernels [44, 45]. As we will see, the SCET approach provides a method to resum these leading singular terms to all orders in perturbation theory.

Upon integration over y and rapidity Y , the total cross-section, differential only in M , is obtained:

$$\frac{d\sigma^{\text{threshold}}}{dM^2} = \frac{4\pi\alpha^2}{3N_c M^2 s} \sum_q e_q^2 \int \frac{dx_1}{x_1} \frac{dx_2}{x_2} C(z, M, \mu_f) [f_{q/N_1}(x_1, \mu_f) f_{\bar{q}/N_2}(x_2, \mu_f) + (q \leftrightarrow \bar{q})], \quad (4.7)$$

where the integration region is bounded from the condition $x_1 x_2 \geq \tau$. We rewrite Eq. (4.7) as

$$\frac{d\sigma^{\text{threshold}}}{dM^2} = \frac{4\pi\alpha^2}{3N_c M^2 s} \int_{\tau}^1 \frac{dz}{z} C(z, M, \mu_f) \mathcal{L}\left(\frac{\tau}{z}, \mu_f\right) \quad (4.8)$$

where we have introduced the parton luminosity

$$\mathcal{L}(y, \mu_f) = \sum_q e_q^2 \int_q^1 \frac{dx}{x} \left[f_{q/N_1}(x, \mu_f) f_{\bar{q}/N_2}\left(\frac{y}{x}, \mu_f\right) + (q \leftrightarrow \bar{q}) \right]. \quad (4.9)$$

4.1.2 Factorization formula for the hard-scattering kernel

The singular part of the coefficient function $C(z, M, \mu_f)$ can be written in a factorized form as

$$C(z, M, \mu_f) = H(M, \mu_f) S(\sqrt{\hat{s}}(1-z), \mu_f), \quad (4.10)$$

where H and S are known respectively as hard function and soft function and will be defined below. This factorization formula has been known for a long time, but it was rederived in Ref. [41] using soft collinear effective theory methods. The hard and soft functions in this way are related to functions – Wilson coefficients – in effective theory, which obey renormalization group (RG) equation. Since the calculation of H and S at a given order is simpler than the calculation of the Drell-Yan cross-section at the same order, Eq. (4.10) is an approximation to the cross-section which reduces the amount of calculational work like the resummed coefficient function in dQCD. Moreover, it is possible to perform threshold resummation directly in z space by solving the RG equations satisfied by H and S .

The starting point of the derivation of the factorization formula is the standard formula for the Drell-Yan cross-section

$$d\sigma = \frac{4\pi\alpha^2}{3sq^2} \frac{d^4q}{(2\pi)^4} \int d^4x e^{-iq \cdot x} \langle N_1(p_1) N_2(p_2) | (-g_{\mu\nu}) J^{\mu\dagger}(x) J^{\nu}(0) | N_1(p_1) N_2(p_2) \rangle, \quad (4.11)$$

where $J^{\mu} = \sum_q e_q \bar{q} \gamma^{\mu} q$ is the electromagnetic current. The factorization formula follows from a sequence of matching steps. The product of current is matched onto operators in SCET; the matching lets a correspondent Wilson coefficient arise. In the case of DY, the matching proceeds in two steps. In the first step a matching with a first version of SCET, which contains soft degrees of freedom along with two types of hard-collinear fields, is performed; in the second step this effective theory is matched onto a SCET version where the soft modes are integrated out and fields of lower virtuality replace the hard-collinear modes. The correspondent Wilson

coefficients are the hard function H and the soft function S . The remaining low-energy matrix element is then identified with the parton luminosity. We will present here the results of this matching procedure; we refer the interested reader to Ref. [41] and references therein for further details.

The physical basis of the factorization formula Eq. (4.10) is made clearer by an intuitive argument, which we will now sketch. We consider the kinematics of the DY process at the parton level, which is shown in Fig. 4.1. Near the partonic threshold, where the energy of the partonic centre-of-mass is just above the invariant mass of the lepton pair, the initial-state partons radiate multiple soft gluons. This soft radiation can be exponentiated and it can be described by objects called Wilson lines, which are phase factors represented by a path ordered exponential of gauge fields. To leading power, the incoming partons are left on the mass-shell; it is therefore possible to describe the DY pair by an on-shell quark form factor, which can be identified with the hard function H . In particular, the hard function H is given by

$$H(M, \mu_f) = |C_V(-M^2 - i\epsilon, \mu_f)|^2 \quad (4.12)$$

where an $i\epsilon$ prescription is required since the Wilson coefficient C_V has a branch cut along the positive q^2 axis. The coefficient C_V is known at 2 loop, and its expression can be found in Appendix A. In Ref. [41] it is finally shown that the soft function can be identified as

$$S(\sqrt{\hat{s}}(1-z), \mu_f) = \sqrt{\hat{s}} W_{\text{DY}}(\sqrt{\hat{s}}(1-z), \mu_f), \quad (4.13)$$

where the Wilson loop W_{DY} is an object which describes the properties of the hadronic final state and whose perturbative expression in position space has been obtained in Ref. [46].

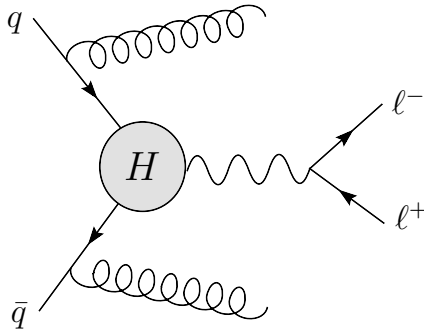


Figure 4.1: Radiation from the initial-state partons in Drell-Yan process at parton level. Figure from Ref. [41].

4.1.3 Resummation in momentum space

The resummation of large logarithms in the threshold region $z \rightarrow 1$ is performed in the SCET approach by solving the renormalization group equation which the hard and the soft function, now characterized as field-theoretic objects, obey.

The matching coefficient C_V obeys the evolution equation

$$\frac{d}{d \log \mu} C_V(-M^2 - i\epsilon, \mu) = \left[\Gamma_{\text{cusp}}(\alpha_s) \left(\log \frac{M^2}{\mu^2} - i\pi \right) + \gamma^V(\alpha_s) \right] C_V(-M^2 - i\epsilon, \mu), \quad (4.14)$$

where the term in Γ_{cusp} is associated with Sudakov double logarithms, whereas γ^V is associated with single logarithms. This equation can be solved exactly; the solution is

$$C_V(-M^2, \mu_f) = \exp[2S(\mu_h, \mu_f) - a_{\gamma^V}(\mu_h, \mu_f) + i\pi a_\Gamma(\mu_h, \mu_f)] \left(\frac{M^2}{\mu_h} \right)^{-a_\Gamma(\mu_h, \mu_f)} C_V(-M^2, \mu_h) \quad (4.15)$$

where a hard matching scale $\mu_h \sim M$, at which C_V is calculated using fixed-order perturbation theory, has been introduced. The Sudakov exponent S and the exponent a_Γ are

$$S(\nu, \mu) = - \int_{\alpha_s(\nu)}^{\alpha_s(\mu)} d\alpha \frac{\Gamma_{\text{cusp}}(\alpha)}{\beta(\alpha)} \int_{\alpha_s(\nu)}^{\alpha} \frac{d\alpha'}{\beta(\alpha')}, \quad a_\Gamma(\nu, \mu) = - \int_{\alpha_s(\nu)}^{\alpha_s(\mu)} d\alpha \frac{\Gamma_{\text{cusp}}(\alpha)}{\beta(\alpha)}. \quad (4.16)$$

with an analogous expression for a_{γ^V} .

The Wilson loop, which is related to the soft function by Eq. (4.13), obeys the following integro-differential equation:

$$\begin{aligned} \frac{dW_{\text{DY}}(\omega, \mu)}{d \log \mu} = & - \left[4\Gamma_{\text{cusp}}(\alpha_s) \log \frac{\omega}{\mu} + 2\gamma^W(\alpha_s) \right] W_{\text{DY}}(\omega, \mu) \\ & - 4\Gamma_{\text{cusp}}(\alpha_s) \int_0^\omega d\omega' \frac{W_{\text{DY}}(\omega', \mu) - W_{\text{DY}}(\omega, \mu)}{\omega - \omega'}, \end{aligned} \quad (4.17)$$

where

$$\gamma^W = 2\gamma^\phi + \gamma^V, \quad (4.18)$$

where γ^ϕ can be obtained by expanding the Altarelli-Parisi splitting function as

$$P_{qq}(z) = \frac{2\Gamma_{\text{cusp}}(\alpha_s)}{[1-z]_+} + 2\gamma^\phi(\alpha_s)\delta(1-z) + \dots \quad (4.19)$$

The solution of Eq. (4.17) is

$$W_{\text{DY}}(\omega, \mu_f) = \exp[-4S(\mu_s, \mu_f) + 2a_{\gamma^W}(\mu_s, \mu_f)] \tilde{s}_{\text{DY}}(\partial_\eta, \mu_s) \frac{1}{\omega} \left(\frac{\omega}{\mu_s} \right)^{2\eta} \frac{e^{-2\gamma_E \eta}}{\Gamma(2\eta)}, \quad (4.20)$$

where we have introduced an auxiliary parameter $\eta = 2a_\Gamma(\mu_s, \mu_f)$. The result Eq. (4.20) is well defined if $\eta > 0$. The result is analytically continued to negative values of η (which is typically the case in DY-like processes) by means of the identity

$$\int_0^\Omega d\omega \frac{f(\omega)}{\omega^{1-2\eta}} = \int_0^\Omega d\omega \frac{f(\omega) - f(0)}{\omega^{1-2\eta}} + \frac{f(0)}{2\eta} \Omega^{2\eta} \quad (4.21)$$

which is valid if $-\frac{1}{2} < \eta < 0$; other subtractions are required for $\eta < \frac{1}{2}$. The function \tilde{s}_{DY} is given by the Laplace transform

$$\tilde{s}_{\text{DY}}(L, \mu_s) = \int_0^\infty d\omega e^{-s\omega} W_{\text{DY}}(\omega, \mu_s), \quad s = \frac{1}{e^{\gamma_E} \mu_s e^{L/2}}. \quad (4.22)$$

The resummed expression for the hard scattering coefficient Eq. (4.10) is given by the product of the solutions of the renormalization group equations Eq. (4.15) and Eq. (4.20). The result can be written as

$$C(z, M, \mu_f) = |C_V(-M^2, \mu_h)|^2 U(M, \mu_h, \mu_s, \mu_f) \times \frac{z^{-\eta}}{(1-z)^{1-2\eta}} \tilde{s}_{\text{DY}} \left(\log \frac{M^2(1-z)^2}{\mu_s^2 z} + \partial_\eta, \mu_s \right) \frac{e^{-2\gamma_E \eta}}{\Gamma(2\eta)} \quad (4.23)$$

where we have defined

$$U(M, \mu_h, \mu_s, \mu_f) = \left(\frac{M^2}{\mu_h^2} \right)^{-2a_\Gamma(\mu_h, \mu_s)} \exp[4S(\mu_h, \mu_s) - 2a_{\gamma^V}(\mu_h, \mu_s) + 4a_{\gamma^\phi}(\mu_s, \mu_f)]. \quad (4.24)$$

The resulting expression is, from a formal point of view, independent of the hard scale μ_h and the soft scale μ_s ; however, in phenomenological applications, one has to truncate the perturbative expansions of C_V , \tilde{s}_{DY} and the anomalous dimensions γ^V and γ^ϕ . Furthermore, the evolution function, which is an exponential, contains all the order in α_s , whereas the hard and the soft function are truncated at fixed perturbative order. For this reason a residual, non trivial dependence on the matching scales cannot be avoided when phenomenological analysis are performed.

4.2 Resummation for the Higgs production process

In this Section we will show how soft collinear effective theory provides a method to resum logarithmically enhanced contribution which arise in the Higgs production in the gluon-gluon fusion process. As for the DY process, the SCET expressions are cast in momentum space and are free of Landau pole.

4.2.1 Fixed-order expressions and factorization formula for Higgs production

We have discussed in some details Higgs production process in gluon-gluon fusion at fixed-order in Sect. 3.2. We have seen that the total cross-section for the production of a Higgs boson of mass m_H in hadronic collisions at centre-of-mass energy \sqrt{s} can be written as

$$\sigma(\tau, M^2) = \tau \sigma_0 \alpha_s^2(\mu_f^2) \sum_{ij} \int \frac{dz}{z} C_{ij}(z, m_t, m_H, \mu_f) \mathcal{L}_{ij} \left(\frac{\tau}{z}, \mu_f \right), \quad (4.25)$$

where

$$\mathcal{L}_{ij}(y, \mu) = \int_y^1 \frac{dx}{x} f_{i/N_1}(x, \mu) f_{j/N_2} \left(\frac{y}{x}, \mu \right) \quad (4.26)$$

are the parton luminosity, $\tau = \frac{m_H^2}{s}$, and C_{ij} are hard scattering kernels. The hard scattering kernels contains terms which are singular in the partonic threshold limit $z \rightarrow 1$, where $\hat{s} \sim m_H^2$. These terms are contained in the hard-scattering kernel C_{gg} , which can be written therefore as

$$C_{gg}(z, m_t, m_H, \mu_f) = C(z, m_t, m_H, \mu_f) + C_{gg}^{\text{reg}}(z, m_t, m_H, \mu_f), \quad (4.27)$$

where C_{gg}^{reg} contains only terms which are not singular in $z = 1$.

It is possible to write the coefficient function $C(z, m_t, m_H, \mu_f)$ in a factorized form, using effective field theory methods in the same way as it was done for the factorized scattering kernel in DY production. As for the DY production, a sequence of matching step is made in order to obtain a factorized formula. One first integrates out the top quark by matching the Standard Model with six quarks flavour onto a five-flavour theory. In this way a Wilson coefficient C_t arises. The five-flavour theory is then matched on SCET in analogy with what was done in DY production; in this way the hard function H and the soft function S arise. The remaining effective-theory matrix element is then identified with the convolution of the parton distribution functions. The resulting coefficient function can be written as

$$C(z, m_t, m_H, \mu_f) = [C_t(m_t^2, \mu_f^2)]^2 H(m_H^2, \mu_f^2) S(\hat{s}(1-z)^2, \mu_f) \quad (4.28)$$

In this way the cross-section is approximated by a factorized formula.

4.2.2 Resummation in momentum space

The hard and soft function H and S are related to Wilson coefficients in SCET. In particular, the hard function can be written as

$$H(m_H^2, \mu^2) = |C_S(-m_H^2 - i\epsilon, \mu^2)|^2, \quad (4.29)$$

where C_S has an expansion in powers of $\alpha_s(\mu^2)$. The soft function is related to the Wilson loop W_{Higgs} , which coincides at two loop order with the Wilson loop W_{DY} after the replacement $C_F \rightarrow C_A$. In particular,

$$\begin{aligned} S(\hat{s}(1-z)^2, \mu_f^2) &= \sqrt{\hat{s}} W_{\text{Higgs}}(\hat{s}(1-z)^2, \mu_f^2) \\ &= \sqrt{\hat{s}} W_{\text{DY}}(\hat{s}(1-z)^2, \mu_f^2) \Big|_{C_F \rightarrow C_A} + \mathcal{O}(\alpha_s^3). \end{aligned} \quad (4.30)$$

The Wilson coefficient C_t , C_S obey RG equations whose solutions provide a method to resum logarithmically enhanced contributions in momentum space. In particular, the Wilson coefficient C_t at scale μ_f is

$$C_t(m_t^2, \mu_f^2) = \frac{\beta(\alpha_s(\mu_f^2))/\alpha_s^2(\mu_f^2)}{\beta(\alpha_s(\mu_t^2))/\alpha_s^2(\mu_t^2)} C_t(m_t^2, \mu_t^2), \quad (4.31)$$

with $\mu_t \sim m_t$, which is the scale at which the top quark is integrated out and C_S can be written as

$$C_S(-m_H^2 - i\epsilon, \mu_f^2) = \exp \left[2S(\mu_h^2, \mu_f^2) - a_\Gamma(\mu_h^2, \mu_f^2) \log \frac{-m_H^2 - i\epsilon}{\mu_h^2} - a_{\gamma_S}(\mu_H^2, \mu_f^2) \right]$$

$$\times C_S(-m_H^2 - i\epsilon, \mu_h^2), \quad (4.32)$$

where a hard matching scale μ_h has been introduced. The solution above depends on the cusp anomalous dimension Γ_{cusp}^A , which controls the double-log evolution, and the anomalous dimension γ^S , which controls the single-log evolution.

The Wilson loop W_{Higgs} obeys an integro-differential equation analogous to Eq. (4.17), whose solution is

$$\omega W_{\text{Higgs}}(\omega^2, \mu_f^2) = \exp[-4S(\mu_s^2, \mu_f^2) + 2a_{\gamma^W}(\mu_s^2, \mu_f^2)] \tilde{s}_{\text{Higgs}}(\partial_\eta, \mu_s^2) \left(\frac{\omega^2}{\mu_s^2} \right)^\eta \frac{e^{-2\gamma_E \eta}}{\Gamma(2\eta)}, \quad (4.33)$$

where $\eta = 2a_\Gamma(\mu_s^2, \mu_f^2)$. The anomalous dimension γ^W is related to γ^S from the equation

$$\gamma^W = \frac{\beta(\alpha_s)}{\alpha_s} + \alpha_s^2 \frac{d}{d\alpha_s} \frac{\beta(\alpha_s)}{\alpha_s^2} + \gamma^S + 2\gamma^B, \quad (4.34)$$

where γ^B is the coefficient of the $\delta(1-z)$ term in $P_{gg}(z)$. The function \tilde{s}_{Higgs} is related to the corresponding function \tilde{s}_{DY} by a simple replacement of color factors. The explicit expressions for the relevant coefficients can be found in Appendix A.

Putting everything together allows one to write the resummed hard-scattering kernel as

$$C(z, m_t, m_H, \mu_f) = [C_t(m_t^2, \mu_t^2)]^2 |C_S(-m_H^2 - i\epsilon, \mu_h^2)|^2 U(m_H, \mu_t, \mu_h, \mu_s, \mu_f) \\ \times \frac{z^{-\eta}}{(1-z)^{1-2\eta}} \tilde{s}_{\text{Higgs}} \left(\log \frac{m_H^2 (1-z)^2}{\mu_s^2 z} + \partial_\eta, \mu_s^2 \right) \frac{e^{2\gamma_E \eta}}{\Gamma(2\eta)} \quad (4.35)$$

where U is the evolution factor defined is

$$U(m_h, \mu_t, \mu_h, \mu_s, \mu_f) = \frac{\alpha_s^2(\mu_s^2)}{\alpha_s^2(\mu_f^2)} \left[\frac{\beta(\alpha_s(\mu_s^2))/\alpha_s^2(\mu_s^2)}{\beta(\alpha_s(\mu_t^2))/\alpha_s^2(\mu_t^2)} \right]^2 \left| \left(\frac{-m_H^2 - i\epsilon}{\mu_h^2} \right)^{-2a_\Gamma(\mu_h^2, \mu_s^2)} \right| \\ \times |\exp[4S(\mu_h^2, \mu_s^2) - 2a_{\gamma^S}(\mu_h^2, \mu_s^2) + 4a_{\gamma^B}(\mu_s^2, \mu_f^2)]|. \quad (4.36)$$

As we emphasized in case of DY production, the resummed hard-scattering coefficient is formally independent of the matching scales μ_s , μ_h and μ_t , but a residual scale dependence remains due to the truncation of perturbation theory.

The total cross-section for the Higgs-boson production is obtained by integrating the resummed coefficient convoluted with the gluon-gluon luminosity \mathcal{L}_{gg} . It is finally necessary to match the result with the fixed-order computation. In the momentum-space approach the double-counting terms are avoided by the simple subtraction

$$\sigma = \sigma^{\text{resummed}} \Big|_{\mu_t, \mu_h, \mu_s, \mu_f} + \left(\sigma^{\text{fixed order}} \Big|_{\mu_f} - \sigma^{\text{resummed}} \Big|_{\mu_t = \mu_h = \mu_s = \mu_f} \right), \quad (4.37)$$

since by construction the last term, where all the evolution scales are evaluated at μ_f , contains only the fixed order truncation of the resummed result.

4.3 The Becher-Neubert scale choice

In the standard dQCD approach soft gluon emission is characterized by an energy scale of order $M(1-z)$, where z is the energy fraction of the observed final state. Therefore, the energy available for unobserved gluon radiation is much smaller than M in the partonic threshold limit $z \rightarrow 1$. As we have previously discussed in Chapter 2, the resummation of $\log(1-z)$ has important phenomenological applications; when a partonic scale is chosen threshold resummation could be important even relatively far from the hadronic threshold, because of the convolution structure of the integral Eq. (4.25).

In the SCET expressions one resums both of $1-z$ and logs of M/μ_s , where M is a hard scale whereas μ_s is a soft scale which can be chosen in different ways. In the SCET approach hence the choice of the soft scale μ_s determines what is being resummed. Different choices are possible. When $\mu_s \sim M$ nothing is resummed and by construction of the SCET expressions fixed-order result in the soft limit is reproduced. The natural partonic choice, $\mu_s \sim M(1-z)$, corresponds to the resummation of logs of $1-z$.

In this last case the resummed SCET coefficient function can be directly compared with the perturbative coefficient function $C_{\text{dQCD}}(z, M^2)$ obtained as the leading-log truncation of the inverse Mellin of the N -space coefficient function $C_{\text{dQCD}}(N, M^2)$. A comparison can hence be done only order by order. On the other hand, the SCET coefficient function in momentum space is formally defined for $\mu_s = M(1-z)$. It was shown in Ref. [49] that, away from the endpoint $z = 1$, all the logarithmically enhanced terms in the partonic cross-section are reproduced order by order with the partonic scale choice. However, the SCET expression with $\mu_s = M(1-z)$ is ill-defined when $z \rightarrow 1$. Moreover, since η depends on z , it is not possible to use Eq. (4.21) to regulate the behaviour of the resummed coefficient function at the endpoint. A possible way out, which consists in a cutoff of the convolution integral at $z = \bar{z} < 1$, was proposed in Ref. [47].

Alternatively, one can choose the soft scale as a function of the hadronic variable τ , which avoids the Landau problem pole. This choice was proposed by Becher and Neubert in Refs. [39, 40, 41, 42]. This particular choice has some puzzling consequences if compared to the standard perturbative approach, since the analytical structure of the integral

$$\sigma_{\text{SCET}}(\tau, M^2) = \int_{\tau}^1 \frac{dz}{z} \mathcal{L}\left(\frac{\tau}{z}\right) C_{\text{SCET}}(z, M^2, \mu_s^2) \quad (4.38)$$

changes. In fact, if the soft scale is chosen as a function of the partonic variable z Eq. (4.38) factorizes upon Mellin transform. This is a sufficient and a necessary condition for parton radiation to respect longitudinal momentum conservation. However, if μ_s depends on τ , the convolution structure is spoiled, and upon Mellin transform the cross-section no longer factorizes and violates longitudinal momentum conservation. In particular, this choice violates the QCD factorization theorem since the partonic coefficient function depends on the hadronic variable τ , while it should not.

The choice of soft scale proposed by Becher and Neubert is

$$\mu_s \sim M(1-\tau). \quad (4.39)$$

However, when τ is small (as for Higgs production at the LHC), with this particular choice $\mu_s \sim M$, which is a hard scale. In this case, as we have discussed, the SCET approach reproduces the soft-limit of the fixed order result. In the small τ case Becher and Neubert

suggest a slightly more general choice of scale. The soft scale Eq. (4.39) is generally rescaled by a function of τ which does not vanish in the hadronic endpoint and which is determined by minimization of perturbative contributions of \tilde{s} to the cross-section. In particular, two criteria are proposed:

- Starting from a high scale, one determines the value of μ_s at which the one-loop correction drops below 15%.
- one choose the value of μ_s for which the one-loop correction is minimized.

In the Drell-Yan case the two resulting scales are chosen as

$$\mu_I = \frac{M(1-\tau)}{1+7\tau} \quad \mu_{II} = \frac{M(1-\tau)}{\sqrt{1+150\tau}}, \quad (4.40)$$

whereas for the Higgs production two different functional forms are chosen, which well interpolates the numerical results obtained from the two criteria proposed. The soft scale is varied between the two scales μ_I and μ_{II} and, somewhat arbitrarily, the average of the two scales is taken as the default choice. We will investigate further the consequences of the BN scale choice in Chapter 5 when we will make a systematical comparison of the dQCD and the SCET approach.

4.4 Phenomenology

We have discussed how SCET provides an alternative way to compute resummed observables. The results depend on various scales from which the SCET predictions are formally independent, but we have seen how a residual dependence cannot be avoided if phenomenological study are performed.

In this Section we will apply soft-gluon resummation in the SCET approach to a specific process, namely the Higgs boson production at the LHC. We will present the prediction for the total cross-section and the K -factor at the resummed level. All the result have been computed setting the matching scales $\mu_h = \mu_t = m_H$, the factorization scale $\mu_f = m_H$ and choosing μ_s as the average value of the two scales μ_I and μ_{II} , which are chosen according to the Becher-Neubert criteria. In Ref. [42] a more detailed study² has been performed, that includes an estimation of the theoretical uncertainties and the resummation of contributions of the form $(C_A\pi\alpha_s)^n$, which arise in the analytic continuation of the gluon form factor C_S . The possibility of the resummation of this enhanced terms, related to the Sudakov logarithms, was observed long time ago [43]. In Ref. [42] π^2 resummation was claimed to lead to large corrections to resummed Higgs cross-section. However, since it is a separate subject, we will not consider it in our phenomenological study.

We show in Fig. 4.2 the resummed cross-section as a function of the Higgs mass m_H at LL, NLL, NNLL compared with the fixed-order results obtained with **ggHiggs**. All the curves have been obtained in the large- m_t limit with the NNPDF2.3 NNLO PDF set and $\alpha_s(m_Z) = 0.0117$. The predictions have been obtained with our own code which we have checked to produce similar results to the public code **RGHiggs** [48]. The effect of soft-gluon resummation is made clearer in Fig. 4.3 where we show the predictions for the K -factor Eq. (3.14). The effect of threshold

²Actually, the results of Ref. [42] include RG improvement up to NNNLL*. In our study, however, we switched from the starred counting used in Ref. [42] to the un-starred counting.

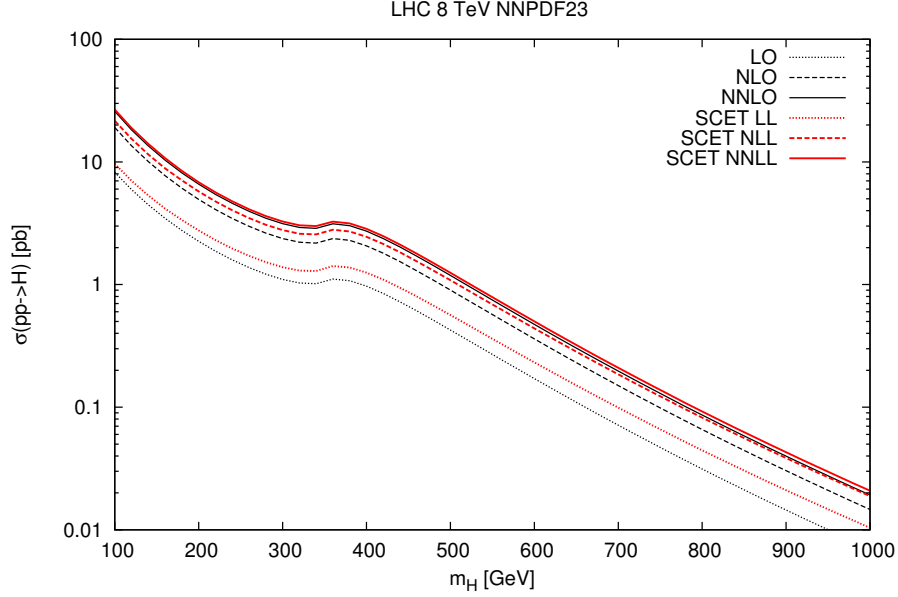


Figure 4.2: Resummed cross-section as a function of the Higgs mass m_H at LL, NLL and NNLL at the LHC. The curves have been calculated with NNPDF2.3 NNLO PDF set, with $\mu_h = \mu_t = m_H = \mu_f$.

resummation is relevant already at LL, where it leads to an increase of the cross-section by 20% up to 50% for a heavy Higgs. The effect is relevant at NLL, where the resummed cross-section gets close to the NNLO result. At NNLL accuracy the effect is slightly reduced and it corresponds to an increase of the cross-section by 10% at most.

Finally, we show in Fig. 4.4 the dependence of the K -factor for the resummed cross-section on the soft scale μ_s , which varies between the two values μ_s^I and μ_s^{II} . As one would expect, the width of the band gets thinner the higher the logarithmic accuracy is.

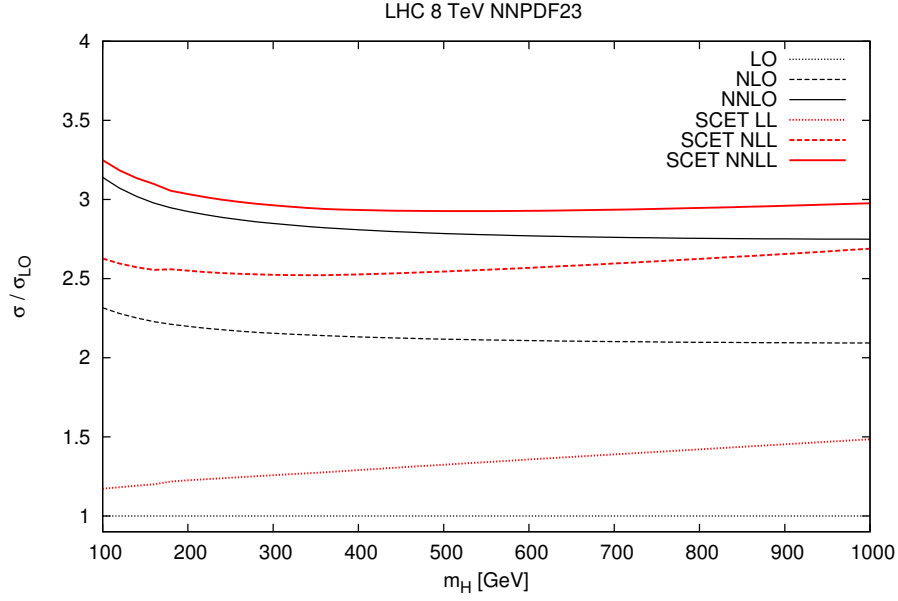


Figure 4.3: K -factor for the resummed cross-section as a function of the Higgs mass m_H at LL, NLL and NNLL at the LHC. The curves have been calculated with NNPDF2.3 NNLO PDF set, with $\mu_h = \mu_t = m_H = \mu_f$.

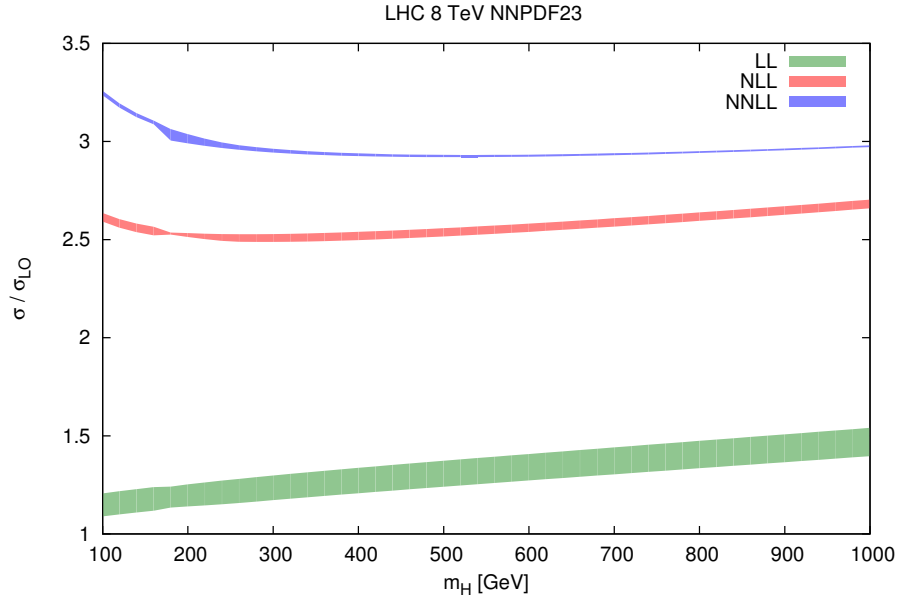


Figure 4.4: Dependence on μ_s of the K -factor for the resummed cross-section as a function of the Higgs mass m_H at LL, NLL and NNLL at the LHC. The curves have been calculated with NNPDF2.3 NNLO PDF set, with $\mu_h = \mu_t = m_H = \mu_f$.

Resummation in SCET and in dQCD: an analytic comparison

In this Chapter we compare soft-gluon resummation in QCD as performed in the standard perturbative QCD formalism, to resummation based on SCET in the Becher-Neubert approach.

In the past years an increasing interest in a deeper understanding of the main similarities and differences in the two methods has grown. Both in Refs. [40, 41, 42] and in Refs. [49, 50] the analytic equivalence of the dQCD and SCET approaches has been explored at various levels. More recently, in Ref. [51], the relationship between the two formalisms has been investigated by focusing on their common basis which relies on soft-gluon factorization properties and then by analyzing how the two formalisms differ in the choice of scales and in the derivation of physical observables.

We will follow the argument presented in Refs. [49, 50] which concentrates on Drell-Yan production and that can be straightforwardly generalized to Higgs boson production. In Sect. 5.1 we will briefly summarize some features of threshold resummation in both the approaches and we will discuss some of the problems which arise in performing such a task in the two formalisms. In Sect. 5.2 we will fix some notation and in Sect 5.3 we will derive a master formula which relates dQCD and SCET. We will finally discuss the logarithmic accuracy of the SCET result with the BN scale choice in Sect. 5.4.

5.1 Threshold resummation

In the previous Chapters we have learned how the resummation of logarithmically enhanced contributions arises naturally when one computes cross-sections in perturbative QCD. In this Section we summarize some of the features we have already encountered in order to have a better understanding of similarities and differences in the dQCD and in the SCET approach.

Standard dQCD resummation is traditionally performed in Mellin space since the truncation of resummed results in momentum space to any finite logarithmic accuracy induces terms which violate the conservation of the longitudinal momentum. As a consequence, it is not possible to perform dQCD resummation in momentum space since this would lead to divergent hadronic cross-sections. In order to obtain finite physical hadronic cross-section one has therefore to perform resummation in N space to finite logarithmic accuracy and subsequently to invert the Mellin transform retaining terms to all logarithmic orders in $1 - z$ (which correspond under

Mellin transform to logs of N).

We have however learned how the running of the coupling introduces new difficulties while performing threshold resummation. In particular, the resummed coefficient function in z space, viewed as a series in α_s Eq. (2.87), where each term is constructed as the exact inverse Mellin transform of Eq. (2.88), does not converge. This divergence is a direct consequence of the presence of the Landau pole in α_s . The fact that the series Eq. (2.87) acquires a nonzero radius of convergences if the Mellin inversion is performed to finite logarithmic accuracy does not help; since upon inverse Mellin transform the hard scale Q^2 is replaced with a scale $Q^2(1-z)^a$ (with $a = 2$ for DY and Higgs production) related to soft-gluon emission the convolution integral Eq. (2.9) always intercepts the region $z \rightarrow 1$ where the running coupling gets over the Landau pole. Fortunately, this non-perturbative divergence can be removed by adding suitable subleading terms: in the MP the particular integration path chosen when performing the Mellin inversion corresponds to the addition of more-than-power suppressed terms, while in the BP the divergent series is made Borel-summable by adding a higher twist term.

On the other hand, approaches based on soft-collinear effective theory are valid alternatives to dQCD and provide a powerful tool in order to obtain resummed observables. In Ref. [39] it was suggested that in the SCET approach resummed expressions in terms of the hadronic kinematic variables could be derived; this allows therefore the resummation of $\log(1-\tau)$, where τ is an (hadronic) dimensionless variable. The divergence due to the presence of the Landau pole can hence be avoided. In fact in the resummed SCET expressions one can choose the soft scale μ_s in terms of the kinematic variables of the hadronic process. With this scale choice resummed expression for different physical processes have been obtained. However, it is not immediate to understand the implications of the BN scale choice in the traditional formalism because one of the main features of dQCD, perturbative factorization – the independence of the partonic cross-section from the hadronic kinematics variables – is lost.

5.2 Resummation of the Drell-Yan process in SCET and dQCD

In this Section we consider for definiteness inclusive Drell-Yan production at a hadron collider; we will however see how the same argument can be applied with minimal modification to Higgs boson production in gluon-gluon fusion. In particular, we concentrate on the invariant mass distribution $\frac{d\sigma_{\text{DY}}}{dM^2}$, where M is the invariant mass of the DY pair. We define the dimensionless cross-section

$$\sigma(\tau, M^2) = \frac{1}{\tau\sigma_0} \frac{d\sigma_{\text{DY}}}{dM^2} \quad (5.1)$$

where σ_0 is the leading order partonic cross section. We can write the invariant mass distribution in the schematic form

$$\sigma(\tau, M^2) = \int_{\tau}^1 \frac{dz}{z} C(z, M^2) \mathcal{L}\left(\frac{\tau}{z}\right). \quad (5.2)$$

From now on, without significant loss of generality, we shall always choose $\mu_F = \mu_R = M$.

5.2.1 Perturbative resummation in dQCD

For convenience of the reader, in this Section we briefly summarize how soft resummation is performed in dQCD. We have discussed at length in Chapter 2 how dQCD resummation is

performed in N space, by considering the Mellin transform of the cross-section

$$\sigma(N, M^2) = \int_0^1 d\tau \tau^{N-1} \sigma(\tau, M^2) = C(N, M^2) \mathcal{L}(N). \quad (5.3)$$

The resummed coefficient function in N space has the form Eq. (2.23) which we report here:

$$C_{\text{dQCD}}^{\text{res}}(N, M^2) = \bar{g}_0(\alpha_s) \exp \bar{S} \left(M^2, \frac{M^2}{N^2} \right) \quad (5.4)$$

where

$$\bar{S} \left(M^2, \frac{M^2}{N^2} \right) = \int_0^1 dz z^{N-1} \left[\frac{1}{1-z} \int_{M^2}^{M^2(1-z)^2} \frac{d\mu^2}{\mu^2} 2A(\alpha_s(\mu^2)) + D(\alpha_s([1-z]^2 M^2)) \right]_+ \quad (5.5)$$

The functions $\bar{g}_0(\alpha_s)$, $A(\alpha_s)$ and $D(\alpha_s)$ are power series in α_s , with $\bar{g}_0(0) = 1$ and $A(0) = D(0) = 0$. We have discussed in Chapter 2 how the inclusion of extra terms in \bar{g}_0 is mandatory in order to improve the accuracy beyond NLL; the inclusion of an extra term in \bar{g}_0 increases the logarithmic accuracy of the coefficient function by half a logarithmic order.

5.2.2 Resummation in the SCET approach

In this Section we collect the relevant expressions for resummed quantities in the SCET approach of Refs. [39, 40, 41, 42]. In order to compare the two approaches it is useful to rewrite the resummed coefficient function Eq. (4.23) as

$$C_{\text{SCET}}^{\text{res}} = H(M^2) U(M^2, \mu_s^2) S(z, M^2, \mu_s^2), \quad (5.6)$$

where the energy scales μ_h and μ_f which appear in Eq. (4.23) are taken for simplicity equal to the hard scale M^2 . In Eq. (5.6) we recognize the hard function $H(M^2)$, which arises from the matching at the hard scale $\mu_h = M$, and which have an expansion in powers of α_s ; the soft function

$$S(z, M^2, \mu_s^2) = \tilde{s}_{\text{DY}} \left(\log \frac{M^2}{\mu_s^2} + \frac{\partial}{\partial \eta}, \mu_s \right) \frac{1}{1-z} \left(\frac{1-z}{\sqrt{z}} \right)^{2\eta} \frac{e^{-2\gamma_E \eta}}{\Gamma(2\eta)} \quad (5.7)$$

where

$$\eta = \int_{M^2}^{\mu_s^2} \frac{d\mu^2}{\mu^2} \Gamma_{\text{cusp}}(\alpha_s(\mu^2)); \quad \Gamma_{\text{cusp}}(\alpha_s) = A(\alpha_s), \quad (5.8)$$

and \tilde{s}_{DY} has a perturbative expansion in powers of $\alpha_s(\mu^2)$. We finally have

$$U(M^2, \mu_s^2) = \exp \left\{ - \int_{M^2}^{\mu_s^2} \frac{d\mu^2}{\mu^2} \left[\Gamma_{\text{cusp}}(\alpha_s(\mu^2)) \log \frac{\mu^2}{M^2} - \gamma_W(\alpha_s(\mu^2)) \right] \right\} \quad (5.9)$$

which accounts RG evolution from the hard scale $\mu_h = M$ to the soft scale μ_s . Observe that $\Gamma_{\text{cusp}}(\alpha_s) = A(\alpha_s)$. We note that the choice of the soft scale μ_s determines the form of the logs, i.e. it determines what is being resummed.

We show in Tab. 5.1 the logarithmic accuracy of the SCET and the dQCD results and its dependence on the perturbative order of the relevant functions. In Refs. [40, 41, 42] the counting is performed at the level of exponents, which corresponds to the $N^k\text{LL}^*$ accuracy.

dQCD:	$A(\alpha_s)$	$D(\alpha_s)$	$\bar{g}_0(\alpha_s)$	accuracy: $\alpha_s^n \ln^k N$
SCET:	$\Gamma_{\text{cusp}}(\alpha_s)$	$\gamma_W(\alpha_s)$	H, \tilde{s}_{DY}	accuracy: $\alpha_s^n \ln^k(\mu_s/M)$
LL	1-loop	—	tree-level	$k = 2n$
NLL*	2-loop	1-loop	tree-level	$2n - 1 \leq k \leq 2n$
NLL	2-loop	1-loop	1-loop	$2n - 2 \leq k \leq 2n$
NNLL*	3-loop	2-loop	1-loop	$2n - 3 \leq k \leq 2n$
NNLL	3-loop	2-loop	2-loop	$2n - 4 \leq k \leq 2n$

Table 5.1: Orders of logarithmic approximations and accuracy of the predicted logarithms in dQCD and SCET. The last columns refers to the content of the coefficient function.

5.3 Comparison at NNLL

In this Section we will derive a master formula which relates the SCET and the dQCD result for a generic choice of the soft scale μ_s . An analytic comparison between the two approaches can be performed in N space, where dQCD admits a perturbative expansion in powers of the strong coupling α_s .

5.3.1 Drell-Yan production

The NNLL resummed expression in dQCD is given by Eq. (2.23), where

$$A(\alpha_s) = A_1\alpha_s + A_2\alpha_s^2 + A_3\alpha_s^3 + \mathcal{O}(\alpha_s^4), \quad (5.10)$$

$$D(\alpha_s) = D_1\alpha_s + D_2\alpha_s^2 + \mathcal{O}(\alpha_s^3), \quad (5.11)$$

$$\bar{g}_0(\alpha_s) = 1 + \bar{g}_{01}\alpha_s + \bar{g}_{02}\alpha_s^2 + \mathcal{O}(\alpha_s^3). \quad (5.12)$$

The analytical expressions for the coefficients A_i , D_i and \bar{g}_{0i} can be found in Appendix A. In Ref. [49] it was proven that

$$\begin{aligned} \bar{S}_{\text{dQCD}} \left(M^2, \frac{M^2}{\bar{N}^2} \right) &= \int_{M^2}^{\frac{M^2}{\bar{N}^2}} \frac{d\mu^2}{\mu^2} \left[A(\alpha_s(\mu^2)) \left(\log \frac{1}{\bar{N}^2} - \log \frac{\mu^2}{M^2} \right) + \hat{D}_2\alpha_s^2(\mu^2) \right] \\ &\quad + 2\zeta_2 \frac{C_F}{\pi} \alpha_s(M^2) \end{aligned} \quad (5.13)$$

where $\bar{N} = Ne^{\gamma_E}$ and

$$\hat{D}(\alpha_s) = \frac{1}{2}D(\alpha_s) - 2\zeta_2 \frac{C_F}{\pi} \beta_0 \alpha_s^2 = \hat{D}_2\alpha_s^2 + \mathcal{O}(\alpha_s^3). \quad (5.14)$$

The dQCD result can be therefore rewritten in the convenient form

$$C_{\text{dQCD}}(N, M^2) = \hat{g}_0(\alpha_s(M^2)) \exp \hat{S}_{\text{dQCD}} \left(M^2, \frac{M^2}{\bar{N}^2} \right) \quad (5.15)$$

where

$$\hat{g}_0(\alpha_s) = \bar{g}_0(\alpha_s) \exp \left[2\zeta_2 A(\alpha_s) + \frac{8}{3}\zeta_3 \beta_0 \frac{C_F}{\pi} \alpha_s^2 \right], \quad (5.16)$$

$$\hat{S}_{\text{dQCD}} \left(M^2, \frac{M^2}{\bar{N}^2} \right) = \int_{M^2}^{M^2/\bar{N}^2} \frac{d\mu^2}{\mu^2} \left[A(\alpha_s(\mu^2)) \log \frac{M^2}{\mu^2 \bar{N}^2} + \hat{D}(\alpha_s(\mu^2)) \right]. \quad (5.17)$$

We now turn to the SCET expression at NNLL. In order to compare the SCET expression to the perturbative QCD result, one has to perform a Mellin transform with respect to z . It is very important to observe that this Mellin transform has to be computed *at fixed* μ_s . Since all the z dependence is contained in the soft function $S(z, M^2, \mu_s^2)$ one has

$$\mathcal{M}[S(z, M^2, \mu_s^2)] = \tilde{s}_{\text{DY}} \left(\log \frac{M^2}{\mu_s^2} + \frac{\partial}{\partial \eta}, \mu_s \right) \frac{\Gamma(N - \eta) \Gamma(2\eta)}{\Gamma(N + \eta)} \frac{e^{-2\gamma_E \eta}}{\Gamma(2\eta)}. \quad (5.18)$$

In the large- N limit this expression turns into

$$\mathcal{M}[S(z, M^2, \mu_s^2)] = \tilde{s}_{\text{DY}} \left(\log \frac{M^2}{\mu_s^2} + \frac{\partial}{\partial \eta}, \mu_s \right) \bar{N}^{-2\eta} + \mathcal{O} \left(\frac{1}{N} \right). \quad (5.19)$$

The analytical comparison between dQCD and SCET of Refs. [49, 50] has been performed in this limit. However, we will investigate in next Chapter if these neglected terms will have any phenomenological effects.

The large- N limit of the SCET expression can be finally written as

$$C_{\text{SCET}}(N, M^2, \mu_s^2) = \hat{H}(M^2) E \left(\frac{M^2}{\bar{N}^2}, \mu_s^2 \right) \exp \hat{S}_{\text{SCET}}(N, M^2, \mu_s^2), \quad (5.20)$$

where

$$\hat{H}(M^2) = H(M^2) \exp \left[\frac{\zeta_2}{2} \frac{C_F}{\pi} \alpha_s(M^2) \right], \quad (5.21)$$

$$E \left(\frac{M^2}{\bar{N}^2}, \mu_s^2 \right) = \tilde{s}_{\text{DY}} \left(\log \frac{M^2}{\mu_s^2 \bar{N}^2}, \mu_s^2 \right) \exp \left[-\frac{\zeta_2}{2} \frac{C_F}{\pi} \alpha_s(\mu_s^2) \right], \quad (5.22)$$

$$\hat{S}_{\text{SCET}}(N, M^2, \mu_s^2) = \int_{M^2}^{\mu_s^2} \frac{d\mu^2}{\mu^2} \left[\Gamma_{\text{cusp}}(\alpha_s(\mu^2)) \log \frac{M^2}{\mu^2 \bar{N}^2} + \hat{\gamma}_W(\alpha_s(\mu^2)) \right] \quad (5.23)$$

and

$$\hat{\gamma}_W(\alpha_s) = \gamma_W(\alpha_s) - \frac{\zeta_2}{2} C_F \pi \beta_0 \alpha_s^2. \quad (5.24)$$

In particular, one has that $\hat{\gamma}_W(\alpha_s) = \hat{D}(\alpha_s)$ at this order.

The ratio $C_r(N, M^2, \mu_s^2)$ between the dQCD and the SCET expressions is defined from

$$C_{\text{dQCD}}(N, M^2) = C_r(N, M^2, \mu_s^2) C_{\text{SCET}}(N, M^2, \mu_s^2). \quad (5.25)$$

We find therefore that

$$C_r(N, M^2, \mu_s^2) = \frac{\hat{g}_0(\alpha_s(M^2))}{\hat{H}(M^2) E \left(\frac{M^2}{\bar{N}^2}, \mu_s^2 \right)} \exp \hat{S} \left(\mu_s^2, \frac{M^2}{\bar{N}^2} \right) \quad (5.26)$$

with

$$\hat{S}\left(\mu_s^2, \frac{M^2}{\bar{N}^2}\right) = \int_{\mu_s^2}^{\frac{M^2}{\bar{N}^2}} \frac{d\mu^2}{\mu^2} \left[A(\alpha_s(\mu^2)) \log \frac{M^2}{\mu^2 \bar{N}^2} + \hat{D}(\alpha_s(\mu^2)) \right]. \quad (5.27)$$

One sees that

$$\frac{\hat{g}_0(\alpha_s(M^2))}{\hat{H}(M^2)E(M^2, M^2)} = 1 + \mathcal{O}(\alpha_s^3(M^2)) \quad (5.28)$$

so that to NNLL accuracy

$$C_r(N, M^2, \mu_s^2) = \frac{E(M^2, M^2)}{E\left(\frac{M^2}{\bar{N}^2}, \mu_s^2\right)} \exp \hat{S}\left(\mu_s^2, \frac{M^2}{\bar{N}^2}\right). \quad (5.29)$$

Using Eq. (5.22) and the 2-loop expression of \tilde{s}_{DY} one has

$$E\left(\frac{M^2}{\bar{N}^2}, \mu_s^2\right) = 1 + E_1(L)\alpha_s(\mu_s^2) + E_2(L)\alpha_s^2(\mu_s^2) + \mathcal{O}(\alpha_s^3), \quad (5.30)$$

where

$$E_1(L) = \frac{A_1}{2} L^2, \quad (5.31)$$

$$\begin{aligned} E_2(L) = & \frac{A_1^2}{8} L^4 - \frac{L^3}{3} \frac{A_1}{2} \beta_0 + \frac{L^2}{2} A_2 + L \hat{D}_2 \\ & + \frac{C_A C_F}{\pi^2} \left[\frac{602}{324} + \frac{67}{144} \zeta_2 - \frac{3}{4} \zeta_2^2 - \frac{11}{72} \zeta_3 \right] \\ & + \frac{C_F n_f}{\pi^2} \left[-\frac{41}{162} - \frac{5}{72} \zeta_2 + \frac{\zeta_3}{36} \right], \end{aligned} \quad (5.32)$$

with

$$L \equiv \log \frac{M^2}{\mu_s^2 \bar{N}^2}. \quad (5.33)$$

In particular, $L = 0$ if the two arguments of E are equal to each other.

We observe that $C_r(N, M^2, \mu_s^2) = 1$ for $\mu_s = M/\bar{N}$, up to subleading (NNNLL*) terms. Therefore with this particular scale choice the SCET result reproduces the dQCD result to NNLL accuracy.

5.3.2 Higgs boson production

In the case of Higgs boson production an equivalent master formula which relates dQCD and SCET exists. The differences between the two process are limited to a rearrangement of color factors and different values of the process-dependent coefficient. In particular, the Higgs resummed coefficients in dQCD are related to the Drell-Yan coefficient by

$$A_k^{\text{Higgs}} = \frac{C_A}{C_F} A_k^{\text{DY}}, \quad D_k^{\text{Higgs}} = \frac{C_A}{C_F} D_k^{\text{DY}}. \quad (5.34)$$

On the other hand, the function \bar{g}_0 in the Higgs case is different from the function \bar{g}_0 in the Drell-Yan case; the first coefficients of its perturbative expansion can be found in Appendix A.

A similar argument also holds for the SCET expression in this case; the values of \tilde{s}_{Higgs} , Γ_{cusp} and γ_W are related to the analogous DY functions by a color factor rearrangement. However, the perturbative expansion of $H(M^2)$ is instead different from the DY one.

The dQCD result in case of Higgs production can be written as

$$C_{\text{dQCD}}(N, M^2) = \hat{g}_0(\alpha_s(M^2)) \exp \hat{S}_{\text{dQCD}} \left(M^2, \frac{M^2}{\bar{N}^2} \right) \quad (5.35)$$

where

$$\hat{g}_0(\alpha_s) = \bar{g}_0(\alpha_s) \exp \left[2\zeta_2 A(\alpha_s) + \frac{8}{3} \zeta_3 \beta_0 \frac{C_A}{\pi} \alpha_s^2 \right], \quad (5.36)$$

$$\hat{S}_{\text{dQCD}} \left(M^2, \frac{M^2}{\bar{N}^2} \right) = \int_{M^2}^{M^2/\bar{N}^2} \frac{d\mu^2}{\mu^2} \left[A(\alpha_s(\mu^2)) \log \frac{M^2}{\mu^2 \bar{N}^2} + \hat{D}(\alpha_s(\mu^2)) \right] \quad (5.37)$$

$$\hat{D}(\alpha_s) = \frac{1}{2} D(\alpha_s) - 2\zeta_2 \frac{C_A}{\pi} \beta_0 \alpha_s^2 = \hat{D}_2 \alpha_s^2 + \mathcal{O}(\alpha_s^3). \quad (5.38)$$

whereas the SCET result is

$$C_{\text{SCET}}(N, M^2, \mu_s^2) = \hat{H}(M^2) E \left(\frac{M^2}{\bar{N}^2}, \mu_s^2 \right) \exp \hat{S}_{\text{SCET}}(N, M^2, \mu_s^2), \quad (5.39)$$

where

$$\hat{H}(M^2) = H(M^2) \exp \left[\frac{\zeta_2}{2} \frac{C_A}{\pi} \alpha_s(M^2) \right], \quad (5.40)$$

$$E \left(\frac{M^2}{\bar{N}^2}, \mu_s^2 \right) = \tilde{s}_{\text{Higgs}} \left(\log \frac{M^2}{\mu_s^2 \bar{N}^2}, \mu_s^2 \right) \exp \left[-\frac{\zeta_2}{2} \frac{C_A}{\pi} \alpha_s(\mu_s^2) \right], \quad (5.41)$$

$$\hat{S}_{\text{SCET}}(N, M^2, \mu_s^2) = \int_{M^2}^{\mu_s^2} \frac{d\mu^2}{\mu^2} \left[\Gamma_{\text{cusp}}(\alpha_s(\mu^2)) \log \frac{M^2}{\mu^2 \bar{N}^2} + \hat{\gamma}_W(\alpha_s(\mu^2)) \right] \quad (5.42)$$

and

$$\hat{\gamma}_W(\alpha_s) = \gamma_W(\alpha_s) - \frac{\zeta_2}{2} C_A \pi \beta_0 \alpha_s^2. \quad (5.43)$$

In particular, also in this case one has that $\hat{\gamma}_W(\alpha_s) = \hat{D}(\alpha_s)$ at this order.

We have checked that also in this case

$$\frac{\hat{g}_0(\alpha_s(M^2))}{\hat{H}(M^2) E(M^2, M^2)} = 1 + \mathcal{O}(\alpha_s^3(M^2)) \quad (5.44)$$

so that to NNLL accuracy Eq. (5.29) holds, where in this case

$$E \left(\frac{M^2}{\bar{N}^2}, \mu_s^2 \right) = 1 + E_1(L) \alpha_s(\mu_s^2) + E_2(L) \alpha_s^2(\mu_s^2) + \mathcal{O}(\alpha_s^3), \quad (5.45)$$

where

$$E_1(L) = \frac{A_1}{2} L^2, \quad (5.46)$$

$$\begin{aligned} E_2(L) = & \frac{A_1^2}{8} L^4 - \frac{L^3}{3} \frac{A_1}{2} \beta_0 + \frac{L^2}{2} A_2 + L \hat{D}_2 \\ & + \frac{C_A^2}{\pi^2} \left[\frac{602}{324} + \frac{67}{144} \zeta_2 - \frac{3}{4} \zeta_2^2 - \frac{11}{72} \zeta_3 \right] \\ & + \frac{C_A n_f}{\pi^2} \left[-\frac{41}{162} - \frac{5}{72} \zeta_2 + \frac{\zeta_3}{36} \right], \end{aligned} \quad (5.47)$$

and L given by Eq. (5.33).

5.3.3 Master formula

We are interested in studying C_r for different scale choices, and in particular with the Becher-Neubert scale choice. It may result useful to recast C_r in a particularly transparent form suitable for analytic comparison by exponentiating the ratio

$$\frac{E(M^2, M^2)}{E\left(\frac{M^2}{N^2}, \mu_s^2\right)}. \quad (5.48)$$

This manipulation introduces terms of order α_s^3 or higher in the ratio, which does not spoil the NNLL accuracy. In this way we can find a final form of C_r which represents the irreducible difference between dQCD and SCET at NNLL accuracy. One has

$$\begin{aligned} \log \frac{E(M^2, M^2)}{E\left(\frac{M^2}{N^2}, \mu_s^2\right)} = & \alpha_s(\mu_s^2) A_1 \frac{L^2}{2} \\ & + \alpha_s^2(\mu_s^2) \left[\beta_0 \frac{A_1}{2} \frac{L^3}{3} - A_2 \frac{L^2}{2} - \hat{D}_2 L \right] + \mathcal{O}(\alpha_s^3). \end{aligned} \quad (5.49)$$

By using

$$\frac{L^{k+1}}{k+1} = \int_{\mu_s^2}^{M^2/\bar{N}^2} \frac{d\mu^2}{\mu^2} \log^k \frac{M^2}{\mu^2 \bar{N}^2}, \quad (5.50)$$

and taking the running of α_s into account, we get to

$$C_r(N, M^2, \mu_s^2) = \exp \int_{\mu_s^2}^{M^2/\bar{N}^2} \frac{d\mu^2}{\mu^2} \log \frac{M^2}{\mu^2 \bar{N}^2} [A(\alpha_s(\mu^2)) - A_1 \alpha_s(\mu^2) - A_2 \alpha_s^2(\mu^2)] \quad (5.51)$$

which is the final NNLL master dQCD-SCET comparison formula of Ref. [50]. We observe that, thanks to the exponentiation, the exponent in Eq. (5.51) is of order α_s^3 .

We remark however that a full numerical comparison between the SCET and dQCD results should rather be performed at first place by using the exact Mellin Eq. (5.18) and only at second place considering the large- N approximation which leads to Eqs. (5.29) and (5.51). Furthermore, one should also consider the effect of subleading terms which change between the expression

Eq. (2.23) and Eq. (5.15) (dQCD) and the Mellin of Eq. (5.6) without analytical manipulation and Eq. (5.20) (SCET). In the next Chapter we will perform such a systematic comparison which will enable us to understand the phenomenological effects of the analytical manipulations which lead to Eq. (5.20).

5.4 Comparison in hadronic space

We now move to the BN scale choice and we compare the dQCD and the SCET result in this case. The BN approach is based on the choice

$$\mu_s \sim M(1 - \tau) \quad (5.52)$$

which, as discussed in Chapter 4, provides a solution to the Landau pole problem. In the following argument we are interested on the logarithmics accuracy of the SCET result and therefore we will discuss the choice $\mu_s = M(1 - \tau)$ and we will not consider the more general choice $\mu_s = M(1 - \tau)g(\tau)$ discussed in Sect. 4.3. Since μ_s depends on a hadronic variable, a partonic comparison cannot be performed, and one must carry out the comparison at the level of hadronic cross-sections. We therefore consider

$$\sigma_{\text{dQCD}}(\tau, M^2) = \int_{\tau}^1 \frac{dz}{z} \mathcal{L}\left(\frac{\tau}{z}\right) C_{\text{QCD}}(z, M^2), \quad (5.53)$$

$$\sigma_{\text{SCET}}(\tau, M^2) = \int_{\tau}^1 \frac{dz}{z} \mathcal{L}\left(\frac{\tau}{z}\right) C_{\text{SCET}}(z, M^2, M^2(1 - \tau)^2) \quad (5.54)$$

where $C_{\text{dQCD}}(z, M^2)$ and $C_{\text{SCET}}(z, M^2, \mu_s^2)$ are the inverse Mellin transform of the N -space coefficient function Eqs. (5.15) and (5.20) and $C_{\text{SCET}}(z, M^2, \mu_s^2)$ has to be calculated as a Mellin transform at fixed μ_s . $C_{\text{dQCD}}(z, M^2)$ should be understood as the order-by-order Mellin inversion at a (arbitrarily high) finite order, since it is given by a divergent series in $\alpha_s(M^2)$. The dQCD cross-section can be written as

$$\sigma_{\text{dQCD}}(\tau, M^2) = \int_{\tau}^1 \frac{dz}{z} \sigma_{\text{SCET}}\left(\frac{\tau}{z}, M^2\right) C_r(z, M^2, M^2(1 - \tau)^2) \quad (5.55)$$

where $C_r(z, M^2, M^2(1 - \tau)^2)$ is the inverse Mellin transform of $C_r(N, M^2, M^2(1 - \tau)^2)$ carried out at fixed μ_s and evaluated at $\mu_s = M(1 - \tau)$.

$C_r(N, M^2, \mu_s^2)$ can be rewritten as

$$\begin{aligned} C_r(N, M^2, \mu_s^2) &= \frac{E(M^2, M^2)}{E(\mu_s^2, \mu_s^2)} \frac{E(\mu_s^2, \mu_s^2)}{E\left(\frac{M^2}{N^2}, \mu_s^2\right)} \exp \hat{S}\left(\mu_s^2, \frac{M^2}{N^2}\right) \\ &= \frac{E(M^2, M^2)}{E(\mu_s^2, \mu_s^2)} \left[1 + F_r\left(\alpha_s(\mu_s^2), \log \frac{M^2}{\mu_s^2 N^2}\right) \right], \end{aligned} \quad (5.56)$$

where $F_r\left(\alpha_s(\mu_s^2), \log \frac{M^2}{\mu_s^2 N^2}\right)$ is of order α_s^3 . Its inverse Mellin transform is [49]

$$C_r(z, M^2, \mu_s^2) = \frac{E(M^2, M^2)}{E(\mu_s^2, \mu_s^2)} \left[\delta(1 - z) + F_r\left(\alpha_s(\mu_s^2), 2 \frac{\partial}{\partial \xi}\right) \frac{(1 - \tau)^{-\xi} \log^{\xi-1} \frac{1}{z}}{e^{\gamma_E \xi} \Gamma(\xi)} \Big|_{\xi=0} \right] \quad (5.57)$$

Plugging this last expression into Eq. (5.55) we obtain

$$\sigma_{\text{dQCD}}(\tau, M^2) = \frac{E(\mu_s^2, \mu_s^2)}{E\left(\frac{M^2}{N^2}, \mu_s^2\right)} \left[\sigma_{\text{SCET}}(\tau, M^2) + F_r \left(\alpha_s(\mu_s^2), 2 \frac{\partial}{\partial \xi} \right) \Sigma(\tau, M^2, \xi) \Big|_{\xi=0} \right] \quad (5.58)$$

where

$$\begin{aligned} \Sigma(\tau, M^2, \xi) &= \frac{(1-\tau)^{-\xi}}{e^{\gamma_E \xi} \Gamma(\xi)} \int_{\tau}^1 \frac{dz}{z} \sigma_{\text{SCET}}\left(\frac{\tau}{z}, M^2\right) \log^{\xi-1} \frac{1}{z} \\ &= \sum_{k=0}^{\infty} c_k(\xi) \frac{d^k \sigma_{\text{SCET}}(\tau, M^2)}{d \log^k(1-\tau)} [1 + \mathcal{O}(1-\tau)] \end{aligned} \quad (5.59)$$

for $\mu_s = M(1-\tau)$. All the logarithmic enhancement are now contained in the ratio

$$\begin{aligned} \frac{E(M^2, M^2)}{E(\mu_s^2, \mu_s^2)} &= 1 + E_2(0)[\alpha_s^2(M^2) - \alpha_s^2(\mu_s^2)] + \dots \\ &= 1 + 4E_2(0)\beta_0\alpha_s^3(M^2)\log(1-\tau) + \mathcal{O}(\alpha_s^4). \end{aligned} \quad (5.60)$$

Therefore the leading difference between dQCD and SCET expressions is

$$\sigma_{\text{dQCD}}(\tau, M^2) - \sigma_{\text{SCET}}(\tau, M^2) = \sigma_{\text{SCET}}(\tau, M^2)[\alpha_s^3 4\beta_0 E_2(0)\log(1-\tau) + \dots] \quad (5.61)$$

where the ellipses stands for terms of relative order $\mathcal{O}(\alpha_s^3)$, without logarithmic enhancement, or terms of relative order $\mathcal{O}(\alpha_s^4)$.

The logarithmic counting is now based on counting powers of $\log(1-\tau)$. Since the SCET expression violates factorization, the difference between dQCD and SCET results is not universal and it depends on parton luminosity through σ_{SCET} . The cross-section σ_{SCET} contains in general leading log terms of form

$$\sigma_{\text{SCET}} \sim \alpha_s^k \log^{2k+p}(1-\tau) \quad (5.62)$$

where terms of order $\alpha_s^k \log^{2k}(1-\tau)$ comes from the coefficient function while terms of order $\alpha_s^k \log^p(1-\tau)$ are due to the parton luminosity.

If we set $p = 0$, which correspond to assume that the parton luminosity does not lead any logarithmic enhancement, the difference between dQCD and SCET is

$$\sigma_{\text{dQCD}} - \sigma_{\text{SCET}} \sim \alpha_s^h \log^{2h-5}(1-\tau); \quad h = k + 3 \quad (5.63)$$

which corresponds to a NNNLL* correction.

In conclusion, SCET and dQCD results differ by a luminosity-dependent term. The BN scale choice avoids the Landau pole problem but the price to pay is the introduction of logarithmically suppressed non-universal terms, in contrast with MP or BP which introduces respectively non universal, but more than power-suppressed terms or power-suppressed universal terms. Moreover, the parton distribution are expected to contain logarithmically enhanced contributions, which may lead the terms introduced by the BN scale choice to become leading or even super-leading.

Finally, when τ is far from threshold one has $\mu_s = M(1 - \tau) \sim M$ and therefore C_r is actually leading log. It was observed in Ref. [49] that this problem could be partially removed through generalizations of the scale μ_s which lead to values of μ_s far from the hard scale M ; these choices however do not change the log counting.

In order to obtain a full understanding of this state of affairs and to investigate the phenomenological implications of the results discussed in this Chapter it seems necessary to appeal to numerical methods. In the next Chapter we will discuss our strategies and we will perform a phenomenological comparison of the two approaches.

Resummation in SCET and in dQCD: a phenomenological comparison

In this Chapter we will perform a systematic comparison of soft-gluon resummation in SCET and in dQCD. In particular, we will present results for Higgs boson production in gluon-gluon fusion in a hadron-hadron collider.

As we have understood, phenomenological predictions in the two formalisms differ significantly in their implementation. The naivest way to compare the two approaches would basically consist of a τ -space comparison of the numerical results. With this results at hand, however, we would not gain any particular understanding of possible sources of differences between SCET and dQCD. On the other hand, we have seen in the previous Chapter how an analytic comparison can be performed in N -space and we have found master formulas which relate the two formalisms. For this reason, it would be of great interest to perform a comparison in τ space but armed with the analytic insight of Chapter 5. We will show how this can be done by means of a saddle-point method. Furthermore, we will show that a saddle-point argument allows the quantification of factorization violation effects in SCET. We will present the results we have obtained with this strategy and we will discuss some open issues which would be interesting to investigate further.

6.1 Comparison of the resummed results

In this Section we will compare the numerical predictions in SCET and in dQCD by looking at the total cross-section and at the K -factor which we have computed numerically. At first, we will show the predictions for the matched results. However, matching with fixed-order calculations reduces the differences between the resummed results; moreover, the analytic comparison of Chapter 5 involves the pure resummed coefficient functions. For this reason, we will move to resummed predictions and we will not consider the matching with the fixed-order.

In Fig. 6.1 we show the predictions for the total cross-section for Higgs boson production at LL, NLL and NNLL, with consistent matching with fixed-order results. The curves have been calculated with NNPDF23 NNLO PDF set in the large- m_t limit and $\alpha_s(m_Z) = 0.0117$. We observe that at LL accuracy the SCET result is larger than the dQCD result, but the situation changes as the logarithmic accuracy grows, and at NNLL accuracy the dQCD prediction is larger

than the SCET prediction. The predictions for the total cross-section in the two formalism can be made more transparent by comparing their ratio. In Fig. 6.2 we show the ratio of the dQCD prediction to the SCET prediction. We observe that at LL accuracy the dQCD prediction is about 10% lower than the dQCD one; at NLL accuracy the predictions are comparable, and at NNLL accuracy the SCET result is 3 – 4% lower than the dQCD result.

We show in Fig. 6.3 the ratio of the resummed predictions without matching with fixed-order results. We observe that in this case the dQCD prediction at NLL accuracy is about 5% larger than the SCET prediction and at NNLL accuracy the dQCD result is up to 15% larger for a light Higgs and more than 10% larger for a heavy Higgs.

From now on, we will not consider anymore the matched results and we will consider the resummed prediction in both formalism. The results obtained give a first feeling for the size of resummation in the two formalisms. However, a more detailed comparison will be carried out in the following Sections.

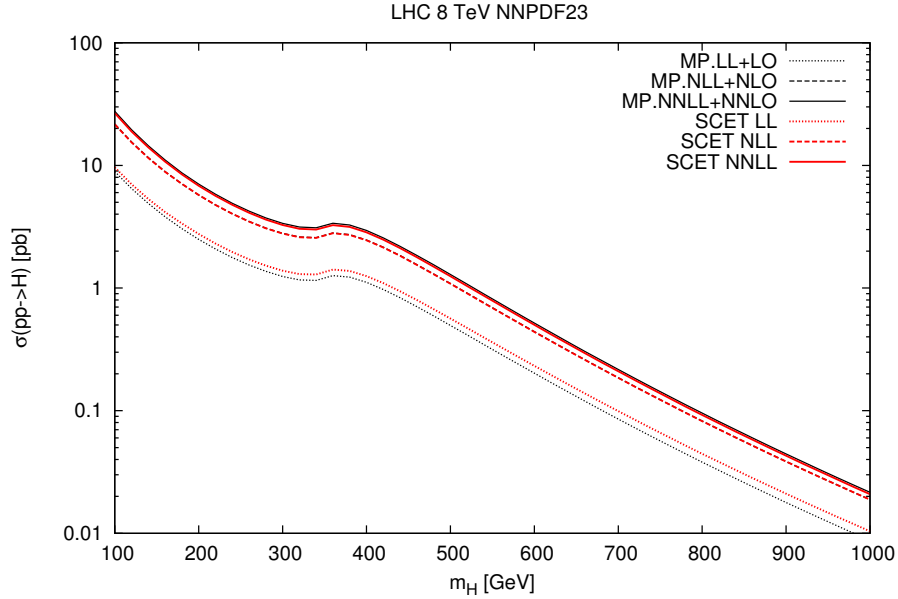


Figure 6.1: Predictions in SCET and in dQCD for the resummed cross-section as a function of the Higgs mass m_H at LL, NLL and NNLL at the LHC.

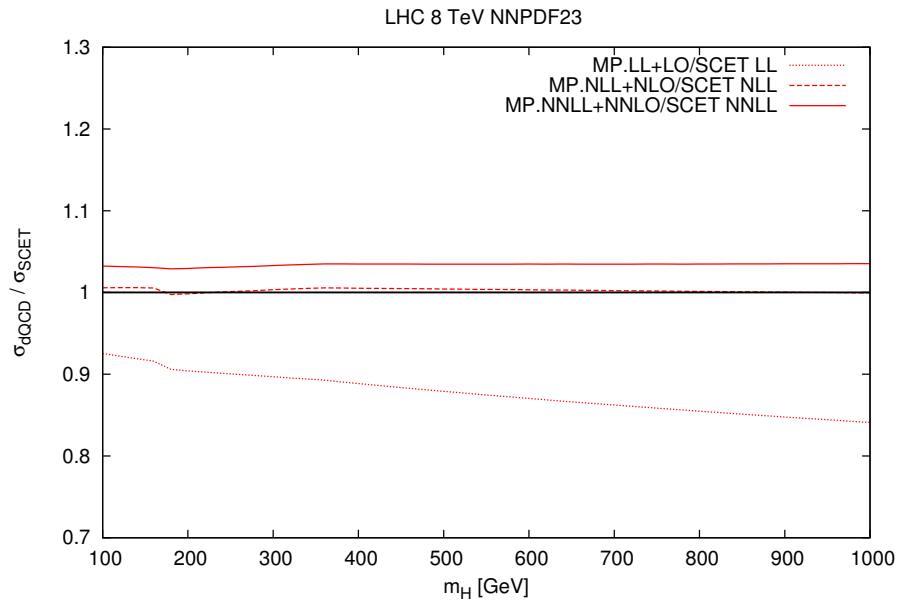


Figure 6.2: Ratio of the dQCD prediction to the SCET prediction for the total cross-section, matched with fixed-order results, as a function of the Higgs mass m_H at LL, NLL and NNLL at the LHC.

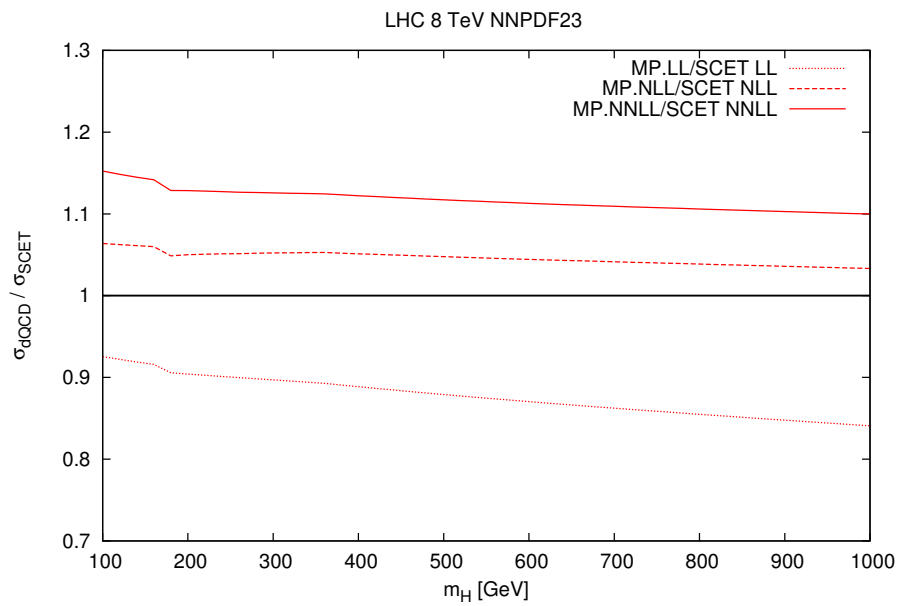


Figure 6.3: Ratio of the dQCD prediction to the SCET prediction for the total cross-section as a function of the Higgs mass m_H at LL, NLL and NNLL at the LHC, without matching with the fixed-order results.

6.2 The resummation region for $gg \rightarrow H$ production mechanism

In the previous Section we have shown a first comparison of the predictions for the cross-section in dQCD and in SCET. However, we learn very little from the previous results, which simply state how much the two approaches differ in their numerical predictions. For this reason, it would be interesting to find a new strategy which would let us study the differences between dQCD and SCET in more detail.

In this Section we will show that a saddle-point argument is particularly suited for this goal and it presents several advantages. First, through a saddle-point argument it is possible to estimate the region which is effected the most by resummation. Second, it is possible to perform a phenomenological comparison with hadronic variables and N -space expressions. Third, the approximate result obtained is very close to the exact result but requires a minimal amount of computational work. Fourth, by means of the saddle-point method it is possible to estimate the effects of factorization violation in SCET.

We will show in Sect. 6.2.1, by means of Mellin-space argument, how it is possible to determine the region of N which provides the dominant contribution to the cross-section. We will discuss how this argument can be applied in the SCET approach in Sect. 6.2.2. We will then apply this argument to Higgs production in gluon-gluon fusion and we will then show in Sect. 6.2.3 the goodness of our approximation by comparing our previous predictions with the results obtained with the saddle point argument. We will finally address the problem of the violation of factorization in SCET and we will try to quantify it in Sect. 6.2.4.

6.2.1 Saddle point argument

In Ref. [23, 52] it was shown that the logarithmic contribution to the coefficient function is sizable or even dominant for $N \gtrsim 2$ and it rapidly deviates from it as N gets smaller. This means that the region where logarithmic effects are important is wider than the region where $\alpha_s \log^2 N \sim 1$. In particular, in this region, where logarithmically enhanced terms behave in a perturbative way, they may lead to a substantial contribution.

As we have seen in Chapter 2, since the hadronic cross-sections are calculated as the convolution of the partonic cross-section with a parton luminosity, the effect of soft-gluon resummation can be relevant far from the hadronic threshold. This can be made quantitative using a saddle-point argument in N -space. More precisely, in Refs. [23, 52] it was shown that for a given process and for any given value of the hadronic ratio τ the cross-section receives the dominant contribution from a narrow range of N , the conjugate to τ upon Mellin transform. In particular, it was shown that the position of the saddle of the Mellin inversion integral is mostly determined by the parton luminosity and that it is not particularly sensitive to the non-perturbative shape of PDFs whereas it is mainly determined by the small- x (low- N) behaviour of the relevant Altarelli-Parisi splitting functions. In particular, if the splitting function has a fast small- x growth, then the average center of mass energy gets smaller and therefore the resummation can be relevant far from the hadronic threshold. In this case, threshold resummation is controlled by perturbative physics. We will see that since the saddle point is mostly determined by luminosity it may be quite large, even if $\tau \ll 1$. The region in which resummation is relevant is therefore extended to small values of τ .

We consider a suitable quantity σ for a hadronic process, related in a simple way to a cross-section or a distribution, characterized by a scale M^2 and a centre-of-mass energy $s = M^2/\tau$

which has the property of factorizing as

$$\sigma(\tau, M^2) = \int_{\tau}^1 \frac{dz}{z} \mathcal{L}(z) C\left(\frac{\tau}{z}, \alpha_s(M^2)\right) \quad (6.1)$$

in terms of a partonic coefficient function C and a parton luminosity

$$\mathcal{L}(z, \mu^2) = \int_z^1 \frac{dx}{x} f_1(x, \mu^2) f_2\left(\frac{z}{x}, \mu^2\right), \quad (6.2)$$

which in turn depends on parton distributions $f_i(x_i, \mu^2)$.

In general, σ receives different contributions from each of the parton channels which contribute in the process. This is however inessential for our discussion. We will concentrate on the dominant channel.

In Eq. (6.1) we recognize the partonic threshold, i.e. the region where the partonic coefficient function is enhanced and soft-gluon resummation is relevant, as the region where $\hat{s} = x_1 x_2 s$ (where $x_1 = x$ and $x_2 = z/x$) is close to M^2 . Since all the values of x_1 and x_2 between τ and 1 are accessible, the relevance of resummation depends on the dominant region in the convolution integral, which can be determined using a saddle point argument.

We consider the Mellin transform of $\sigma(\tau, M^2)$

$$\sigma(N, M^2) = \int_0^1 d\tau \tau^{N-1} \sigma(\tau, M^2), \quad (6.3)$$

with inverse

$$\sigma(\tau, M^2) = \frac{1}{2\pi i} \int_{c-i\infty}^{c+i\infty} dN \tau^{-N} \sigma(N, M^2) = \frac{1}{2\pi i} \int_{c-i\infty}^{c+i\infty} dN e^{E(\tau, N; M^2)} \quad (6.4)$$

where we have defined

$$E(\tau, N; M^2) \equiv N \log \frac{1}{\tau} + \log \sigma(N, M^2). \quad (6.5)$$

The function $E(\tau, N; M^2)$ always has a minimum on the real positive N axis at some N_0 , since $\sigma(N, M^2)$ is a decreasing function of N (the area below $\tau^{N-1} \sigma(\tau, M^2)$ decreases as N increases). Therefore the inversion integral is dominated by the region $N \sim N_0$, and it can be approximated by a saddle-point argument looking at the expansion of $E(\tau, N; M^2)$ around N_0 .

$E(\tau, N)$ has a minimum on the real N axis where $N = N_0(\tau)$, whith

$$E'(\tau, N_0(\tau)) = \log \frac{1}{\tau} + \frac{\sigma'(N_0(\tau), M^2)}{\sigma(N_0(\tau), M^2)} = 0, \quad (6.6)$$

where we have denoted with a prime the differentiation with respect to N . Hence the inversion integral can be approximated by

$$\begin{aligned} \sigma(\tau, M^2) &\approx \int_{c-i\infty}^{c+i\infty} dN e^{E(\tau, N_0(\tau)) + \frac{E''(\tau, N_0(\tau))}{2} (N - N_0(\tau))^2} \\ &= \frac{1}{\sqrt{2\pi}} \frac{e^{E(\tau, N_0(\tau))}}{\sqrt{E''(\tau, N_0(\tau))}} \end{aligned} \quad (6.7)$$

which has been calculated by changing the variable $N = N_0 + it$ and performing the gaussian integral.

It was shown in Refs. [23, 52] that the position of the saddle point for the fixed order cross-section in case of DY process and Higgs process is mostly determined by the PDFs and it is very much larger than the one calculated with only the coefficient function. As a consequence, the convolution with PDFs greatly enhances the impact of resummation and it extends it to a wider kinematic region.

The saddle-point strategy is particularly useful because it allows a transparent comparison of the SCET and the dQCD expression at the parton level. As we know, the SCET expression depends through μ_s on a hadronic scale τ . Since the SCET expression is no longer in the form of a convolution product, and therefore it does not factorize into a parton luminosity and a partonic cross-section, it is not immediate to perform a partonic comparison. However, through a saddle-point argument we can obtain an approximate factorized expression both for dQCD and SCET. By considering the first order of the saddle-point approximation we obtain

$$\begin{aligned}\sigma(\tau, M^2) &\approx \frac{1}{\sqrt{2\pi}} e^{E(\tau, N_0(\tau))} \\ &= \frac{1}{\sqrt{2\pi}} \tau^{-N_0(\tau)} \mathcal{L}(N_0(\tau), M^2) C(N_0(\tau), M^2).\end{aligned}\quad (6.8)$$

In this way the cross-section is factorized into a luminosity and a coefficient function, evaluated at the saddle-point N_0 . In the next Section we will discuss how the saddle-point argument can be used in SCET; however, it is clear that if one can obtain an analogous expression for the SCET case a partonic comparison could be possible.

6.2.2 The saddle point in SCET

In the previous Section we have seen how the saddle point depends on the Mellin transform of the cross-section $\sigma(\tau, M^2)$ Eq. (6.3). In Mellin space the cross-section calculated in dQCD factorizes in the product of the parton luminosity and a coefficient function:

$$\sigma(N, M^2) = \mathcal{L}(N, M^2) C(N, M^2). \quad (6.9)$$

This is not the case if one considers the Mellin transform of the SCET expression in the BN approach. In fact, since the BN choice of μ_s depends on the hadronic variable τ , the cross-section $\sigma(\tau, M^2)$ is not a convolution:

$$\sigma^{\text{SCET}}(\tau, M^2) = \int_{\tau}^1 \frac{dz}{z} \mathcal{L}(z) C\left(\frac{\tau}{z}, M^2, \mu_s^2(\tau)\right) \quad (6.10)$$

It is however possible to compute the Mellin transform of $\sigma^{\text{SCET}}(\tau, M^2)$ at fixed μ_s and then consider

$$\sigma^{\text{SCET}}(N, M^2; \tau) = \mathcal{L}(N, M^2) C(N, M^2, \mu_s^2(\tau)), \quad (6.11)$$

where with an abuse of notation we have denoted the the cross-section in N space as σ^{SCET} , even if it is not the Mellin transform of $\sigma^{\text{SCET}}(\tau, M^2)$. The cross-section can be calculated as

$$\sigma^{\text{SCET}}(\tau, M^2) = \frac{1}{2\pi i} \int_{c-i\infty}^{c+i\infty} dN \tau^{-N} \sigma^{\text{SCET}}(N, M^2; \tau) = \frac{1}{2\pi i} \int_{c-i\infty}^{c+i\infty} dN e^{E^{\text{SCET}}(\tau, N; M^2)} \quad (6.12)$$

keeping in mind that $\sigma^{\text{SCET}}(N, M^2; \tau)$ is not the Mellin transform of $\sigma^{\text{SCET}}(\tau, M^2)$ if μ_s depends on τ . Following the steps of the previous Section it is possible to look for the saddle-point of the integral Eq. (6.12). In this case $E^{\text{SCET}}(\tau, N)$ will have a minimum on the real N axis where $N = \bar{N}_0(\tau)$, whith

$$E^{\text{SCET}'}(\tau, \bar{N}_0(\tau)) = \log \frac{1}{\tau} + \frac{\sigma^{\text{SCET}'}(\bar{N}_0(\tau), M^2; \tau)}{\sigma^{\text{SCET}}(\bar{N}_0(\tau), M^2; \tau)} = 0, \quad (6.13)$$

where in principle $N_0(\tau) \neq \bar{N}_0(\tau)$.

We can now compare the saddle-point approximation of the cross-section in the two approaches, which at first order read:

$$\sigma^{\text{dQCD}}(\tau, M^2) \approx \frac{1}{\sqrt{2\pi}} \tau^{-N_0(\tau)} \mathcal{L}(N_0(\tau), M^2) C^{\text{dQCD}}(N_0(\tau), M^2) \quad (6.14)$$

$$\sigma^{\text{SCET}}(\tau, M^2) \approx \frac{1}{\sqrt{2\pi}} \tau^{-\bar{N}_0(\tau)} \mathcal{L}(\bar{N}_0(\tau), M^2) C^{\text{SCET}}(\bar{N}_0(\tau), M^2, \mu_s^2(\tau)). \quad (6.15)$$

If $N_0 = \bar{N}_0$ we conclude that

$$\frac{\sigma^{\text{dQCD}}(M^2, \tau)}{\sigma^{\text{SCET}}(M^2, \tau, \mu_s^2(\tau))} \simeq \frac{C^{\text{dQCD}}(M^2, \tau)}{C^{\text{SCET}}(M^2, \tau, \mu_s^2(\tau))} = C_r(N_0(\tau), M^2, \mu_s^2(\tau)). \quad (6.16)$$

It is therefore possible a comparison of the two approaches trough partonic expressions.

However, it is not obvious that the two saddle point should be equal. In fact we expect a very small difference between N_0 and \bar{N}_0 because the coefficient function in SCET and in dQCD are two different functions; however, a potentially bigger difference between the two saddle-point descends from the non-trivial dependence of C^{SCET} on the hadronic variable τ . By comparing the resulting expressions it is hence possible to investigate the factorization violation of the SCET result. The study of the saddle-point positions in dQCD and in SCET therefore allows one to quantify the violation of factorization in the SCET formalism. Since the dependence of the saddle-point is mostly determined by PDFs, we will find this violation small.

6.2.3 Results

In this Section we show the results obtained in the specific case of Higgs production in gluon-gluon fusion. In this particular case the quantity $\sigma(\tau, M^2)$ of Eq. (6.1) is

$$\sigma(\tau, M^2) = \frac{1}{\tau \sigma_0} \frac{d\sigma_{gg \rightarrow H}}{dM^2}(\tau, M^2). \quad (6.17)$$

We concentrate on the gg channel, which is dominant.

We determine the position of the saddle-point N_0 for the production of a Higgs boson of invariant mass $m_H = 125$ GeV in a pp collider, with a parton luminosity determined using NNPDF2.3 NNLO parton distributions with $\alpha_s(m_Z) = 0.117$. In Fig. 6.4 we show the saddle point determined using the resummed coefficient function Eq. (2.23) in dQCD and Eq. (4.35) in SCET with $\mu_h = \mu_t = \mu_f = m_H$ and choosing μ_s as the average value of the two scales μ_I and μ_{II} according to BN criteria. We will discuss below the consequences of such a choice. The saddle point has been determined in both plots using the NNLL resummed coefficient. The

vertical black line denotes the saddle-point region for a Higgs boson of 125 GeV produced in the LHC 14 TeV kinematics, where $\tau \sim 0.0001$, whereas the vertical purple line denotes the saddle-point region for a 125 GeV Higgs boson produced in the LHC 8 TeV kinematics where $\tau \sim 0.00025$. We find that in these particular kinematics settings the saddle point is close to the point $N = 2$, in good agreement with what was found using fixed-order partonic coefficient functions in Ref. [52]. We show in Fig. 6.5 the position of the saddle-point as a function of m_H in the LHC 8 TeV kinematics.

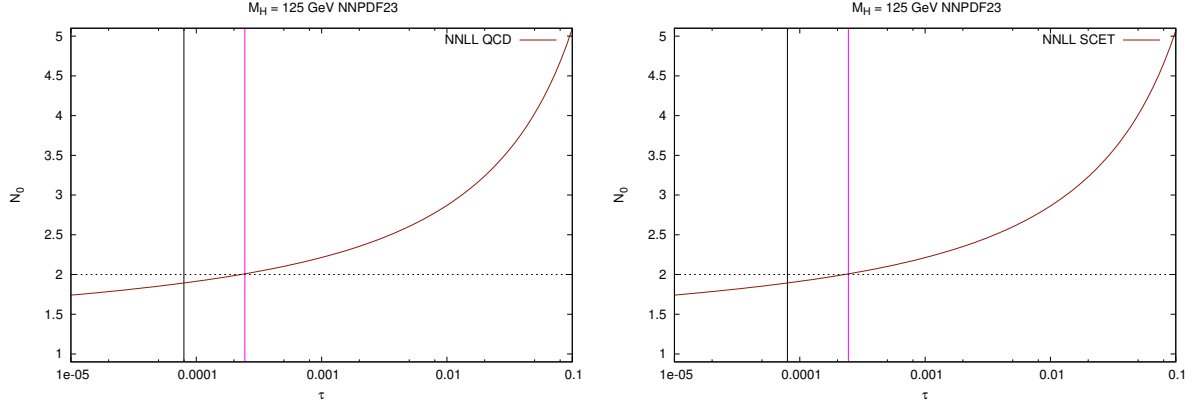


Figure 6.4: The position of the saddle-point N_0 for the Mellin inversion integral as a function of τ with $m_H = 125$ GeV using NNPDF2.3 NNLO parton distributions. Left: dQCD; right: SCET. The vertical black line marks the saddle point region when $\sqrt{s} = 14$ TeV whereas the vertical purple line marks the saddle point region when $\sqrt{s} = 8$ TeV. Left: dQCD; right: SCET.

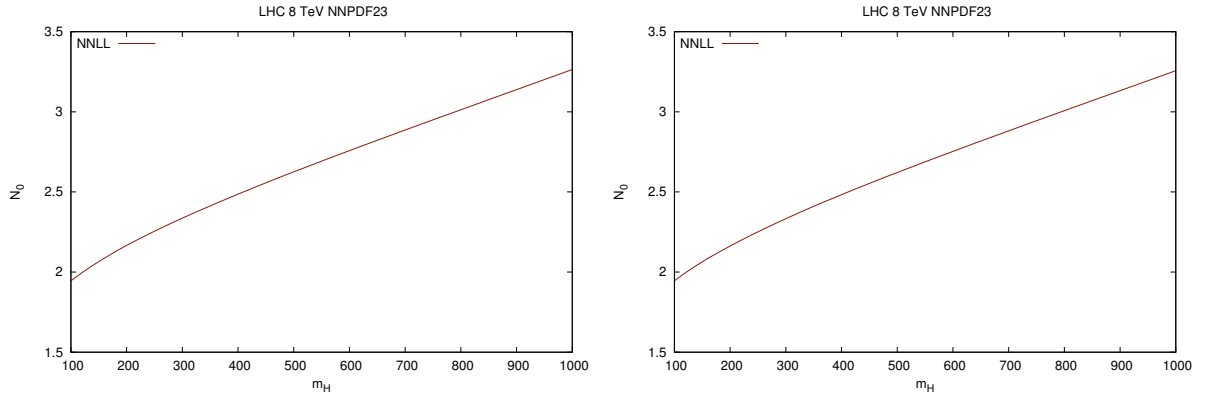


Figure 6.5: The position of the saddle-point N_0 for the Mellin inversion integral as a function of m_H with $\sqrt{s} = 8$ TeV using NNPDF2.3 NNLO parton distributions. Left: dQCD; right: SCET.

In Fig. 6.6 we show the position of the saddle obtained omitting the parton luminosity and omitting the coefficient function, in case of dQCD. As expected, the position of N_0 depends mostly on the behaviour of the parton distribution functions.

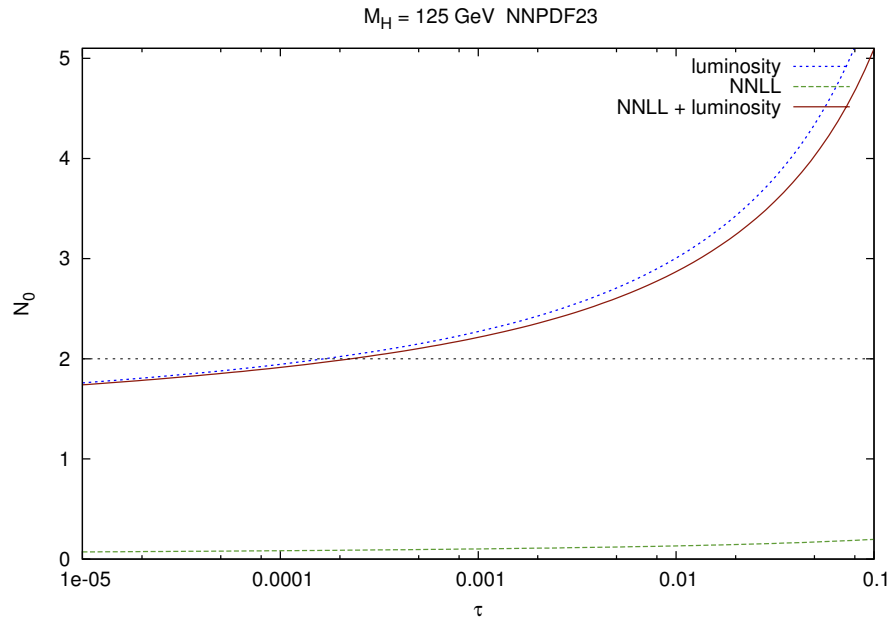


Figure 6.6: The position of the saddle-point N_0 for the Mellin inversion integral as a function of τ with $m_H = 125 \text{ GeV}$ using NNPDF2.3 NNLO parton distributions. Green dashed curve: position of the saddle point omitting the parton luminosity; blue dashed curve: position of the saddle point omitting the partonic coefficient function.

We note that the saddle-point depends weakly on the mass of the Higgs boson. In particular, we show in Fig. 6.7 the saddle-point as a function of τ with different values of the Higgs mass from 125 GeV to 1 TeV. The saddle-point has been calculated using the dQCD resummed coefficient with NNLL accuracy.

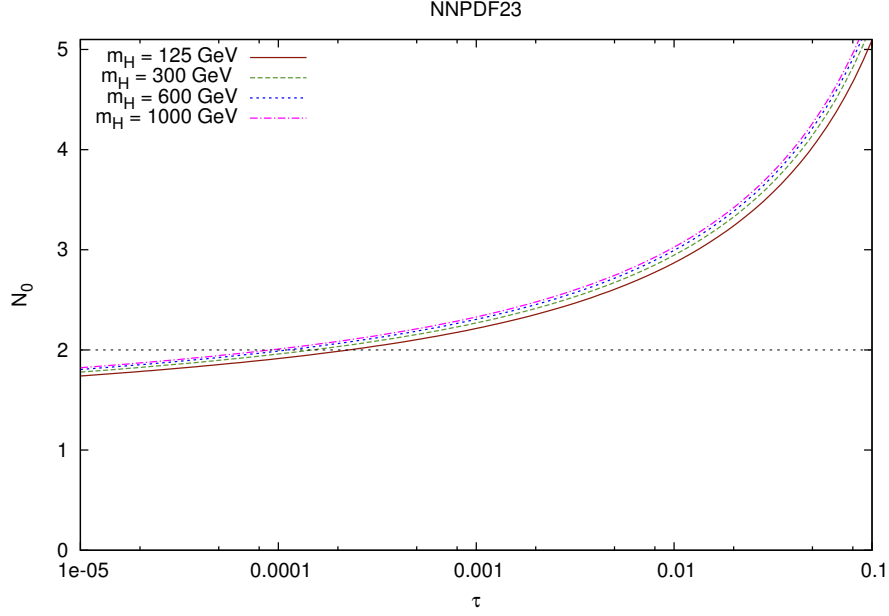


Figure 6.7: The position of the saddle-point N_0 for the Mellin inversion integral as a function of τ using NNPDF2.3 NNLO parton distributions, with different values of m_H .

In Figs. 6.8 we compare the results obtained for the resummed cross-section in dQCD and in SCET with the approximation Eq. (6.7). We observe that thanks to the saddle-point argument it is possible to obtain an approximation of the resummed cross-section with accuracy at the percent level on a wide mass range, both at NLL and NNLL. We observe that the saddle-point approximation has the same level of accuracy both for the SCET and dQCD; in both cases the value obtained with Eq. (6.7) slightly overestimates the exact value.

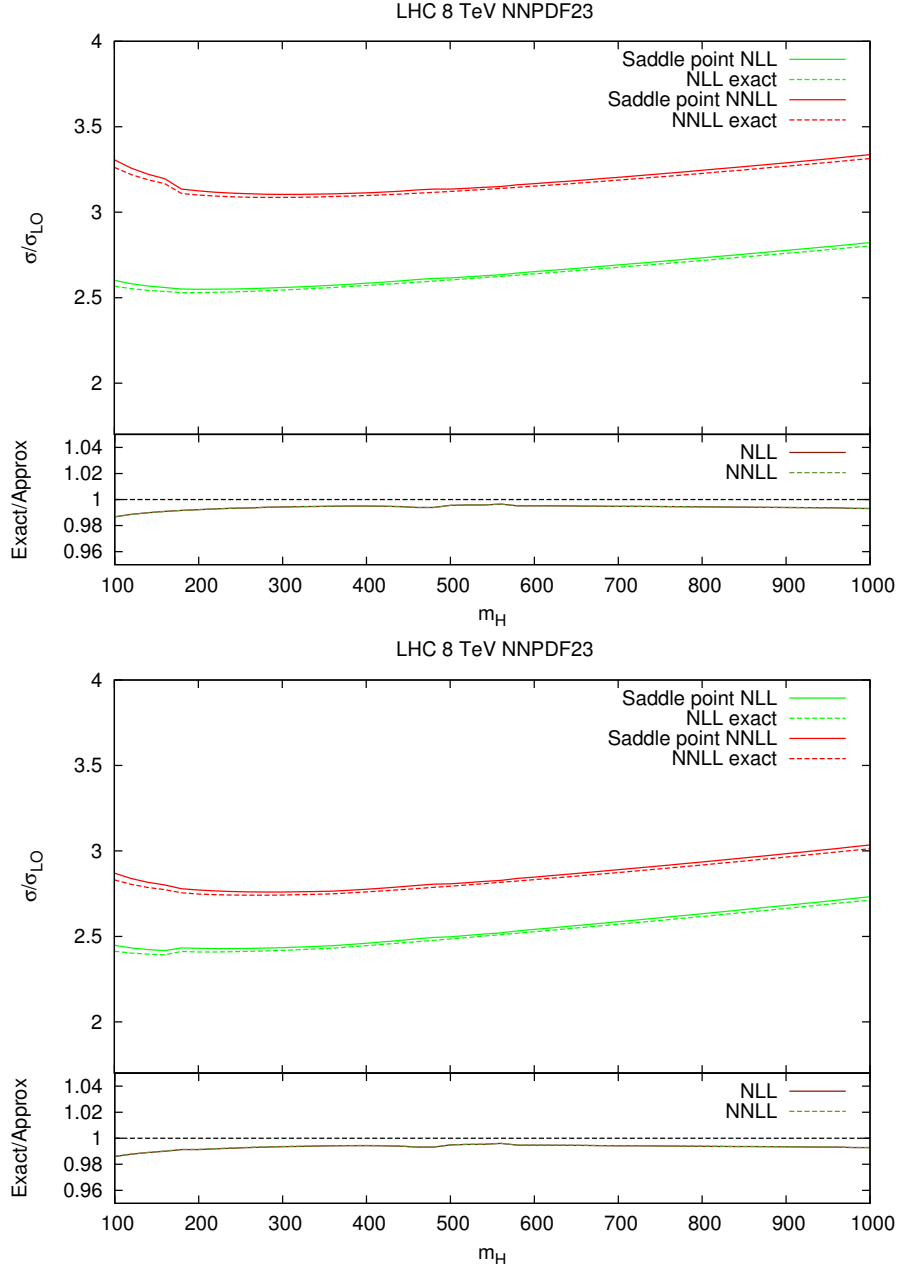


Figure 6.8: Upper plot: the exact K -factor for the resummed cross-section as a function of the Higgs mass m_H at NLL and NNLL compared with the K -factor calculated with the saddle point approximation Eq. (6.7) using NNPFD2.3 NNLO parton distributions, with $\sqrt{s} = 8$ TeV. Small lower plots: ratio between the exact and the approximate K -factor. Up: dQCD; low: SCET.

6.2.4 Factorization violation in SCET

In this Section we quantify the effect of violation of factorization in SCET by comparing the position of the saddle point of the SCET result to the position of the saddle point in dQCD. Since we have seen that the position of N_0 saddle depends very strongly on luminosity, we expect small effects.

In Fig. 6.9 we show a comparison of the position of the saddle point for the Mellin inversion integral as a function of τ and a Higgs boson mass of 125 GeV. We use the NNPDF2.3 NNLO PDF set and we compare the predictions obtained using the NNLL coefficient function. We observe that the saddle points differ by less than 1‰ for a large range of the variable τ and reach the level of 1‰ only for values of τ much larger than the interesting values at LHC. We have checked that the violation of factorization is negligible in a large τ range even for the production of a Higgs with a mass of the TeV order.

In Fig. 6.10 we show the position of the saddle point for SCET and dQCD as a function of the Higgs mass and with the center of mass energy equal to 8 TeV. We observe that also in this case the differences between the values of the saddle point is at the per thousand level for all the mass range considered.

We conclude that no significant difference exists between the position of the saddle point in the two approaches and that therefore the effects of the violation of factorization in SCET are indeed small.

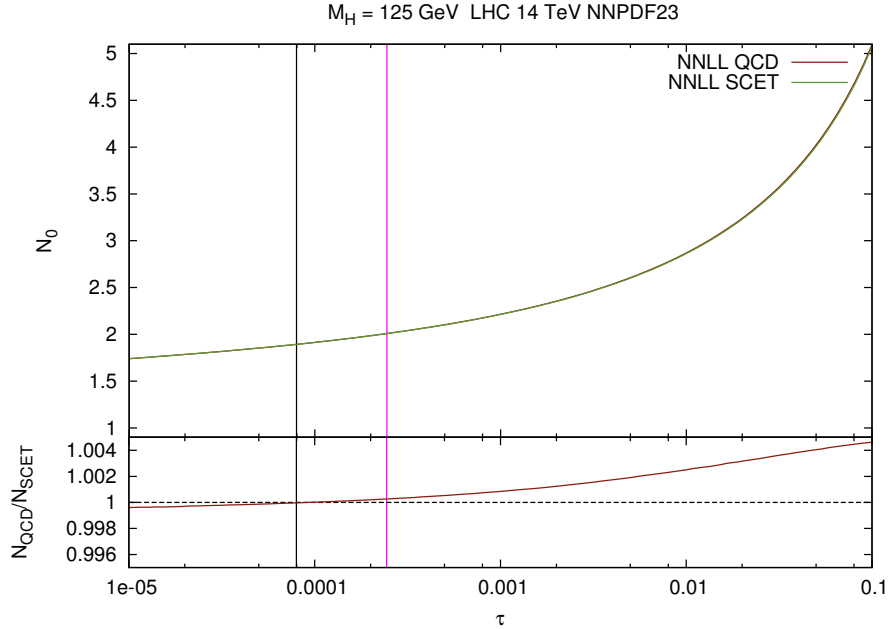


Figure 6.9: Upper plot: the position of the saddle-point N_0 for the Mellin inversion integral as a function of τ with $m_H = 125$ GeV using NNPDF2.3 NNLO parton distributions for dQCD and for SCET. Lower plot: ratio between the saddle point N_0^{dQCD} and N_0^{SCET} . The vertical black line marks the saddle point region when $\sqrt{s} = 14$ TeV whereas the vertical purple line marks the saddle point region when $\sqrt{s} = 8$ TeV.

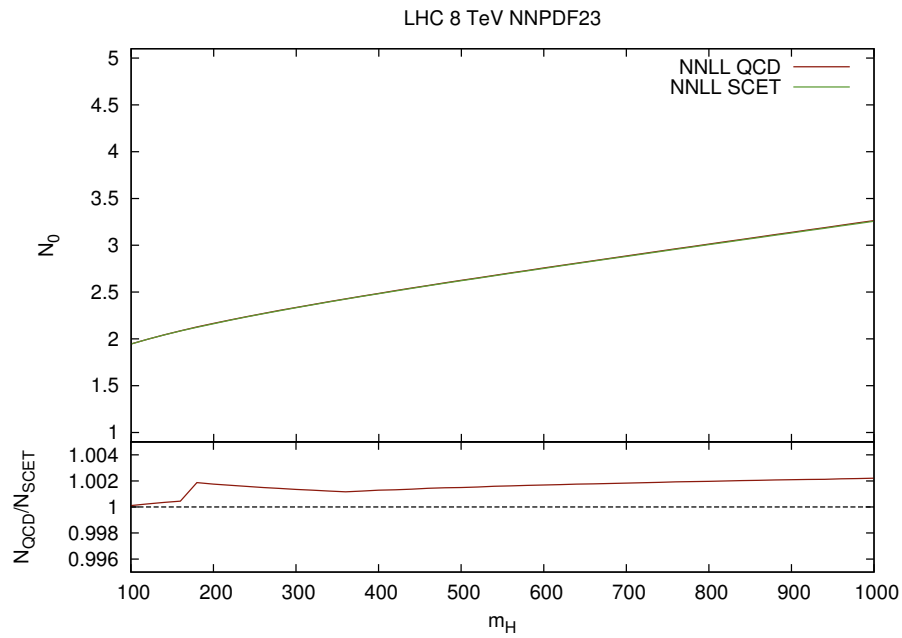


Figure 6.10: Upper plot: The position of the saddle-point N_0 for the Mellin inversion integral as a function of m_H with $\sqrt{s} = 8$ TeV using NNPDF2.3 NNLO parton distributions for dQCD and for SCET. Lower plot: ratio between the saddle point N_0^{dQCD} and N_0^{SCET} .

6.3 Higgs resummed results: N -space comparison

In the previous Section we have found a way to perform a phenomenological comparison between SCET and dQCD by using N -space expressions with hadronic variables. The study of N -space quantities can hence be used in order to obtain a better assesment of the differences between the two approaches. We are particularly interested in the study of the ratio between the dQCD resummed coefficient function and the SCET resummed coefficient function. We have observed that, thanks to the saddle-point argument, the difference between the predictions for the total cross-section can be related in an extremely simple way to $C_r(N, M^2, \mu_s^2)$.

By comparing the values of $C_r(N, M^2, \mu_s^2)$ to the ratio of the dQCD on the SCET cross-section we are therefore able on one hand to validate the saddle-point strategy and on the other hand to verify once more that the factorization violation is to all effects small. Moreover, we are able to quantify the consequences of the analytic manipulations of $C_r(N, M^2, \mu_s^2)$ and we are able to inspect the differences between SCET and dQCD at various levels.

We show in Fig. 6.11 the partonic coefficients functions both for SCET and for dQCD, evaluated at $N_0(\tau)$, as a function of the Higgs mass m_H at NLL and at NNLL accuracy. We observe that both at NLL and at NNLL accuracy the dQCD coefficient functions are bigger than the SCET coefficient functions; however, we observe that whereas the difference is small at NLL accuracy, it gets above the 10% level at NNLL accuracy. For this numerical evaluation we have used the dQCD expression Eq. (2.23) and the exact N -space Mellin transform of Eq. (4.35) with $\mu_t = \mu_h = \mu_f = m_H$ and μ_s equal to the average value of the two scales μ_I and μ_{II} , which are chosen according to the Becher-Neubert criteria.

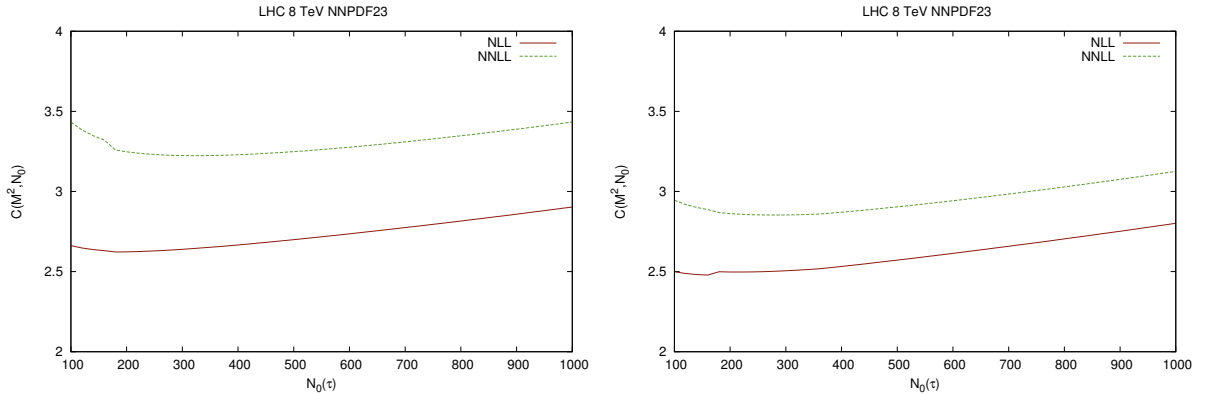


Figure 6.11: The partonic coefficient function evaluated in the saddle point N_0 as a function of the Higgs mass m_H at NLL and NNLL accuracy. Left: dQCD; right: SCET.

We show in Fig. 6.12 the value of $C_r(N_0(\tau), M^2, \mu_s^2)$ as a function of the Higgs mass m_H at NLL accuracy and at NNLL accuracy. The value of $C_r(N_0(\tau), M^2, \mu_s^2)$ is evaluated as the ratio of the partonic coefficient function depicted in Fig. 6.11. We will study how the value of C_r is modified by the manipulations of Chapter 5 in Sect. 6.4.1. We observe that the value of C_r is about 1.05 at NLL accuracy and is about 1.15 at NNLL accuracy, i.e. the effect of resummation is higher in dQCD than in SCET.

We show in Fig. 6.13 the ratio of the dQCD cross-section to the SCET cross-section compared with the value of $C_r(N_0(\tau), M^2, \mu_s^2)$ as a function of the Higgs mass m_H at NLL accuracy and

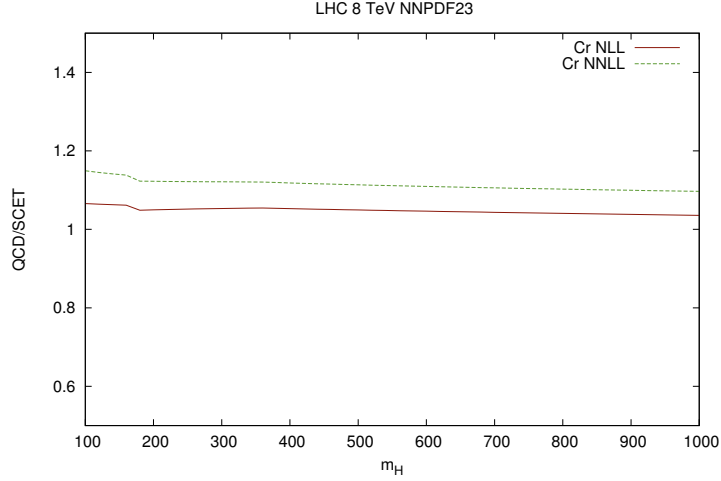


Figure 6.12: $C_r(N_0(\tau), M^2, \mu_s^2)$ as a function of the Higgs mass m_H at NLL and NNLL accuracy.

at NNLL accuracy. In both cases we have chosen μ_s as the average value of the two soft scales proposed by Becher and Neubert in Ref. [42]. In the lower plot we show the ratio of the two values. We observe that the results are in remarkable agreement both at NLL and at NNLL.

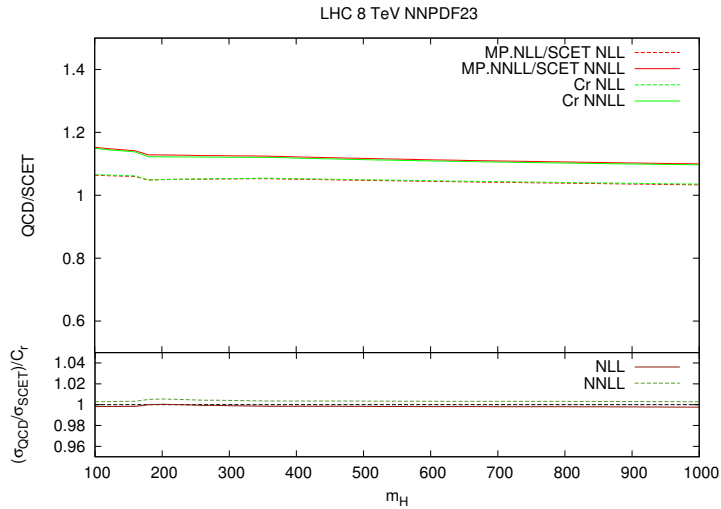


Figure 6.13: Upper plot: the ratio of the dQCD cross-section to the SCET cross-section compared with the value of $C_r(N_0(\tau), M^2, \mu_s^2)$ as a function of the Higgs mass m_H at NLL accuracy and at NNLL accuracy. Lower plot: ratio of the two curves at NLL accuracy and at NNLL accuracy.

6.4 Detailed comparison

In the previous Section we have compared the numerical predictions obtained in the SCET and in the dQCD approaches. We have observed that at NNLL accuracy the results differ at 15% level and we have traced this difference to the value of $C_r(N, M^2, \mu_s^2)$ evaluated at the saddle point N_0 . Now we would like to understand the origin of this difference. This will be done in two steps.

First, we would like to concentrate on the analytic comparison of Chapter 5. After some analytical manipulations, we have found the final NNLL master dQCD-SCET comparison formula Eq. (5.51). However, we would like to better understand the consequences of those analytical manipulation.

Second, we would like to investigate the phenomenological consequences of the BN scale choice. Since the soft scale μ_s determines what is being resummed, it is important to understand the effect of the factors which lead to values of μ_s far from the hard scale thus determining the resummation enhancement. We address these problems in this Section.

6.4.1 Connection with the analytical comparison

In Sect. 5.3.3 we have obtained a master formula which relates SCET and dQCD. In particular, we have defined the ratio $C_r(N, M^2, \mu_s^2)$ as

$$C_{\text{dQCD}}(N, M^2) = C_r(N, M^2, \mu_s^2) C_{\text{SCET}}(N, M^2, \mu_s^2). \quad (6.18)$$

We have shown in the previous Section the values of $C_r(N, M^2, \mu_s^2)$ computed as the exact ratio of the dQCD and the SCET expression at NNLL, without any analytical manipulation, and we have found that the value of C_r is about 1.15.

However, all the master formulas of Chapter 5, which relate the SCET and dQCD results, were obtained using the large- N limit of the SCET expression. In particular, the exact Mellin transform of the soft function

$$\mathcal{M}[S(z, M^2, \mu_s^2)] = \tilde{s} \left(\log \frac{M^2}{\mu_s^2} + \frac{\partial}{\partial \eta}, \mu_s \right) \frac{\Gamma(N - \eta) \Gamma(2\eta)}{\Gamma(N + \eta)} \frac{e^{-2\gamma_E \eta}}{\Gamma(2\eta)} \quad (6.19)$$

in the large- N limit becomes

$$\mathcal{M}[S(z, M^2, \mu_s^2)] = \tilde{s} \left(\log \frac{M^2}{\mu_s^2} + \frac{\partial}{\partial \eta}, \mu_s \right) \bar{N}^{-2\eta} + \mathcal{O} \left(\frac{1}{N} \right). \quad (6.20)$$

We have seen in Sect. 6.2.3 that the value of the saddle point N_0 lies between 2 and 3. Therefore one may ask whether the large- N limit is a good approximation or not. We will see that the large- N limit does indeed make a difference.

We will finally show the value of $C_r(N, M^2, \mu_s^2)$ Eq. (5.51), which is the final NNLL master dQCD-SCET comparison formula of Ref. [50]. This corresponds to the irreducible difference between the two approaches provided that SCET and dQCD are treated exactly in the same way up to NNNLL* terms. However, since SCET does not exponentiate all the resummed terms, which are contained both in the evolution function U and in soft function S , we expect a difference between this last master formula and the value of C_r evaluated as the ratio of the

dQCD resummed coefficient function Eq. (2.23) and the Mellin transform of the SCET resummed coefficient function Eq. (4.35) in the large- N limit.

Our results are collected in Fig. 6.14 and in Fig. 6.15. In particular, we show in Fig. 6.14 the value of $C_r(N_0, M^2, \mu_s^2)$ as a function of the Higgs mass m_H and center-of-mass energy of 8 TeV and in Fig. 6.15 the value of $C_r(N_0, M^2, \mu_s^2)$ as a function of τ with $m_H = 125$ GeV. We observe that in the large- N limit the value of C_r is about 0.98, which corresponds to a difference of almost 20% with respect to the value of C_r computed with the exact Mellin transform of the SCET coefficient function. The value of C_r computed as Eq. (5.51) is almost equal to 1, the difference being well below 1% percent. It appears from Fig. 6.14 that there is a small dependence on mass for the large- N and for the final C_r , whereas the exact Mellin C_r gets closer to 1 as the mass grows. This behaviour can be easily understood since the larger is the Higgs mass, the bigger is the saddle-point N_0 , the closer is the value of the exact Mellin to the large- N C_r . One observes the same dependence, this time on τ , in Fig. 6.15.

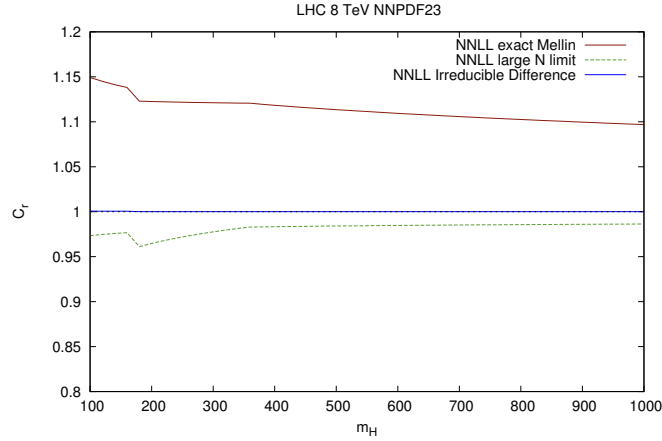


Figure 6.14: $C_r(N_0(\tau), M^2, \mu_s^2)$ as a function of the Higgs mass m_H in different approximations.

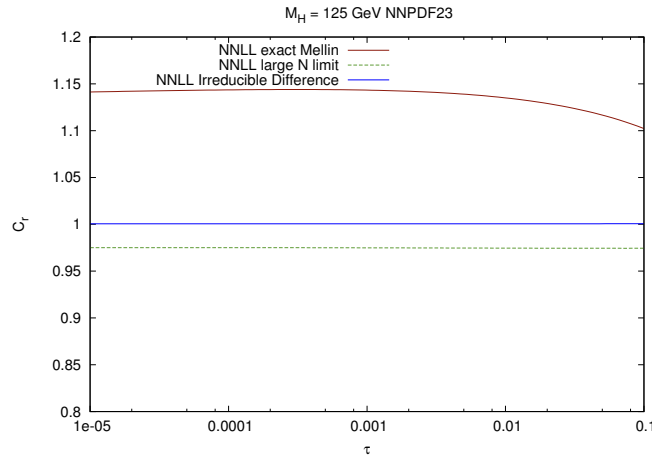


Figure 6.15: $C_r(N_0(\tau), M^2, \mu_s^2)$ as a function of τ in different approximations.

We have seen that the main difference between SCET and dQCD is due to the fact that the two approaches treat differently the subleading terms. If we move back to z space, we can compare the soft function S in the original formalism, namely

$$S(z, M^2, \mu_s^2) = \tilde{s} \left(\log \frac{M^2}{\mu_s^2} + \frac{\partial}{\partial \eta}, \mu_s \right) \frac{1}{1-z} \left(\frac{1-z}{\sqrt{z}} \right)^{2\eta} \frac{e^{-2\gamma_E \eta}}{\Gamma(2\eta)} \quad (6.21)$$

to the soft function in the large N limit

$$S(z, M^2, \mu_s^2) = \tilde{s} \left(\log \frac{M^2}{\mu_s^2} + \frac{\partial}{\partial \eta}, \mu_s \right) (-\log z)^{-1+2\eta} \frac{e^{-2\gamma_E \eta}}{\Gamma(2\eta)}. \quad (6.22)$$

In particular, we observe that in the first case the action of the η derivative produces logs of z , whereas in the second case it produces logs of $\log(z)$. Note that

$$(-\log z)^{-1+2\eta} = \sqrt{z} \frac{z^{-\eta}}{(1-z)^{1-2\eta}} [1 + \mathcal{O}((1-z)^2)]. \quad (6.23)$$

Therefore, different classes of logs are resummed. These choices are equivalent from the point of view of resummation, as they differ by subleading terms. Nevertheless, the difference in their effects on the prediction is not negligible.

In order to assess the impact of the subleading terms, we show in Fig. 6.16 the value of $C_r(N, M^2, \mu_s = M/\bar{N})$, computed as the exact ratio of the dQCD and the SCET expression, without any analytical manipulation, at LL, NLL, NNLL, compared to the value of $C_r(N, M^2, \mu_s = M/\bar{N})$ in the large- N limit at the same logarithmic accuracy, as a function of N . We note that the result is close to 1 only at NNLL, where the effect of the subleading terms is smaller. However, we note that for small N the difference between curves with different logarithmic accuracy is comparable, or even smaller, than the difference between the curves evaluated at the same logarithmic accuracy but which differ by $\mathcal{O}(1/N)$ terms.

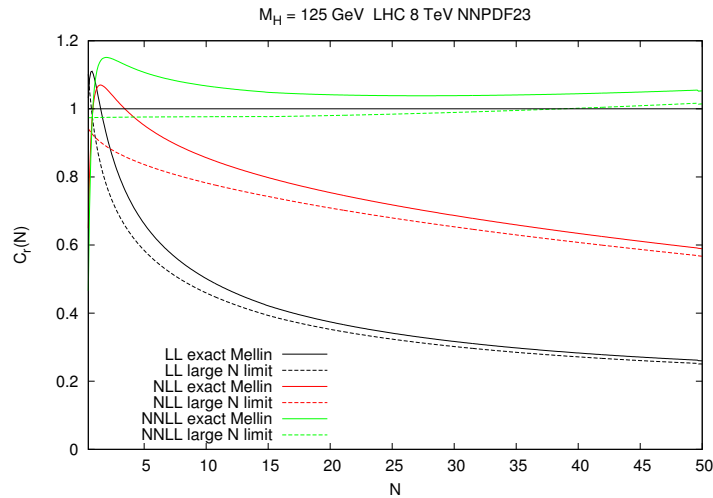


Figure 6.16: Exact $C_r(N, M^2, \mu_s^2 = M^2/\bar{N}^2)$ and large- N $C_r(N, M^2, \mu_s^2 = M^2/\bar{N}^2)$ as a function of N at LL, NLL and NNLL accuracy.

6.4.2 The Becher-Neubert scale choice

The Becher-Neubert scale choice is

$$\mu_s = M(1 - \tau)g(\tau) \quad (6.24)$$

where the function $g(\tau)$ is chosen in order to minimize the contributions of \tilde{s} to the cross-section according to the two criteria discussed in Sect. 4.3. If τ is small, as for Higgs production at the LHC, the naive choice $\mu_s = M(1 - \tau)$ would not enhance the cross-section, by construction of SCET. The value of the factors hence determines the impact of soft-gluon resummation in the SCET formalism by rescaling the soft scale to a value which is smaller than the hard scale M . In this Section we inspect the phenomenological consequences of such a choice.

We know that with the choice $\mu_s = M/\tilde{N}$ the SCET results in the large N limit reproduce the dQCD results. Therefore it is natural to compare the BN soft scale with the scale $\mu_s = M/\tilde{N}_0$. In Fig. 6.17 we show the values of different choices of the soft scale μ_s as a function of the Higgs mass m_H , with centre-of-mass energy of 8 TeV. We observe that the soft scale is almost equal to the Higgs mass m_H if the naive choice $\mu_s = m_H$ is made. However, if μ_s is chosen according to the two criteria proposed by Becher and Neubert, we find that the value of the soft scale gets closer to the value $\mu_s = M/\tilde{N}_0$ depicted in red in Fig. 6.17. We show in Fig. 6.18 the values of the same choices of the soft scale as a function of τ and with $m_H = 125$ GeV. We observe that the naive choice leads to a almost constant value of μ_s except for large values of τ . The Becher-Neubert choice on the other hand lies closer to the choice $\mu_s = M/\tilde{N}_0$.

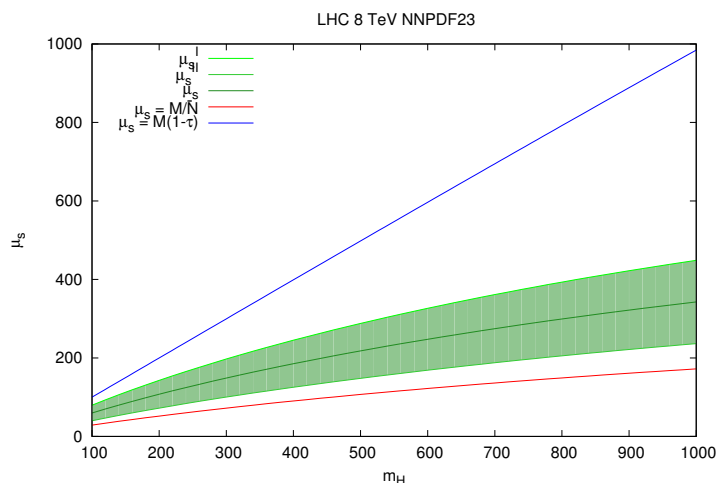


Figure 6.17: Values of different choices of the soft scale μ_s as a function of the Higgs mass m_H , with centre-of-mass energy of 8 TeV.

We expect therefore a small difference between the results obtained with the BN scale choice and the results obtained with the choice $\mu_s = M/\tilde{N}_0$. In Fig. 6.19 we compare the value of the large- N limit $C_r(N_0(\tau), M^2, \mu_s^2)$ and of the final $C_r(N_0(\tau), M^2, \mu_s^2)$ computed with the BN choice of μ_s and with the choice $\mu_s = M/\tilde{N}_0$ as a function of τ . We show results at NNLL accuracy evaluated with $m_H = 125$ GeV. We observe that the difference is indeed very small.

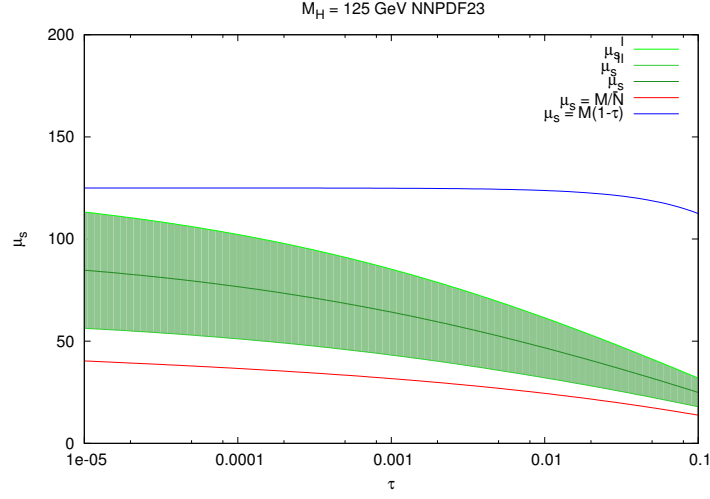


Figure 6.18: Values of different choices of the soft scale μ_s as a function of τ , with $m_H = 125$ GeV.

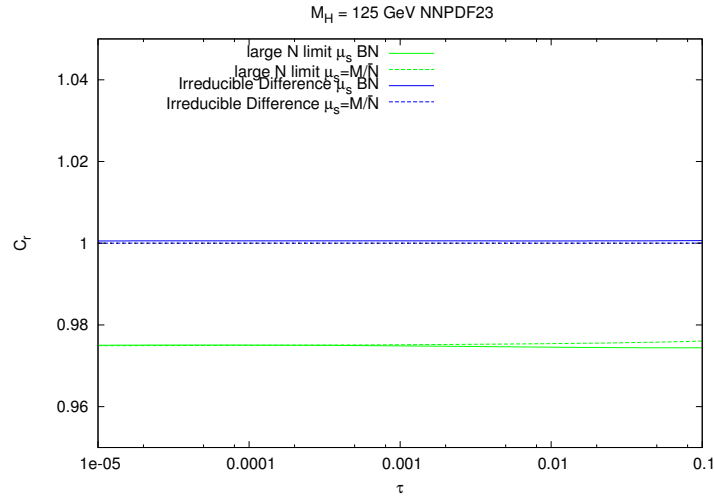


Figure 6.19: Value of the large- N limit $C_r(N_0(\tau), M^2, \mu_s^2)$ and of the final $C_r(N_0(\tau), M^2, \mu_s^2)$ computed with the BN choice of μ_s and with the choice $\mu_s = M/\bar{N}_0$ as a function of τ .

It is natural to ask why the BN choice is not dissimilar from the choice $\mu_s = M/\bar{N}_0$. A simple qualitative argument provides the answer to this question. The Mellin transform of the soft function reads

$$\mathcal{M}[S(z, M^2, \mu_s^2)] = \left[1 + \frac{C_A}{2\pi} \alpha_s(\mu_s^2) \left(\log^2 \frac{M^2}{\mu_s^2 \bar{N}^2} + \frac{\pi^2}{6} \right) \right] \bar{N}^{-2\eta} + \mathcal{O}\left(\frac{1}{\bar{N}}\right). \quad (6.25)$$

According to the BN criteria, μ_s is chosen in order to minimize the contributions of \tilde{s} to the cross-section. Since the integral is very well approximated by its value in the saddle point, we conclude by looking at Eq. (6.25) that a value of $\mu_s \sim M/\bar{N}_0$ does indeed minimize the first loop collection of \tilde{s} . Some difference persists because of the shift induced by the constant $\frac{\pi^2}{6}$ and, more subtly, by the fact that in the SCET approach one has to consider the exact Mellin of the SCET moment-space coefficient function.

6.4.3 Summary and outlook

In Sect. 6.2.4 we have shown that the factorization violation effects in SCET are to all practical purposes negligible for a large range of τ . Thanks to a saddle point argument, we have hence been able to relate the difference between the SCET and dQCD predictions to the value of $C_r(N, M^2, \mu_s^2)$ in the saddle point N_0 . We have therefore performed a detailed comparison of soft gluon resummation in SCET and in dQCD.

We have first concentrated on the analytical structure of the SCET and the dQCD result and we have assessed the impact of the subleading terms with the choice $\mu_s = M/\bar{N}$, with which SCET reproduces the standard dQCD results. In particular, we have shown that for small N the difference between the curves evaluated at the same logarithmic accuracy, but which differ by $\mathcal{O}(1/N)$ terms (which we will call subdominant terms), is significant, and is greater than the difference between predictions at different logarithmic accuracy. The situation changes as N grows, where the effect of the subleading terms is greater than the effect of the subdominant terms up to NNLL accuracy.

However, in SCET one resums logs of μ_s which is chosen according to BN criteria. We have therefore compared the BN scale choice to the choice $\mu_s = M/\bar{N}$. We have seen that the difference is small and that the BN choice is similar to the choice $\mu_s = M/\bar{N}_0$. However, we would like to obtain a better understanding of the factors which reduce the value of the soft scale μ_s . In particular, we would like to understand how the choice of μ_s according to BN criteria changes as the mass grows. In this way the value of the saddle point would be in the large- N region, which we have not studied in detail.

In conclusion, we have found that the main difference between SCET and dQCD resummed result is due to subdominant terms. Therefore a significant ambiguity in the resummation procedure exists. One may conclude therefore that resummation cannot be used. However, a possible way out of the ambiguity due to the choice of the subleading terms consists in the comparison of the results which differ by vanishing terms in the large- N limit to the fixed order result. We mean to further clarify this issues with further analytical analysis as a prosecution of this Thesis.

Conclusions

In this Thesis we have presented a systematic comparison of soft-gluon resummation in the more standard dQCD approach and in a SCET approach. We have focused on Higgs boson production in gluon-gluon fusion. We now summarize our main results.

From the theoretical point of view, we have verified that the results of Refs. [49, 50] can be straightforwardly extended to Higgs boson production in gluon-gluon fusion. We have then tackled the challenge of performing a phenomenological comparison between the dQCD and the SCET resummed result on various levels.

We have developed a strategy which allows for a comparison between the SCET and dQCD expressions by means of partonic expressions, for which an analytical comparison can be performed in an easier way, despite the fact that the SCET result depend on hadronic variables. This comparison can be performed provided the fact that the effect of violation of factorization in SCET is small. Our results have indeed confirmed that this effect is negligible. Furthermore, our strategy allows to obtain resummed cross-section with a minimal amount of computational work and with very good accuracy.

We have reduced the difference between the SCET and the dQCD resummed results to the value of the ratio between the dQCD and the SCET resummed coefficient function $C_r(N, M^2, \mu_s^2)$ evaluated in the saddle point $N_0(\tau)$ of the Mellin inversion integral. We have shown how the value of C_r depends on various approximations and we have studied the resulting effects on the SCET and the dQCD predictions. In particular, we have concluded that the main difference between the two approaches is related to subleading terms in N space. However, we have studied a process for which resummation is perturbative and for which the effect of these subleading terms has a considerable phenomenological effect.

We have investigated the consequences of the Becher-Neubert scale choice and we have performed a comparison between this scale choice and the scale M/\bar{N} which is the scale which is naturally resummed in dQCD. By a qualitative analysis, we have understood how the BN scale choice is similar to the saddle point-driven scale M/\bar{N}_0 .

In our work we have inspected some issues which we would like to further investigate. In particular, we have observed that SCET and dQCD resummation formulae agree in the large- N or $x \rightarrow 1$ soft limit, but disagree by subleading terms. Therefore, there are two possibilities: either resummation cannot be used because of these large ambiguities, or else a comparison

with the fixed order result could be a possible way to resolve the ambiguity in the resummation procedure. A deeper analytical insight is needed in order to obtain a more complete comprehension of the resummation procedure in the two formalisms. To this purpose, it would be worthwhile to perform a more detailed study of the ambiguities of the resummation by using different prescriptions in the traditional dQCD approach. The Borel resummation prescription could therefore result particularly useful, in particular as a mean to assess the different treatments of the subleading terms.

Finally, it would be interesting to perform an analogous systematic comparison of dQCD and SCET predictions focusing on Drell-Yan process in hadron-hadron collider. It would be then possible to discuss the relevance of resummation in SCET and dQCD for the production of light mass states (W , Z production) and for the production of heavy dileptons, with masses in the TeV region.

Analytical expressions

In this Appendix we collect various analytical expressions which complete the discussion of the resummation procedure.

A.1 Soft-gluon resummation formulae in dQCD

The general structure of the resummed coefficient function for Drell-Yan and Higgs production is

$$C^{\text{res}}(N, M^2) = g_0(\alpha_s) \exp \mathcal{S}(\bar{\alpha}L, \bar{\alpha}) \quad (\text{A.1})$$

$$\bar{\alpha} \equiv 2\beta_0\alpha, \quad L \equiv \log \frac{1}{N}, \quad (\text{A.2})$$

where g_0 collects all the constant terms and has the expansion

$$g_0(\alpha_s) = 1 + \sum_{j=1}^{\infty} g_{0j} \alpha_s^j, \quad (\text{A.3})$$

and the Sudakov form factor has the logarithmic expansion

$$\mathcal{S}(\bar{\alpha}L, \bar{\alpha}) = \frac{1}{\bar{\alpha}} g_1(\bar{\alpha}L) + g_2(\bar{\alpha}L) + \bar{\alpha} g_3(\bar{\alpha}L) + \bar{\alpha}^2 g_4(\bar{\alpha}L) + \dots \quad (\text{A.4})$$

In this Section we use the expansion coefficient of the β function defined from the renormalization-group equation

$$\mu^2 \frac{d}{d\mu^2} \alpha_s(\mu^2) = \beta(\alpha_s(\mu^2)) \quad (\text{A.5})$$

where

$$\begin{aligned} \beta(\alpha_s) &= -\alpha_s^2(\beta_0 + \beta_1 + \beta_2 \alpha_s^2 + \dots) \\ &= -\beta_0 \alpha_s^2(1 + b_1 \alpha_s + b_2 \alpha_s^2 + \dots) \end{aligned} \quad (\text{A.6})$$

and $\beta_k = b_k \beta_0$ for $k \geq 1$. So far the first four coefficients are known [54, 55]. The first three coefficients are

$$\beta_0 = \frac{11C_A - 4T_F n_f}{12\pi} = \frac{33 - 2n_f}{12\pi} \quad (\text{A.7a})$$

$$\beta_1 = \frac{17C_A^2 - (10C_A + 6C_F)T_F n_f}{24\pi^2} = \frac{153 - 19n_f}{24\pi^2} \quad (\text{A.7b})$$

$$\begin{aligned} \beta_2 &= \frac{1}{(4\pi)^3} \left[\frac{2857}{54} C_A^3 + \left(2C_F^2 - \frac{205}{9} C_F C_A - \frac{1415}{27} C_A^2 \right) T_F n_f \right. \\ &\quad \left. + \left(\frac{44}{9} C_F + \frac{158}{27} C_A \right) T_F^2 n_f^2 \right] \\ &= \frac{1}{128\pi^3} \left[2857 - \frac{5033}{9} n_f + \frac{325}{27} n_f^2 \right]. \end{aligned} \quad (\text{A.7c})$$

A.1.1 Drell-Yan process

In this Section we give the explicit expressions of the functions g_i which appear in the resummed Drell-Yan cross-section. We have [14]

$$g_1(\lambda) = \frac{2A_1}{\beta_0} [(1 + \lambda) \log(1 + \lambda) - \lambda] \quad (\text{A.8a})$$

$$\begin{aligned} g_2(\lambda) &= \frac{A_2}{\beta_0^2} [\lambda - \log(1 + \lambda)] + \frac{A_1}{\beta_0} \left[\log(1 + \lambda) \left(\log \frac{M^2}{\mu_R^2} - 2\gamma_E \right) - \lambda \log \frac{\mu_F^2}{\mu_R^2} \right] \\ &\quad + \frac{A_1 b_1}{\beta_0^2} \left[\frac{1}{2} \log^2(1 + \lambda) + \log(1 + \lambda) - \lambda \right] \end{aligned} \quad (\text{A.8b})$$

$$\begin{aligned} g_3(\lambda) &= \frac{1}{4\beta_0^3} (A_3 - A_1 b_2 + A_1 b_1^2 - A_2 b_1) \frac{\lambda^2}{1 + \lambda} \\ &\quad + \frac{A_1 b_1^2}{2\beta_0^3} \frac{\log(1 + \lambda)}{1 + \lambda} \left[1 + \frac{1}{2} \log(1 + \lambda) \right] + \frac{A_1 b_2 - A_1 b_1^2}{2\beta_0^3} \log(1 + \lambda) \\ &\quad + \left(\frac{A_1 b_1}{\beta_0^2} \gamma_E + \frac{A_2 b_1}{2\beta_0^3} \right) \left[\frac{\lambda}{1 + \lambda} - \frac{\log(1 + \lambda)}{1 + \lambda} \right] \\ &\quad - \left(\frac{A_1 b_2}{2\beta_0^3} + \frac{A_1}{\beta_0} (\gamma_E^2 + \zeta_2) + \frac{A_2}{\beta_0^2} \gamma_E - \frac{D_2}{4\beta_0^2} \right) \frac{\lambda}{1 + \lambda} \\ &\quad + \left[\left(\frac{A_1}{\beta_0} \gamma_E + \frac{A_2 - A_1 b_1}{2\beta_0^2} \right) \frac{\lambda}{1 + \lambda} + \frac{A_1 b_1}{2\beta_0^2} \frac{\log(1 + \lambda)}{1 + \lambda} \right] \log \frac{M^2}{\mu_R^2} \\ &\quad - \frac{A_2}{2\beta_0^2} \lambda \log \frac{\mu_F^2}{\mu_R^2} + \frac{A_1}{4\beta_0} \left[\lambda \log^2 \frac{\mu_F^2}{\mu_R^2} - \frac{\lambda}{1 + \lambda} \log^2 \frac{M^2}{\mu_R^2} \right]. \end{aligned} \quad (\text{A.8c})$$

The full expression of the coefficient g_{0k} is given by [56, 5]

$$g_{01} = \frac{C_F}{\pi} \left[4\zeta_2 - 4 + 2\gamma_E^2 + \left(\frac{3}{2} - 2\gamma_E \right) \log \frac{M^2}{\mu_F^2} \right] \quad (\text{A.9a})$$

$$g_{02} = \frac{C_F}{16\pi^2} \left\{ C_F \left(\frac{511}{4} - 198\zeta_2 - 60\zeta_3 + \frac{552}{5}\zeta_2^2 - 128\gamma_E^2 + 128\gamma_E^2\zeta_2 + 32\gamma_E^4 \right) \right.$$

$$\begin{aligned}
& + C_A \left(-\frac{1535}{12} + \frac{376}{3} \zeta_2 + \frac{604}{9} \zeta_3 - \frac{92}{5} \zeta_2^2 + \frac{1616}{27} \gamma_E - 56 \gamma_E \zeta_3 \right. \\
& \quad \left. + \frac{536}{9} \gamma_E^2 - 16 \gamma_E^2 \zeta_2 + \frac{176}{9} \gamma_E^3 \right) \\
& + n_f \left(\frac{127}{6} - \frac{64}{3} \zeta_2 + \frac{8}{9} \zeta_3 - \frac{224}{27} \gamma_E - \frac{80}{9} \gamma_E^2 - \frac{32}{9} \gamma_E^3 \right) \\
& + \log^2 \frac{M^2}{\mu_F^2} \left[C_F (32 \gamma_E^2 - 48 \gamma_E + 18) + C_A \left(\frac{44}{3} \gamma_E - 11 \right) + n_f \left(2 - \frac{8}{3} \gamma_E \right) \right] \\
& + \log \frac{M^2}{\mu_F^2} \left[C_F (48 \zeta_3 + 72 \zeta_2 - 93 - 128 \gamma_E \zeta_2 + 128 \gamma_E + 48 \gamma_E^2 - 64 \gamma_E^3) \right. \\
& \quad \left. + C_A \left(\frac{193}{3} - 24 \zeta_3 - \frac{88}{3} \zeta_2 + 16 \gamma_E \zeta_2 - \frac{536}{9} \gamma_E - \frac{88}{3} \gamma_E^2 \right) \right. \\
& \quad \left. + n_f \left(\frac{16}{3} \zeta_2 - \frac{34}{3} + \frac{80}{9} \gamma_E + \frac{16}{3} \gamma_E^2 \right) \right] \Bigg\} \\
& - \frac{\beta_0 C_F}{\pi} \left[4 \zeta_2 - 4 + 2 \gamma_E^2 + \left(\frac{3}{2} - 2 \gamma_E \right) \log \frac{M^2}{\mu_F^2} \right] \log \frac{\mu_F^2}{\mu_R^2} .
\end{aligned} \tag{A.9b}$$

For completeness, we list the coefficients \bar{g}_{0k} [50]:

$$\bar{g}_{01} = \frac{C_F}{\pi} (2 \zeta_2 - 4) \tag{A.10a}$$

$$\begin{aligned}
\bar{g}_{02} = & \frac{C_F}{16 \pi^2} \left[C_A \left(-\frac{12}{5} \zeta_2^2 + \frac{592}{9} \zeta_2 + 28 \zeta_3 - \frac{1535}{12} \right) \right. \\
& + C_F \left(\frac{72}{5} \zeta_2^2 - 70 \zeta_2 - 60 \zeta_3 + \frac{511}{4} \right) \\
& \left. + n_f \left(8 \zeta_3 - \frac{112}{9} \zeta_2 + \frac{127}{6} \right) \right] .
\end{aligned} \tag{A.10b}$$

The coefficients appearing in the previous functions are

$$\begin{aligned}
A_1 &= \frac{C_F}{\pi} \\
A_2 &= \frac{C_F}{2 \pi^2} \left[C_A \left(\frac{67}{18} - \frac{\pi^2}{6} \right) - \frac{10}{9} T_F n_f \right] \\
A_3 &= \frac{C_F}{4 \pi^3} \left[C_A^2 \left(\frac{245}{24} - \frac{67}{9} \zeta_2 + \frac{11}{6} \zeta_3 + \frac{11}{5} \zeta_2^2 \right) + \left(-\frac{55}{24} + 2 \zeta_3 \right) C_F n_f \right. \\
& \quad \left. + \left(-\frac{209}{108} + \frac{10}{9} \zeta_2 - \frac{7}{3} \zeta_3 \right) C_A n_f - \frac{1}{27} n_f^2 \right] \\
D_2 &= \frac{C_F}{16 \pi^2} \left[C_A \left(-\frac{1616}{27} + \frac{88}{9} \pi^2 + 56 \zeta_3 \right) + \left(\frac{224}{27} - \frac{16}{9} \pi^2 \right) n_f \right] .
\end{aligned} \tag{A.11}$$

A.1.2 Higgs production

The Higgs resummation coefficient are simply related to those of Drell-Yan process and can be obtained by [14]

$$A_k^{\text{Higgs}} = \frac{C_A}{C_F} A_k^{\text{DY}}, \quad D_k^{\text{Higgs}} = \frac{C_A}{C_F} D_k^{\text{DY}}. \quad (\text{A.12})$$

The coefficients g_{0k} , which collect the constant terms, can be found in Ref. [35] with full scale dependence. They are:

$$g_{01} = \frac{C_A}{\pi} \left[4\zeta_2 + 2\gamma_E^2 + \frac{2}{3}\pi\beta_0 \log \frac{\mu_R^2}{\mu_F^2} - 2\gamma_E \log \frac{M^2}{\mu_F^2} \right] + \frac{11}{2\pi} \quad (\text{A.13a})$$

$$\begin{aligned} g_{02} = & \frac{1}{\pi^2} \left\{ \delta g_{02} + \gamma_E \left(\frac{101}{3} - \frac{14}{9}n_f - \frac{63}{2}\zeta_3 \right) + \gamma_E^2 \left(\frac{133}{2} - \frac{5}{3}n_f + \frac{63}{2}\zeta_3 \right) + 4\gamma_E^3\pi b_0 + 18\gamma_E^4 \right. \\ & + \left(\frac{133}{2} - \frac{5}{3}n_f \right) \zeta_2 + \frac{261}{2}\zeta_4 + \left(22 - \frac{4}{3}n_f \right) \zeta_3 \\ & + \left[\left(-\frac{165}{4} + \frac{5}{2}n_f \right) \gamma_E + 18\gamma_E^2 + 18\zeta_2 \right] \log^2 \frac{M^2}{\mu_F^2} \\ & + 18\pi\gamma_E b_0 \log \frac{M^2}{\mu_F^2} \log \frac{M^2}{\mu_R^2} - 18\pi b_0 (\gamma_E^2 + \zeta_2) \log^2 \frac{M^2}{\mu_R^2} \\ & \left. + \left[12(\pi b_0 - 3\gamma_E) \gamma_E^2 + \left(-\frac{133}{2} + \frac{5}{3}n_f - 63\zeta_2 \right) \gamma_E + 12\pi b_0 \zeta_2 - 72\zeta_3 \right] \log \frac{M^2}{\mu_F^2} \right\} \\ \delta g_{02} = & \frac{11399}{144} + \frac{133}{2}\zeta_2 - \frac{9}{20}\zeta_2^2 - \frac{165}{4}\zeta_3 \\ & + \left(\frac{19}{8} + \frac{2}{3}n_f \right) \log \frac{M^2}{m_t^2} + n_f \left(-\frac{1189}{144} - \frac{5}{3}\zeta_2 + \frac{5}{6}\zeta_3 \right) + 3b_0^2\pi^2 \log^2 \frac{\mu_F^2}{\mu_R^2} - 18\zeta_2 \log^2 \frac{M^2}{\mu_F^2} \\ & + \left(\frac{169}{4} + \frac{171}{2}\zeta_3 - \frac{19}{6}n_f + 12\pi b_0 \zeta_2 \right) \log \frac{M^2}{\mu_F^2} \\ & + \left(-\frac{465}{8} + \frac{13}{3}n_f - 18\pi b_0 \zeta_2 \right) \log \frac{M^2}{\mu_R^2}. \end{aligned} \quad (\text{A.13b})$$

The function $\bar{g}_0(\alpha_s)$ is related to $g_0(\alpha_s)$ by [25]

$$\bar{g}_0(\alpha_s) = g_0(\alpha_s) \exp \left[- \sum_{n=1}^{\infty} \alpha_s^n \sum_{k=0}^n b_{n,k} \frac{\Gamma^{(k+1)}(1)}{k+1} \right]. \quad (\text{A.14})$$

where (omitting scale dependence)

$$b_{1,1} = \frac{4C_A}{\pi}, \quad (\text{A.15a})$$

$$b_{1,0} = 0, \quad (\text{A.15b})$$

$$b_{2,2} = \frac{1}{\pi^2} \left(-\frac{11}{3}C_A^2 + \frac{2}{3}C_A n_f \right) \quad (\text{A.15c})$$

$$b_{2,1} = \frac{1}{\pi^2} \left[\left(\frac{67}{9} - 2\zeta_2 \right) C_A^2 - \frac{10}{9} C_A n_f \right] \quad (\text{A.15d})$$

$$b_{2,0} = \frac{1}{\pi^2} \left[\left(-\frac{101}{27} + \frac{11}{3} \zeta_2 + \frac{7}{2} \zeta_3 \right) C_A^2 + \left(\frac{14}{27} - \frac{2}{3} \zeta_2 \right) C_A n_f \right]. \quad (\text{A.15e})$$

The coefficients \bar{g}_{0k} can be straightforwardly determined as

$$\bar{g}_{0,n} = g_{0,n} - r_n \quad (\text{A.16})$$

where r_n can be read off Eq. (A.14) order by order in α_s . We obtain, setting $C_A = 3$ and omitting scale dependence,

$$\bar{g}_{01} = \frac{11}{2\pi} + \pi \quad (\text{A.17a})$$

$$\begin{aligned} \bar{g}_{02} = & \frac{133}{12} - \frac{165\zeta_3}{4\pi^2} + \frac{11399}{144\pi^2} + \frac{3\pi^2}{16} \\ & + \left(\frac{19}{8\pi^2} + \frac{2}{3\pi^2} n_f \right) \log \frac{M^2}{m_t^2} \\ & + n_f \left(\frac{5\zeta_3}{6\pi^2} - \frac{1189}{144\pi^2} - \frac{5}{18} \right). \end{aligned} \quad (\text{A.17b})$$

A.1.3 Matching

It is necessary to compute and subtract double counting terms when matching the resummed expression with the fixed order results. In order to do so, one first expand Eqs. (A.8a) in powers of λ :

$$g_1(\lambda) = \frac{A_1}{\beta_0} \left[\lambda^2 - \frac{1}{3} \lambda^3 + \mathcal{O}(\lambda^4) \right] \quad (\text{A.18a})$$

$$g_2(\lambda) = \frac{A_1}{\beta_0} \left(\log \frac{M^2}{\mu_F^2} - 2\gamma_E \right) \lambda + \left(\frac{A_2}{2\beta_0^2} + \frac{A_1}{2\beta_0} \left(2\gamma_E - \log \frac{M^2}{\mu_R^2} \right) \right) \lambda^2 + \mathcal{O}(\lambda^3) \quad (\text{A.18b})$$

$$\begin{aligned} g_3(\lambda) = & \left(-\frac{A_1}{\beta_0} (\gamma_E^2 + \zeta_2) - \frac{A_2}{\beta_0^2} \gamma_E + \frac{D_2}{4\beta_0^2} \right) \lambda \\ & + \left(\frac{A_1}{\beta_0} \gamma_E \log \frac{M^2}{\mu_R^2} + \frac{A_2}{2\beta_0^2} \log \frac{M^2}{\mu_F^2} - \frac{A_1}{4\beta_0} \left(\log^2 \frac{M^2}{\mu_R^2} - \log^2 \frac{\mu_F^2}{\mu_R^2} \right) \right) \lambda + \mathcal{O}(\lambda^2). \end{aligned} \quad (\text{A.18c})$$

It is possible to obtain the double-counting term as the Taylor expansion in powers of α_s of $g_0(\alpha_s) \exp \mathcal{S}(\lambda, \bar{\alpha})$:

$$\begin{aligned} g_0(\alpha_s) \exp \mathcal{S}(\lambda, \bar{\alpha}) &= (1 + \alpha_s g_{01} + \alpha_s^2 g_{02}^2 + \dots) e^{\alpha_s \mathcal{S}_1 + \alpha_s^2 \mathcal{S}_2 + \dots} \\ &= 1 + (\mathcal{S}_1 + g_{01}) \alpha_s + \left(\frac{\mathcal{S}_1^2}{2} + \mathcal{S}_2 + \mathcal{S}_1 g_{01} + g_{02} \right) \alpha_s^2 + \mathcal{O}(\alpha_s^3). \end{aligned} \quad (\text{A.19})$$

In particular, one gets

$$\alpha_s \mathcal{S}_1 = \left[\frac{A_1}{\beta_0} \left(\frac{\lambda}{\bar{\alpha}} + \log \frac{M^2}{\mu_F^2} - 2\gamma_E \right) \right] \lambda \quad (\text{A.20})$$

$$\alpha_s^2 \mathcal{S}_2 = \left[-\frac{A_1}{3\beta_0} \frac{\lambda}{\bar{\alpha}} + \left(\frac{A_2}{2\beta_0^2} + \frac{A_1}{2\beta_0} \left(2\gamma_E - \log \frac{M^2}{\mu_R^2} \right) \right) + \left\{ -\frac{A_1}{\beta_0} (\gamma_E^2 + \zeta_2) - \frac{A_2}{\beta_0^2} \gamma_E + \frac{D_2}{4\beta_0^2} \right. \right. \\ \left. \left. + \frac{A_1}{\beta_0} \gamma_E \log \frac{M^2}{\mu_R^2} + \frac{A_2}{2\beta_0^2} \log \frac{M^2}{\mu_F^2} - \frac{A_1}{4\beta_0} \left(\log^2 \frac{M^2}{\mu_R^2} - \log^2 \frac{\mu_F^2}{\mu_R^2} \right) \right\} \frac{\bar{\alpha}}{\lambda} \right] \lambda^2. \quad (\text{A.21})$$

A.2 Soft-gluon resummation formulae in SCET

In this Section we list the perturbative expansions of the various matching coefficients and anomalous dimensions required to evaluate the RG-improved result. We use the same notation of Refs. [41, 42] where the β function is defined as

$$\beta(\alpha_s) = -2\alpha_s \left[\beta_0 \frac{\alpha_s}{4\pi} + \beta_1 \left(\frac{\alpha_s}{4\pi} \right)^2 + \beta_2 \left(\frac{\alpha_s}{4\pi} \right)^3 + \dots \right]. \quad (\text{A.22})$$

The expansion coefficients for the QCD β -function to four-loop order are

$$\begin{aligned} \beta_0 &= \frac{11}{3} C_A - \frac{4}{3} T_F n_f, \\ \beta_1 &= \frac{34}{3} C_A^2 - \frac{20}{3} C_A T_F n_f - 4 C_F T_F n_f, \\ \beta_2 &= \frac{2857}{54} C_A^3 + \left(2C_F^2 - \frac{205}{9} C_F C_A - \frac{1415}{27} C_A^2 \right) T_F n_f + \left(\frac{44}{9} C_F + \frac{158}{27} C_A \right) T_F^2 n_f^2, \\ \beta_3 &= \frac{149753}{6} + 3564\zeta_3 - \left(\frac{1078361}{162} + \frac{6508}{27} \zeta_3 \right) n_f + \left(\frac{50065}{162} + \frac{6472}{81} \zeta_3 \right) n_f^2 + \frac{1093}{729} n_f^3. \end{aligned} \quad (\text{A.23})$$

The value of β_3 corresponds to $N_c = 3$ and $T_F = \frac{1}{2}$.

A.2.1 Drell-Yan production

Two-loop matching coefficients

The Wilson coefficient C_V has the expansion [40]

$$C_V(-M^2 - i\epsilon, \mu) = 1 + \frac{C_F \alpha_s}{4\pi} \left(-L^2 + 3L - 8 + \frac{\pi^2}{6} \right) + C_F \left(\frac{\alpha_s}{4\pi} \right)^2 [C_F H_F + C_A H_A + T_F n_f H_f], \quad (\text{A.24})$$

where

$$\begin{aligned} H_F &= \frac{L^4}{2} - 3L^3 + \left(\frac{25}{2} - \frac{\pi^2}{6} \right) L^2 + \left(-\frac{45}{2} - \frac{3\pi^2}{2} + 24\zeta_3 \right) L + \frac{255}{8} + \frac{7\pi^2}{2} - \frac{83\pi^4}{360} - 30\zeta_3, \\ H_A &= \frac{11}{9} L^3 + \left(-\frac{233}{18} + \frac{\pi^2}{3} \right) L^2 + \left(\frac{2545}{54} + \frac{11\pi^2}{9} - 26\zeta_3 \right) L \\ &\quad - \frac{51157}{648} - \frac{337\pi^2}{108} + \frac{11\pi^4}{45} + \frac{313}{9} \zeta_3, \\ H_f &= -\frac{4}{9} L^3 + \frac{38}{9} L^2 + \left(-\frac{418}{27} - \frac{4\pi^2}{9} \right) L + \frac{4085}{162} + \frac{23\pi^2}{27} + \frac{4}{9} \zeta_3, \end{aligned} \quad (\text{A.25})$$

and $L = \ln(M^2/\mu^2) - i\pi$.

The two-loop expression for the soft function reads

$$\widetilde{s}_{\text{DY}}(L, \mu) = 1 + \frac{C_F \alpha_s}{4\pi} \left(2L^2 + \frac{\pi^2}{3} \right) + C_F \left(\frac{\alpha_s}{4\pi} \right)^2 [C_F W_F + C_A W_A + T_F n_f W_f], \quad (\text{A.26})$$

where

$$\begin{aligned} W_F &= 2L^4 + \frac{2\pi^2}{3} L^2 + \frac{\pi^4}{18} = \frac{1}{2} \left(2L^2 + \frac{\pi^2}{3} \right)^2, \\ W_A &= -\frac{22}{9} L^3 + \left(\frac{134}{9} - \frac{2\pi^2}{3} \right) L^2 + \left(-\frac{808}{27} + 28\zeta_3 \right) L + \frac{2428}{81} + \frac{67\pi^2}{54} - \frac{\pi^4}{3} - \frac{22}{9} \zeta_3, \\ W_f &= \frac{8}{9} L^3 - \frac{40}{9} L^2 + \frac{224}{27} L - \frac{656}{81} - \frac{10\pi^2}{27} + \frac{8}{9} \zeta_3. \end{aligned} \quad (\text{A.27})$$

Three-loop anomalous dimensions

Here we list expressions for the anomalous dimensions quoting all results in the $\overline{\text{MS}}$ renormalization scheme. The expansion coefficients of the anomalous dimensions are defined as

$$\Gamma_{\text{cusp}}(\alpha_s) = \Gamma_0 \frac{\alpha_s}{4\pi} + \Gamma_1 \left(\frac{\alpha_s}{4\pi} \right)^2 + \Gamma_2 \left(\frac{\alpha_s}{4\pi} \right)^3 + \dots \quad (\text{A.28})$$

and similarly for the other anomalous dimensions.

The expansion coefficients of the cusp anomalous dimension Γ_{cusp} are [7]

$$\begin{aligned} \Gamma_0 &= 4C_F, \\ \Gamma_1 &= 4C_F \left[\left(\frac{67}{9} - \frac{\pi^2}{3} \right) C_A - \frac{20}{9} T_F n_f \right], \\ \Gamma_2 &= 4C_F \left[C_A^2 \left(\frac{245}{6} - \frac{134\pi^2}{27} + \frac{11\pi^4}{45} + \frac{22}{3} \zeta_3 \right) + C_A T_F n_f \left(-\frac{418}{27} + \frac{40\pi^2}{27} - \frac{56}{3} \zeta_3 \right) \right. \\ &\quad \left. + C_F T_F n_f \left(-\frac{55}{3} + 16\zeta_3 \right) - \frac{16}{27} T_F^2 n_f^2 \right]. \end{aligned} \quad (\text{A.29})$$

The anomalous dimension γ^V is

$$\begin{aligned} \gamma_0^V &= -6C_F, \\ \gamma_1^V &= C_F^2 (-3 + 4\pi^2 - 48\zeta_3) + C_F C_A \left(-\frac{961}{27} - \frac{11\pi^2}{3} + 52\zeta_3 \right) + C_F T_F n_f \left(\frac{260}{27} + \frac{4\pi^2}{3} \right), \\ \gamma_2^V &= C_F^3 \left(-29 - 6\pi^2 - \frac{16\pi^4}{5} - 136\zeta_3 + \frac{32\pi^2}{3} \zeta_3 + 480\zeta_5 \right) \\ &\quad + C_F^2 C_A \left(-\frac{151}{2} + \frac{410\pi^2}{9} + \frac{494\pi^4}{135} - \frac{1688}{3} \zeta_3 - \frac{16\pi^2}{3} \zeta_3 - 240\zeta_5 \right) \\ &\quad + C_F C_A^2 \left(-\frac{139345}{1458} - \frac{7163\pi^2}{243} - \frac{83\pi^4}{45} + \frac{7052}{9} \zeta_3 - \frac{88\pi^2}{9} \zeta_3 - 272\zeta_5 \right) \end{aligned}$$

$$\begin{aligned}
& + C_F^2 T_F n_f \left(\frac{5906}{27} - \frac{52\pi^2}{9} - \frac{56\pi^4}{27} + \frac{1024}{9} \zeta_3 \right) \\
& + C_F C_A T_F n_f \left(-\frac{34636}{729} + \frac{5188\pi^2}{243} + \frac{44\pi^4}{45} - \frac{3856}{27} \zeta_3 \right) \\
& + C_F T_F^2 n_f^2 \left(\frac{19336}{729} - \frac{80\pi^2}{27} - \frac{64}{27} \zeta_3 \right). \tag{A.30}
\end{aligned}$$

The anomalous dimension γ^ϕ is known to three-loop order from the NNLO calculation of the Altarelli-Parisi splitting functions [7]. The expansion coefficients are

$$\begin{aligned}
\gamma_0^\phi &= 3C_F, \\
\gamma_1^\phi &= C_F^2 \left(\frac{3}{2} - 2\pi^2 + 24\zeta_3 \right) + C_F C_A \left(\frac{17}{6} + \frac{22\pi^2}{9} - 12\zeta_3 \right) - C_F T_F n_f \left(\frac{2}{3} + \frac{8\pi^2}{9} \right), \\
\gamma_2^\phi &= C_F^3 \left(\frac{29}{2} + 3\pi^2 + \frac{8\pi^4}{5} + 68\zeta_3 - \frac{16\pi^2}{3} \zeta_3 - 240\zeta_5 \right) \\
& + C_F^2 C_A \left(\frac{151}{4} - \frac{205\pi^2}{9} - \frac{247\pi^4}{135} + \frac{844}{3} \zeta_3 + \frac{8\pi^2}{3} \zeta_3 + 120\zeta_5 \right) \\
& + C_F^2 T_F n_f \left(-46 + \frac{20\pi^2}{9} + \frac{116\pi^4}{135} - \frac{272}{3} \zeta_3 \right) \\
& + C_F C_A^2 \left(-\frac{1657}{36} + \frac{2248\pi^2}{81} - \frac{\pi^4}{18} - \frac{1552}{9} \zeta_3 + 40\zeta_5 \right) \\
& + C_F C_A T_F n_f \left(40 - \frac{1336\pi^2}{81} + \frac{2\pi^4}{45} + \frac{400}{9} \zeta_3 \right) \\
& + C_F T_F^2 n_f^2 \left(-\frac{68}{9} + \frac{160\pi^2}{81} - \frac{64}{9} \zeta_3 \right). \tag{A.31}
\end{aligned}$$

Using these results, one can compute the expansion coefficients for the anomalous dimension γ^W of the Drell-Yan soft function from the relation $\gamma^W = 2\gamma^\phi + \gamma^V$. This yields for the first two coefficients

$$\begin{aligned}
\gamma_0^W &= 0, \\
\gamma_1^W &= C_F C_A \left(-\frac{808}{27} + \frac{11\pi^2}{9} + 28\zeta_3 \right) + C_F T_F n_f \left(\frac{224}{27} - \frac{4\pi^2}{9} \right). \tag{A.32}
\end{aligned}$$

Renormalization-group functions

We now give the perturbative expansions of the functions S and a_Γ . The resulting expression for a_Γ is given by

$$\begin{aligned}
a_\Gamma(\nu, \mu) &= \frac{\Gamma_0}{2\beta_0} \left\{ \ln \frac{\alpha_s(\mu)}{\alpha_s(\nu)} + \left(\frac{\Gamma_1}{\Gamma_0} - \frac{\beta_1}{\beta_0} \right) \frac{\alpha_s(\mu) - \alpha_s(\nu)}{4\pi} \right. \\
& \quad \left. + \left[\frac{\Gamma_2}{\Gamma_0} - \frac{\beta_2}{\beta_0} - \frac{\beta_1}{\beta_0} \left(\frac{\Gamma_1}{\Gamma_0} - \frac{\beta_1}{\beta_0} \right) \right] \frac{\alpha_s^2(\mu) - \alpha_s^2(\nu)}{32\pi^2} + \dots \right\}. \tag{A.33}
\end{aligned}$$

Similar expressions with the Γ_i replaced by the coefficients γ_i^V or γ_i^ϕ hold for the functions a_{γ^V} and a_{γ^ϕ} , respectively. The expression for the Sudakov exponent S are [40]

$$\begin{aligned}
S(\nu, \mu) = & \frac{\Gamma_0}{4\beta_0^2} \left\{ \frac{4\pi}{\alpha_s(\nu)} \left(1 - \frac{1}{r} - \ln r \right) + \left(\frac{\Gamma_1}{\Gamma_0} - \frac{\beta_1}{\beta_0} \right) (1 - r + \ln r) + \frac{\beta_1}{2\beta_0} \ln^2 r \right. \\
& + \frac{\alpha_s(\nu)}{4\pi} \left[\left(\frac{\beta_1\Gamma_1}{\beta_0\Gamma_0} - \frac{\beta_2}{\beta_0} \right) (1 - r + r \ln r) + \left(\frac{\beta_1^2}{\beta_0^2} - \frac{\beta_2}{\beta_0} \right) (1 - r) \ln r \right. \\
& \left. \left. - \left(\frac{\beta_1^2}{\beta_0^2} - \frac{\beta_2}{\beta_0} - \frac{\beta_1\Gamma_1}{\beta_0\Gamma_0} + \frac{\Gamma_2}{\Gamma_0} \right) \frac{(1-r)^2}{2} \right] \right\}, \tag{A.34}
\end{aligned}$$

where $r = \alpha_s(\mu)/\alpha_s(\nu)$.

A.2.2 Higgs production

Two-loop matching coefficients

To NNLO, the short-distance coefficient C_t is [58, 59]

$$\begin{aligned}
C_t(m_t^2, \mu^2) = & 1 + \frac{\alpha_s(\mu^2)}{4\pi} (5C_A - 3C_F) \\
& + \left(\frac{\alpha_s(\mu^2)}{4\pi} \right)^2 \left[\frac{27}{2} C_F^2 + \left(11 \ln \frac{m_t^2}{\mu^2} - \frac{100}{3} \right) C_F C_A - \left(7 \ln \frac{m_t^2}{\mu^2} - \frac{1063}{36} \right) C_A^2 \right. \\
& \left. - \frac{4}{3} C_F T_F - \frac{5}{6} C_A T_F - \left(8 \ln \frac{m_t^2}{\mu^2} + 5 \right) C_F T_F n_f - \frac{47}{9} C_A T_F n_f \right]. \tag{A.35}
\end{aligned}$$

The two-loop expression for the Wilson coefficient C_S can be extracted from the results of [53]. We write its perturbative series in the form

$$C_S(-m_H^2 - i\epsilon, \mu^2) = 1 + \sum_{n=1}^{\infty} c_n(L) \left(\frac{\alpha_s(\mu^2)}{4\pi} \right)^n, \tag{A.36}$$

where $L = \ln[(-m_H^2 - i\epsilon)/\mu^2]$. The one- and two-loop coefficients are found to be

$$\begin{aligned}
c_1(L) = & C_A \left(-L^2 + \frac{\pi^2}{6} \right), \\
c_2(L) = & C_A^2 \left[\frac{L^4}{2} + \frac{11}{9} L^3 + \left(-\frac{67}{9} + \frac{\pi^2}{6} \right) L^2 + \left(\frac{80}{27} - \frac{11\pi^2}{9} - 2\zeta_3 \right) L \right. \\
& + \frac{5105}{162} + \frac{67\pi^2}{36} + \frac{\pi^4}{72} - \frac{143}{9} \zeta_3 \left. \right] + C_F T_F n_f \left(4L - \frac{67}{3} + 16\zeta_3 \right) \\
& + C_A T_F n_f \left[-\frac{4}{9} L^3 + \frac{20}{9} L^2 + \left(\frac{104}{27} + \frac{4\pi^2}{9} \right) L - \frac{1832}{81} - \frac{5\pi^2}{9} - \frac{92}{9} \zeta_3 \right]. \tag{A.37}
\end{aligned}$$

The associated soft function \tilde{s}_{Higgs} is obtained from that in the Drell-Yan case by the replacement $C_F \rightarrow C_A$. This yields

$$\tilde{s}_{\text{Higgs}}(L, \mu^2) = 1 + \frac{\alpha_s(\mu^2)}{4\pi} C_A \left(2L^2 + \frac{\pi^2}{3} \right) + \left(\frac{\alpha_s(\mu^2)}{4\pi} \right)^2 (C_A^2 W_A + C_A T_F n_f W_f), \tag{A.38}$$

with

$$\begin{aligned} W_A &= 2L^4 - \frac{22}{9}L^3 + \frac{134}{9}L^2 + \left(-\frac{808}{27} + 28\zeta_3\right)L + \frac{2428}{81} + \frac{67\pi^2}{54} - \frac{5\pi^4}{18} - \frac{22}{9}\zeta_3, \\ W_f &= \frac{8}{9}L^3 - \frac{40}{9}L^2 + \frac{224}{27}L - \frac{656}{81} - \frac{10\pi^2}{27} + \frac{8}{9}\zeta_3. \end{aligned} \quad (\text{A.39})$$

Three-loop anomalous dimensions

The cusp anomalous dimension in the adjoint representation is given (at least up to three-loop order) by C_A/C_F times that in the fundamental representation Eq. (A.29). The explicit expressions for the evolution functions S and a_Γ have the form shown in Sect. A.2.1.

The first three expansion coefficients of the anomalous dimension γ^S entering the evolution equation of the matching coefficient C_S are [60, 57]

$$\begin{aligned} \gamma_0^S &= 0, \\ \gamma_1^S &= C_A^2 \left(-\frac{160}{27} + \frac{11\pi^2}{9} + 4\zeta_3 \right) + C_A T_F n_f \left(-\frac{208}{27} - \frac{4\pi^2}{9} \right) - 8C_F T_F n_f, \\ \gamma_2^S &= C_A^3 \left[\frac{37045}{729} + \frac{6109\pi^2}{243} - \frac{319\pi^4}{135} + \left(\frac{244}{3} - \frac{40\pi^2}{9} \right) \zeta_3 - 32\zeta_5 \right] \\ &\quad + C_A^2 T_F n_f \left(-\frac{167800}{729} - \frac{2396\pi^2}{243} + \frac{164\pi^4}{135} + \frac{1424}{27} \zeta_3 \right) \\ &\quad + C_A C_F T_F n_f \left(\frac{1178}{27} - \frac{4\pi^2}{3} - \frac{16\pi^4}{45} - \frac{608}{9} \zeta_3 \right) + 8C_F^2 T_F n_f \\ &\quad + C_A T_F^2 n_f^2 \left(\frac{24520}{729} + \frac{80\pi^2}{81} - \frac{448}{27} \zeta_3 \right) + \frac{176}{9} C_F T_F^2 n_f^2. \end{aligned} \quad (\text{A.40})$$

The first three coefficients of the anomalous dimension γ^B , which equals one half of the coefficient of the $\delta(1-x)$ term in the Altarelli-Parisi splitting function $P_{gg}(x)$, are [6]

$$\begin{aligned} \gamma_0^B &= \frac{11}{3} C_A - \frac{4}{3} T_F n_f = \beta_0, \\ \gamma_1^B &= 4C_A^2 \left(\frac{8}{3} + 3\zeta_3 \right) - \frac{16}{3} C_A T_F n_f - 4C_F T_F n_f, \\ \gamma_2^B &= C_A^3 \left[\frac{79}{2} + \frac{4\pi^2}{9} + \frac{11\pi^4}{54} + \left(\frac{536}{3} - \frac{8\pi^2}{3} \right) \zeta_3 - 80\zeta_5 \right] \\ &\quad + C_A^2 T_F n_f \left(\frac{233}{9} + \frac{8\pi^2}{9} + \frac{2\pi^4}{27} + \frac{160}{3} \zeta_3 \right) \\ &\quad - \frac{241}{9} C_A C_F T_F n_f + 2C_F^2 T_F n_f + \frac{58}{9} C_A T_F^2 n_f^2 + \frac{44}{9} C_F T_F^2 n_f^2. \end{aligned} \quad (\text{A.41})$$

From the relation $\gamma^W = \frac{\beta(\alpha_s)}{\alpha_s} + \gamma^t + \gamma^S + 2\gamma^B$, where $\gamma^t = \alpha_s^2 \frac{d}{d\alpha_s} \frac{\beta(\alpha_s)}{\alpha_s^2}$ we obtain

$$\begin{aligned} \gamma_0^W &= 0, \\ \gamma_1^W &= C_A^2 \left(-\frac{808}{27} + \frac{11\pi^2}{9} + 28\zeta_3 \right) + C_A T_F n_f \left(\frac{224}{27} - \frac{4\pi^2}{9} \right). \end{aligned} \quad (\text{A.42})$$

References

- [1] R. Ellis, W. Stirling, and B. Webber, *QCD and collider physics*, vol. 8, Camb. Monogr. Part. Phys. Nucl. Phys. Cosmol., 1996.
- [2] G. Altarelli, *Collider Physics within the Standard Model: a Primer* [arXiv:1303.2842 [hep-ph]].
- [3] P. Nason, *Introduction to perturbative QCD*, in “Particles and fields. Proceedings, 11th Jorge Andre Swieca Summer School, Campos do Jordao, Sao Paulo, Brazil, January 14-27, 2001”, ed. G. A. Alves, O. J. P. Eboli and V. O. Rivelles, River Edge, USA: World Scientific (2002) 665 p
- [4] J.C. Collins, D.E. Soper and George Sterman, *Factorization of Hard Processes in QCD* in “Perturbative QCD”, ed. A.H. Mueller, World Scientific Publ., 1989.
- [5] M. Bonvini, *Resummation of soft and hard gluon radiation in perturbative QCD* [arXiv:1212.0480 [hep-ph]].
- [6] A. Vogt, S. Moch and J. A. M. Vermaseren, *The Three-loop splitting functions in QCD: The Singlet case*, Nucl. Phys. B **691** (2004) 129 [hep-ph/0404111].
- [7] S. Moch, J. A. M. Vermaseren and A. Vogt, *The Three loop splitting functions in QCD: The Nonsinglet case*, Nucl. Phys. B **688** (2004) 101 [hep-ph/0403192].
- [8] G. F. Sterman, *Summation of Large Corrections to Short Distance Hadronic Cross-Sections*, Nucl. Phys. B **281** (1987) 310.
- [9] S. Catani and L. Trentadue, *Resummation of the QCD Perturbative Series for Hard Processes*, Nucl. Phys. B **327** (1989) 323.
- [10] H. Contopanagos, E. Laenen and G. F. Sterman, *Sudakov factorization and resummation* Nucl. Phys. B **484** (1997) 303 [hep-ph/9604313].
- [11] S. Forte and G. Ridolfi, *Renormalization group approach to soft gluon resummation*, Nucl. Phys. B **650** (2003) 229 [hep-ph/0209154].

- [12] P. Bolzoni, S. Forte and G. Ridolfi, *Renormalization group approach to Sudakov resummation in prompt photon production*, Nucl. Phys. B **731** (2005) 85 [hep-ph/0504115].
- [13] J. C. Collins, D. E. Soper and G. F. Sterman, *Factorization of Hard Processes in QCD* Adv. Ser. Direct. High Energy Phys. **5** (1988) 1 [hep-ph/0409313].
- [14] S. Moch, J. A. M. Vermaseren and A. Vogt, *Higher-order corrections in threshold resummation*, Nucl. Phys. B **726** (2005) 317 [hep-ph/0506288].
- [15] S. Catani, *Higher order QCD corrections in hadron collisions: Soft gluon resummation and exponentiation*, Nucl. Phys. Proc. Suppl. **54A** (1997) 107 [hep-ph/9610413].
- [16] S. Catani, *Soft gluon resummation: A Short review*, in “QCD and high energy hadronic interactions. Proceedings, 32nd Rencontres de Moriond, Les Arcs, France, March 22-29, 1997” ed. J. Tran Thanh Van, Ed. Frontieres (1997) 673 p [hep-ph/9709503].
- [17] E. Laenen, G. Stavenga and C. D. White, *Path integral approach to eikonal and next-to-eikonal exponentiation*, JHEP **0903** (2009) 054 [arXiv:0811.2067 [hep-ph]].
- [18] E. Laenen, L. Magnea, G. Stavenga and C. D. White, *Next-to-eikonal corrections to soft gluon radiation: a diagrammatic approach*, JHEP **1101** (2011) 141 [arXiv:1010.1860 [hep-ph]].
- [19] S. Forte, G. Ridolfi, J. Rojo and M. Ubiali, *Borel resummation of soft gluon radiation and higher twists*, Phys. Lett. B **635** (2006) 313 [hep-ph/0601048].
- [20] S. Catani, M. L. Mangano, P. Nason and L. Trentadue, *The Resummation of soft gluons in hadronic collisions*, Nucl. Phys. B **478** (1996) 273 [hep-ph/9604351].
- [21] P. Bolzoni, *Threshold resummation of Drell-Yan rapidity distributions*, Phys. Lett. B **643** (2006) 325 [hep-ph/0609073].
- [22] R. Abbate, S. Forte and G. Ridolfi, *A New prescription for soft gluon resummation*, Phys. Lett. B **657** (2007) 55 [arXiv:0707.2452 [hep-ph]].
- [23] M. Bonvini, S. Forte and G. Ridolfi, *Soft gluon resummation of Drell-Yan rapidity distributions: Theory and phenomenology*, Nucl. Phys. B **847** (2011) 93 [arXiv:1009.5691 [hep-ph]].
- [24] M. Grazzini, *QCD Effects in Higgs Boson Production at Hadron Colliders*, PoS RADCOR **2009** (2010) 047 [arXiv:1001.3766 [hep-ph]].
- [25] R. D. Ball, M. Bonvini, S. Forte, S. Marzani and G. Ridolfi, *Higgs production in gluon fusion beyond NNLO*, Nucl. Phys. B **874** (2013) 746 [arXiv:1303.3590 [hep-ph]].
- [26] C. Anastasiou, C. Duhr, F. Dulat, E. Furlan, T. Gehrmann, F. Herzog and B. Mistlberger, *Higgs boson gluon-fusion production at threshold in N³LO QCD* [arXiv:1403.4616 [hep-ph]].
- [27] S. Marzani, R. D. Ball, V. Del Duca, S. Forte and A. Vicini, *Finite-top-mass effects in NNLO Higgs production*, Nucl. Phys. Proc. Suppl. **186** (2009) 98 [arXiv:0809.4934 [hep-ph]].

-
- [28] S. Marzani, R. D. Ball, V. Del Duca, S. Forte and A. Vicini, *Higgs production via gluon-gluon fusion with finite top mass beyond next-to-leading order*, Nucl. Phys. B **800** (2008) 127 [arXiv:0801.2544 [hep-ph]].
 - [29] C. Anastasiou, R. Boughezal and F. Petriello, *Mixed QCD-electroweak corrections to Higgs boson production in gluon fusion*, JHEP **0904** (2009) 003 [arXiv:0811.3458 [hep-ph]].
 - [30] K. G. Chetyrkin, B. A. Kniehl and M. Steinhauser, *Decoupling relations to α_s^3 and their connection to low-energy theorems*, Nucl. Phys. B **510** (1998) 61 [hep-ph/9708255].
 - [31] R. V. Harlander and W. B. Kilgore, *Soft and virtual corrections to $pp \rightarrow H + X$ at NNLO*, Phys. Rev. D **64** (2001) 013015 [hep-ph/0102241].
 - [32] C. Anastasiou and K. Melnikov, *Higgs boson production at hadron colliders in NNLO QCD*, Nucl. Phys. B **646** (2002) 220 [hep-ph/0207004].
 - [33] S. Dawson, *Radiative corrections to Higgs boson production*, Nucl. Phys. B **359** (1991) 283.
 - [34] S. Dawson and R. Kauffman, *QCD corrections to Higgs boson production: nonleading terms in the heavy quark limit*, Phys. Rev. D **49** (1994) 2298 [hep-ph/9310281].
 - [35] S. Catani, D. de Florian, M. Grazzini and P. Nason, *Soft gluon resummation for Higgs boson production at hadron colliders*, JHEP **0307** (2003) 028 [hep-ph/0306211].
 - [36] L. Reina, *TASI 2011: lectures on Higgs-Boson Physics* [arXiv:1208.5504 [hep-ph]].
 - [37] <http://www.ge.infn.it/~bonvini/higgs/>
 - [38] A. V. Manohar, *Deep inelastic scattering as $x \rightarrow 1$ using soft collinear effective theory*, Phys. Rev. D **68** (2003) 114019 [hep-ph/0309176].
 - [39] T. Becher and M. Neubert, *Threshold resummation in momentum space from effective field theory*, Phys. Rev. Lett. **97** (2006) 082001 [hep-ph/0605050].
 - [40] T. Becher, M. Neubert and B. D. Pecjak, *Factorization and Momentum-Space Resummation in Deep-Inelastic Scattering*, JHEP **0701** (2007) 076 [hep-ph/0607228].
 - [41] T. Becher, M. Neubert and G. Xu, *Dynamical Threshold Enhancement and Resummation in Drell-Yan Production*, JHEP **0807** (2008) 030 [arXiv:0710.0680 [hep-ph]].
 - [42] V. Ahrens, T. Becher, M. Neubert and L. L. Yang, *Renormalization-Group Improved Prediction for Higgs Production at Hadron Colliders*, Eur. Phys. J. C **62** (2009) 333 [arXiv:0809.4283 [hep-ph]].
 - [43] G. Parisi, *Summing Large Perturbative Corrections in QCD*, Phys. Lett. B **90** (1980) 295.
 - [44] C. Anastasiou, L. J. Dixon, K. Melnikov and F. Petriello, *Dilepton rapidity distribution in the Drell-Yan process at NNLO in QCD*, Phys. Rev. Lett. **91** (2003) 182002 [hep-ph/0306192].
 - [45] C. Anastasiou, L. J. Dixon, K. Melnikov and F. Petriello, *High precision QCD at hadron colliders: Electroweak gauge boson rapidity distributions at NNLO*, Phys. Rev. D **69** (2004) 094008 [hep-ph/0312266].

- [46] A. V. Belitsky, *Two loop renormalization of Wilson loop for Drell-Yan production*, Phys. Lett. B **442** (1998) 307 [hep-ph/9808389].
- [47] M. Beneke, P. Falgari, S. Klein and C. Schwinn, *Hadronic top-quark pair production with NNLL threshold resummation*, Nucl. Phys. B **855** (2012) 695 [arXiv:1109.1536 [hep-ph]].
- [48] <http://rghiggs.hepforge.org>
- [49] M. Bonvini, S. Forte, M. Ghezzi and G. Ridolfi, *Threshold Resummation in SCET vs. Perturbative QCD: An Analytic Comparison*, Nucl. Phys. B **861** (2012) 337 [arXiv:1201.6364 [hep-ph]].
- [50] M. Bonvini, S. Forte, M. Ghezzi and G. Ridolfi, *The scale of soft resummation in SCET vs perturbative QCD*, Nucl. Phys. Proc. Suppl. **241-242** (2013) 121 [arXiv:1301.4502 [hep-ph]].
- [51] G. Sterman and M. Zeng, *Quantifying Comparisons of Threshold Resummations*, arXiv:1312.5397 [hep-ph].
- [52] M. Bonvini, S. Forte and G. Ridolfi, *The Threshold region for Higgs production in gluon fusion*, Phys. Rev. Lett. **109** (2012) 102002 [arXiv:1204.5473 [hep-ph]].
- [53] R. V. Harlander, *Virtual corrections to $gg \rightarrow H$ to two loops in the heavy top limit*, Phys. Lett. B **492**, 74 (2000) [arXiv:hep-ph/0007289].
- [54] J. A. M. Vermaseren, S. A. Larin and T. van Ritbergen, *The four loop quark mass anomalous dimension and the invariant quark mass*, Phys. Lett. B **405** (1997) 327 [hep-ph/9703284].
- [55] M. Czakon, *The Four-loop QCD beta-function and anomalous dimensions*, Nucl. Phys. B **710** (2005) 485 [hep-ph/0411261].
- [56] S. Moch and A. Vogt, *Higher-order soft corrections to lepton pair and Higgs boson production*, Phys. Lett. B **631** (2005) 48 [hep-ph/0508265].
- [57] A. Idilbi, X. d. Ji and F. Yuan, *Transverse momentum distribution through soft-gluon resummation in effective field theory*, Phys. Lett. B **625**, 253 (2005) [arXiv:hep-ph/0507196].
- [58] M. Kramer, E. Laenen and M. Spira, *Soft gluon radiation in Higgs boson production at the LHC*, Nucl. Phys. B **511**, 523 (1998) [arXiv:hep-ph/9611272].
- [59] K. G. Chetyrkin, B. A. Kniehl and M. Steinhauser, *Hadronic Higgs decay to order α_s^4* , Phys. Rev. Lett. **79**, 353 (1997) [arXiv:hep-ph/9705240].
- [60] A. Idilbi, X. d. Ji, J. P. Ma and F. Yuan, *Threshold resummation for Higgs production in effective field theory*, Phys. Rev. D **73**, 077501 (2006) [arXiv:hep-ph/0509294].
- [61] R. D. Ball, V. Bertone, S. Carrazza, C. S. Deans, L. Del Debbio, S. Forte, A. Guffanti and N. P. Hartland *et al.*, *Parton distributions with LHC data*, Nucl. Phys. B **867** (2013) 244 [arXiv:1207.1303 [hep-ph]].